APPLICATIONS OF GRAPHENE TRANSISTORS IN BIOLOGICAL SENSING

ZHANG MENG

Ph.D

The Hong Kong Polytechnic University

2015

The Hong Kong Polytechnic University

Department of Applied Physics

Applications of Graphene Transistors in Biological Sensing

ZHANG Meng

A thesis submitted in partial fulfillment of the requirements for the degree of Doctor of Philosophy

October 2014

CERTIFICATE OF ORIGINALITY

I hereby declare that this thesis is my own work and that, to the best of my knowledge and belief, it reproduces no material previously published or written, nor material that has been accepted for the award of any other degree or diploma, except where due acknowledgement has been made in the text.

_____ (Signed)

ZHANG MENG (Name of student)

Abstract

Graphene, a carbon nanomaterial with a honeycomb 2D single atomic layer structure, has aroused great attention in scientific research since 2004. Due to its unique physical, chemical and electrical properties, graphene has been viewed as a potential candidate for many biomedical applications such as chemical and biological sensors. Among all kinds of graphene based sensors, solution-gated graphene transistor (SGGT) which can operate in electrolyte has been widely studied as promising candidate for high-performance sensors. SGGTs have several advantages over conventional methods, 1. The transistor-based structure of SGGT has both the sensing and the amplification functions, which implies higher sensitivity. 2. SGGTs can operate in aqueous environment with relatively low working voltages, which is important for many chemical and biological processes. 3. SGGTs are feasible for miniaturization and integration process because the device performance is dependent on the ratio of the channel width to length rather than device size.

In this thesis, whole graphene solution-gated transistors with graphene as both channel and gate electrodes were fabricated and used as dopamine sensors. The limit of detection (LOD) of dopamine reached as low as 1 nM, which is three orders of magnitude better than that of conventional electrochemical measurements. The sensing mechanism is attributed to the change of effective gate voltage applied on the transistor induced by the electro-oxidation of dopamine at the graphene gate electrodes.

The interference from glucose, uric acid (UA), and ascorbic acid (AA) on the dopamine sensor is characterized. In purpose of improving the selectivity of dopamine to the interferences, a thin Nafion film was modified on the graphene gate by solution process. After the modification, the device exhibited LOD of 1 nM to dopamine, 1 μM to AA and 10 μM to UA.

Enzyme induced reactions on the gate electrodes of SGGTs could induce the change of effective gate voltage applied on the channel, and thus induce the variation of the conductance. Based on this mechanism, SGGTs with functionalized gate electrodes were designed and fabricated for hydrogen peroxide (H_2O_2) and glucose detection. Firstly, the graphene gate electrodes were modified by Pt nanoparticles through electrodeposition process. The sensitivity of the PtNP-modified SGGTs towards H_2O_2 could reach as low as 30 nM. Based on the as-prepared highly sensitive H_2O_2 sensor, glucose oxidase was immobilized on the gate electrode by using biocompatible polymers (Chitosan, Nafion). The LOD of the functionalized device towards glucose could reach as low as 0.5 μM.

Due to the good biocompatibility and chemical stability of graphene, SGGTs were also developed as cellular interface platform in this thesis. Hepatocellular carcinoma epithelial cancer cell lines (HepG2), osteogenic cell lines (SAOS2), and fibroblast cell lines (HFF1) were cultured on the graphene channel of SGGTs, exhibited excellent biocompatibility. Cell activities on the SGGTs were monitored and analyzed during the adhesion process. The results indicated that the adherent cells could influence the

electrical properties of SGGTs. Meanwhile, during the cell culture, constant electrical fields were applied on all the three electrodes of SGGTs, formed sequential Fermi level change on the SGGT channel. The corresponding distribution of different cell lines on the SGGTs was discussed.

In summary, SGGT-based chemical sensors and biological sensors with specific functions were designed and fabricated. For many sensing applications, SGGTs performance biomedical detections.

List of Publications

1. **Meng Zhang,** Peng Lin, Mo Yang and Feng Yan, Fabrication of Organic Electrochemical Transistor Arrays for Biosensing, *Biochimica et Biophysica Acta (BBA) - General Subjects,1830, 4402-4406 (2013)*.

2. **Meng Zhang**, Caizhi Liao, Yanli Yao, Zhike Liu, Fengfei Gong and Feng Yan, High-Performance Dopamine Sensors Based on Whole-Graphene Solution-Gated Transistors, *Adv. Funct. Mater. 24, 978-985 (2014).*

3. **Meng Zhang**, Caizhi Liao, Chun Hin Mak, Peng You, Chee Leung Mak, Feng Yan, Highly sensitive glucose sensors based on enzyme-modified whole-graphene solution-gated transistors, *Scientific Reports, 8311, (2015)* .

4. Feng Yan, **Meng Zhang** and Jinhua Li, Solution-Gated Graphene Transistors for Chemical and Biological Sensors, *Adv. Healthcare Mater. 3, 313-331 (2014).*

5. Caizhi Liao, **Meng Zhang**, Liyong Niu, Zijian Zheng and Feng Yan, Solution gated graphene transistor with graphene-modified gate electrodes for highly sensitive and selective dopamine sensors, *J. Mater. Chem. B, 2, 191-200 (2014).*

6. Caizhi Liao, **Meng Zhang**, Liyong Niu, Zijian Zheng and Feng Yan, Highly selective and sensitive glucose sensors based on solution gated graphene transistor with graphene-modified gate electrodes, *J. Mater. Chem. B, 1, 3820-3829 (2013).*

7. Caizhi Liao, Chunhin Mak, **Meng Zhang**, Helen L.W. Chan and Feng Yan, Flexible Organic Electrochemical Transistors for Highly Selective Enzyme Biosensors and Used for Saliva Testing, *Adv.Mater. (2015). DOI: 10.1002/adma.201404378*.

8. Caizhi Liao, **Meng Zhang**, Mei Yu Yao, Tao Hua, Li Li, Feng Yan, Flexible Organic Electronics in Biology: Materials and Devices, *Adv. Mater. (2015). DOI: 10.1002/adma.201402625.*

Acknowledgments

From the bottom of my heart, I want to express my gratitude to my chief supervisor Prof. Yan Feng for his guidance, encouragement and great patience during the past three years. With out his support I would never finish this thesis. I respect him for his persistence and perseverence attitude towards science and life. In the three-year studies and life, he guided me in the academic field as well as in life, help me to broaden my horizon and start my new journey.

Secondly, I would like to express my thanks to Prof. Zhao Xingzhong in Wuhan University. I would never forget his advices and selfless help in my life. And I want to thank all my teachers, friends and collegues who have helped me to finish this thesis. Dr. Hardy Lui from Material Research Center, Dr. Terrace Wong, Dr Albert Choi from Applied Physics Department helped me a lot for many experiment techniques used in this thesis.

Thirdly, I would like to offer my special thanks to Dr. Lin Peng, Dr. Li Jinhua, Dr. Yao Yanli, Dr. Wang Lu, Dr. Tai Qidong, Dr. Sun Zhenhua, Dr. Liu Zhike, Dr. He Rongxiang, Dr. Zhu Hongwei, Mr. Bu Chenghao, Mr. Leo Mak, Mr You Peng, Mr Liu Shenghua, Mr Liao Caizhi, Mr Liu Yuzhe from our group for their great support and advices for my research. I wish to acknowledge the help provided by Mr. Wang Ning, Dr Tang Libing, Dr Cheng Bolei, Mr Zhao Yuda, Miss Chen Li, Miss Guo Ming, Miss Lin Mei, and Miss Jie Wenjing in our department for their assistance and useful

discussions. I would express my thanks to Dr. Lily Li, Mr Liu Chunling, Mr Tong Jiahui, Dr Fu Ying and Miss Liu Xuan from Institute of Textiles and Clothing, the Hong Kong Polytechnic University for their help.

I would also like to thank my collaborators, Dr Yang Mo, Mr Ron Chan, Dr Ye Weiwei from Department of Biomedicine Engineering for their useful help, assistance, and discussions in experiments.

I owe a lot of thanks to my friends, Ms Lin Ling, Miss Ding Jing, Miss Sun Qiong, Miss Zheng Keqing, Mr Zhao Meng, Miss Xiang Ruoxi, Mr Andy Tam, Miss Hou Jia, Miss Xin Yin, Miss Bu Shanshan in PolyU. With all your guys together, I enjoyed a happy time and created a lot of precious memories in Hong Kong.

Finally, I would like to express the greatest gratitude and love to my family, my mama and papa, you always love me and support me without any reservation. I dedicate this thesis to my family, I love you forever.

Table of Contents

List of Figures

List of Tables

Abbreviation

Abbreviation	***Description***
AB	Amyl butyrate
AFM	Atomic force microscopy
BSA	Bovine Serum Albumin
CV	Cyclic voltammetry
CVD	Chemical vapor deposition
EDL	Electrical double layer
GO	Graphene oxide
HepG2	Human hepatocellular carcinoma cell line
HFF-1	Human foreskin fibroblasts cell line
IgE	Immunoglobulin E

ISFET	Ion-sensitive field-effect transistor
PASE	1-pyrenebutanoic succinimidyl ester
PDMS	poly dimethylsiloxane
PMMA	Polymethy methacrylate
PNA	Peptide nuclei acid
PSA–ACT	Prostate specific antigen/alantichymotrypsin
PtNP	Platinum nanoparticle
SAOS2	Human sapien osteosarcoma cell lines
SGFET	Solution-gated graphene field effect transistor
SGGT	Solution-gated graphene transistor

Chapter 1 Introduction

Since single-layer graphene firstly been exfoliated in 2004, many types of sensors and electronics were developed by ultilizing the unique electrical, optical, chemical properties of graphene. Until recently, graphene and its derives were widely used to detect multiple types of chemistry and biological analytes. In this chapter, the research background for chemical and biological sensors based on solution-gated graphene transistors will be introduced. Furthermore, the objective of my research as well as the outline of the whole thesis will be given in this chapter.

1.1 Background

Nowadays, there is a growing need for precise detection and monitoring chemistry and biological activities. Sensors with high sensitivity, high selectivity and rapid response are required urgently in many fields, including medical analysis, healthcare products, food safety tests, environmental monitoring, agriculture industry, security, and so on. With the development of nanotechnology, many chemical and biological sensors or electronics based on novel nanomaterials were widely investigated. Graphene, because of its unique physical properties, has been regarded as a promising material in the chemical and biological sensors [1-6]. In this thesis, graphene based solution-gated transistors were systematically studied as biosensing platforms.

After Novoselov et al. firstly separated stable single-layer graphene in ambient conditions in 2004 [7],much progress has been made in developing graphene devices in various types of sensors. Among all kinds of graphene- based chemical sensors and biosensors, solution-gated graphene transistor (SGGT), in which the gate and the graphene channel are separated by electrolyte instead of dielectric insulator, has shown to be the most promising one for real-time, highly sensitive, and high-throughput chemical and biological sensors. Basically, transistor-based sensor implies many advantages, such as amplification of signals detection, feasible method for further integration and so on. Meanwhile, the high mobilities and high conductance of graphene suggests devices could have high sensitivies.

1.2 Objective of Research

Although many progresses have been made for the sensing applications based on SGGTs, the physics of devices and the mechanism of sensors are still needing further researching and understanding. Thus, exploring the device physics and sensor mechanisms of SGGTs is indispensible. Besides, many other types of applications based on SGGTs should be developed to meet the requirements of scientific research, practical applications. Based on the reasons above, the objective of this thesis is settle as following:

The first objective of this thesis is to review the previous research of SGGTs based biosensors and chemical sensors, study and summary the device physics and the sensing mechanisms.

Secondly, the objective is to develop highly sensitive biosensors (such as neurotransimitter sensor, carbonhydrates sensor) based on the understanding of the theory of the SGGTs. SGGT-based sensors are designed in purpose of improving the limit of detection and the detection range for certain analytes, and improve the performance comparing to conventional methods. The third objective is to develop integrated sensing platform based on SGGTs, such as cell-based biosensor, which could not only be used for sensing but also for manipulating chemical and biological activities. All these kinds of SGGT-based sensors have potential applications for real time monitoring various of chemical and bio-analytes and activities.

1.3 Outline of Thesis

Chapter 1: Introduction. In this chapter, we basically introduced the background of chemical and biological sensors based on solution gated graphene transistors (SGGTs). The objectives and outline of this thesis are also contained in this chapter.

Chapter 2: In this chapter, the basic structure, materials and typical sensing mechanism was introduced and discussed. Also we reviewed recent progresses of chemical and biological sensors based on solution gated graphene transistors (SGGTs).

Chapter 3: High performance dopamine sensors based on whole graphene solution-gated transistors. In this chapter, we developed a whole graphene SGGTs for dopamine detection. The fabrication procedures of whole graphene based SGGTs are introduced and descriped. Meanwhile, the behavior and mechanism of SGGTs were discussed.

Chapter 4: Highly sensitive glucose sensors based on SGGTs. In this chapter, SGGTs are designed and fabricated as highly sensitive H_2O_2 sensors and glucose sensors. The enzyme-based functionalized method are discussed and used for specific sensing applications. The behavior and mechanisms are discussed in this chapter.

Chapter 5: Cell sensing platform integrated with SGGTs. In this chapter, SGGTs are used as cell activity sensing platforms. The platform are used to monitor cell activity such as cell adhesion, cell apoptosis and control cell density distribution. The device behavior and mechanism are also discussed in this chapter.

Chapter 6: Conclusions and Future Outlook. In this chapter, the works of this thesis are concluded and future works are proposed.

Chapter 2 Overview of chemical and biological sensors based on Solution-Gated Graphene Transistors

In this chapter, the basic structure, materials and typical sensing mechanism of solution gated graphene transistors (SGGTs) will be introduced and discussed. An overall point of view in this area is provided. Also, recent progresses of chemical and biological sensors based on SGGTs are reviewed in the chapter.

2.1 Basic concepts of SGGT

Solution-gated graphene transistors (SGGTs), which is also known as solution-gated graphene field effect transistors (SGFET), is one kind of electronic devices comprised by three metal contacts (source, drain, and gate) and a graphene channel fabricated on a substrate as shown in Figure 2.1

Two different voltages are applied on the drain and the gate eletrodes while the source is grounded. SGGTs have similar working principles as typical eletrolyte gated field effect transistors which are widely used in electronics, the graphene channel and the gate are exposed to an electrolyte. Gate voltage is applied through the electrolyte and

the conductance of the graphene channel can be modulated by the gate voltage due to change of carrier densities in the channel.

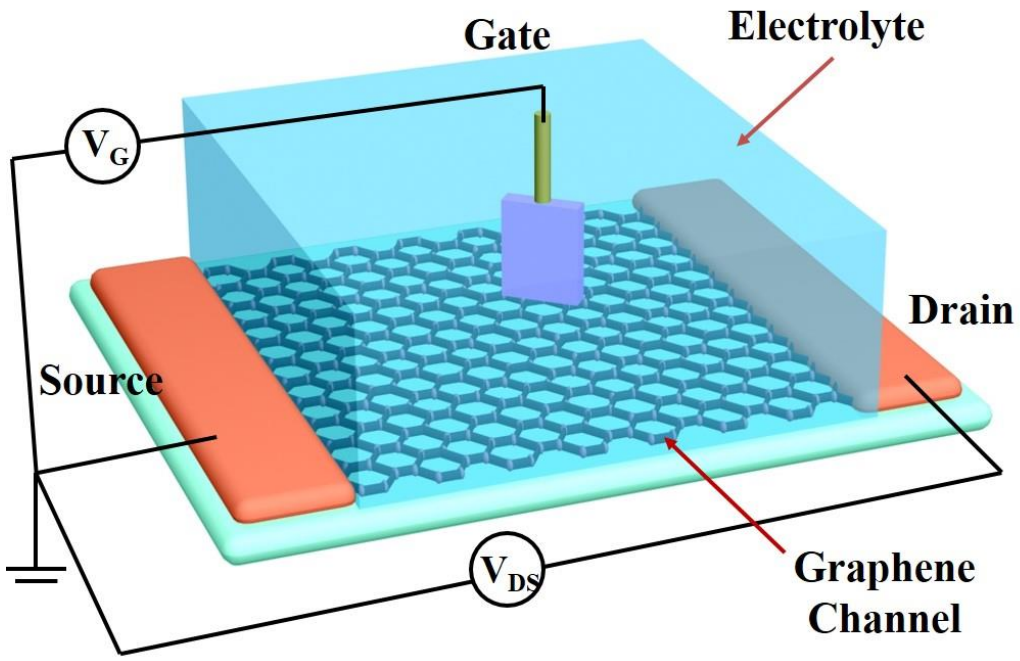

Figure 2.1 Typical configuration of a SGGT, containing three electrodes(source, drain,gate), a graphene channel and electrolyte.

One obvious difference of SGGTs from other kind of eletrolyte gated FETs is the channel material. Graphene, a novel allotrope of nanocarbon materials which has a so-called honeycomb 2D single-atomic-layer structure is used for channel conducting. Graphene is constructed by a sheet of sp^2-bonded carbon atoms, which has been viewed as the basic structure of many other carbon allotropes, such as graphite and

carbon nanotubes. The carbon–carbon bond length in graphene is about 0.142 nm. The unique 2D structure of graphene has led to many remarkable physical properties including massless carriers (both electrons and holes), high transparency (97.7% for single layer), high conductivity, and extremely high carrier mobilities up to 10^5 $cm^2/(V\ s)$, which is about 2–3 orders of magnitude higher than those of typical semiconductors such as silicon. [8] Because of the excellent properties, graphene has been intensely investigated for the applications in transistors, solar cells, transparent conducting electrodes, sensors, and so on. Graphene holds advantages particularly in the sensing applications because it is chemically robust and bioinert. More importantly, graphene is extremely sensitive to electric field and charges around it because every carbon atom of a graphene sheet is exposed to the environment.

Graphene was firstly prepared by mechanical exfoliation method. [9] However, it is very difficult to obtain large-area graphene films using this technique. Then, several more convenient approaches, such as chemical vapor deposition (CVD) on metal substrates, epitaxial growth on SiC, and reduction from separated graphene oxide (GO) flakes, and so on, have been extensively studied by many research groups. Some approaches are potentially low cost and suitable for mass production. It is notable that large-area and high-quality single- or few-layer graphene has been successfully fabricated by CVD methods,which paved the way for the development of high performance, high density, and multifunctional graphene-based devices for many applications including the chemical and biological sensors.

SGGTs operate in electrolytes in direct contact with analytes, which is meaningful for the detection of many biological relevant molecules and reactions in aqueous solutions. SGGT-based sensors are expected to have high sensitivities because of the following factors. Firstly, a transistor-based sensor could serve as both a sensor and an amplifier. A small variation of voltage could induce a pronounced response of channel current due to the inherent amplification function of the device. [10] Secondly, graphene shows much higher carrier mobilities than many other semiconductors used in transistor-based sensors, [9] such as organic semiconductors, [11]silicon nanowires, [12] and carbon nanotubes. [1] Therefore, SGGTs have higher transconductance (i.e., the ratio of channel current response to the gate voltage change) than other types of transistors, which is a key factor to the signal amplification of the devices. [13]Thirdly, SGGTs have the operational voltages normally less than 1 V, [14]so the devices are very sensitive to small potential changes induced by analytes near the interfaces on the channel or the gate. Of particular interest is the factor that SGGTs can be miniaturized without the degradation of device performance because the channel current is proportional to the ratio of the channel width to length rather than the actual device size, so the devices are promising in the applications as high-density and multifunctional microarrays that can provide unprecedented simultaneous and multiplexed analysis in a high- throughput screening format [10].

In this chapter, we will focus on the recent progress and the performance of SGGT-based chemical and biological sensors in the detection of pH, ions, biological analytes

and bioreactions, as shown in Table 1 and Table 2. The detailed working principle and the fabrication of SGGTs are introduced first. Then, the sensors are sorted by their applications and described in the two sessions: 1) chemical sensors, including pH and ion sensors; 2) biosensors, including glucose, DNA, cell, bacterial, and protein sensors. It is notable that all of the sensors are potentially useful in healthcare products.

2.2 Introduction to graphene: properties and fabrication

2.2.1 Mechanically Exfoliated Graphene

Pristine graphene without any functionalization is insoluble in any solvent. Therefore, pristine graphene channel can be fabricated by directly transferring graphene sheets onto the substrate by mechanical cleavage, known as the "scotch-tape" method. [9, 15] The technique is easy to achieve, using adhesive tape to repeatedly peel layers off of highly oriented pyrolytic graphite and pressing it onto an target substrate. The pristine single- or few-layer graphene exhibits the best electronic and structural qualities, high carrier mobilities at room temperature, and low intrinsic noises as compared with other nano- structured graphene films. So that it is used very often to study the intrinsic properties of graphene and related devices. However, it is difficult to control the shape, size, and location of this kind of graphene, as shown in Figure 2.2. Hence, the yield of

the devices is extremely low. It is obvious that mechanically exfoliated graphene is more suitable for fundamental study than practical applications, such as SGGTs.

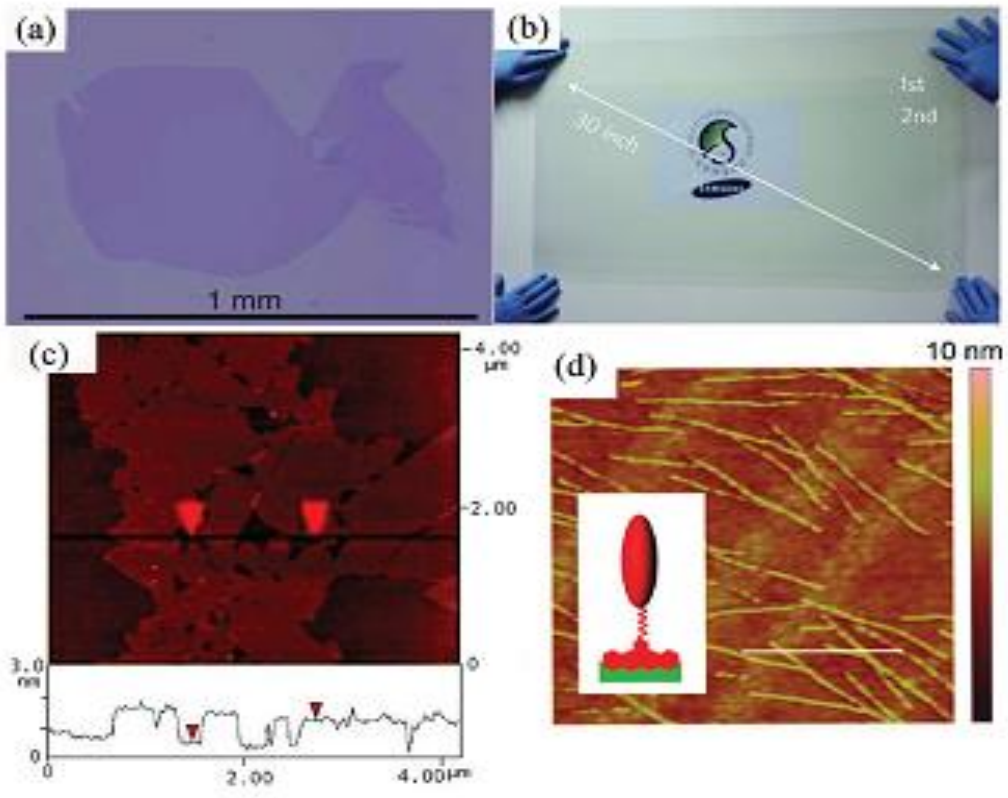

Figure 2.2 a) Optical microscopy image of exfoliation graphene prepared on a oxidized Si wafer by the scotch-tape technique[8].b) A transparent ultralarge-area CVD-grown graphene film transferred on a 35-in. polyethylene terephthalate (PET) sheet [16].c) AFM image of GO sheets on freshly cleaved mica, the height difference between two arrows is 1 nm, indicating a single-layer GO[17]. d) AFM image of phages bound to mechanically exfoliated pristine graphene film (scale bars 1 μm) [18].

2.2.2 Graphene Prepared by CVD

CVD method has emerged to be one of the most promising techniques for the large-scale production of single- and multi-layer graphene films. Carbon atoms can be dissolved in metal (e.g., Ni, Ru, and Cu) foils at high temperature and then precipitated onto the metal surfaces to form graphene films upon cooling. By using this method, graphene films could be prepared on the metal substrates particularly on Cu foils that can lead to single-layer yield as high as 95% [19]. As shown in Figure 2.2b, large-area graphene with a size up to tens of inches can be prepared by a CVD method. So this technique can enable the mass production of SGGTs with high reproducibility for many practical applications. Another advantage of CVD growth is the feasibility of substitutional doping by introducing heteroatoms (nitrogen, boron, etc.) into the carbon lattice [16], which is also important in functionalizing or optimizing the graphene transistors. Because of the large size of CVD grown graphene, arrays of SGGTs with designed shapes and sizes could be achieved by microfabrication techniques, which shows great potential for miniaturized multifunctional sensing arrays and lab-on-a-chip applications. [20, 21].

On the other hand, there are still many shortcomings of this technique. The CVD-grown graphene can only be prepared on certain metallic substrates and needs to be transferred to target substrates by wet-chemical process with the assistance of a layer of polymer, such as polymathy methacrylate (PMMA) [22], coated on the surface to

stabilize the graphene film before the metal substrate is etched away. The transfer process adds additional complications to the quality and consistency of samples such as cracking, contaminations, and destruction of graphene sheets, causes deterioration of the physical and electronic properties. So the transfer process needs to be optimized in the fabrication of high-performance SGGTs. In addition, the substrate can also influence the physical properties of graphene dramatically due to the interaction between them as evidenced by many reports. Therefore, the substrate modification or treatment is another issue needs to be considered in the fabrication of graphene transistors [22].

Alternatively, another method to obtain an arbitrarily large graphene film is to decompose silicon carbide (SiC) to graphene at high temperatures. [23, 24]However, several issues limit its practical applications. It is difficult to precisely control the properties of graphene epitaxially grown on SiC and it also needs additional transfer steps for device fabrication. More importantly, this technique is not suitable for mass-production for the high price of single-crystal SiC.

2.2.3 GO and rGO

Chemical exfoliation of graphite into GO provides an opportunity to produce solution-processable graphene, which enables the mass production of graphene-based electronics at low cost. [6] Different from direct physical cleavage, chemicals were used to intercalate bulk graphite by inserting reactants between layers that weaken the

cohesive van der waals force. Typically, a stable, homogeneous GO aqueous suspension could be generated by a modified Hummers method, [17] graphite is oxidized with sulfuric acid and potassium permanganate and exfoliated as a result. As shown in Figure 2.2c, the lateral dimensions of GO flakes ranging from several hundred nanometers to several micrometers. This method has relatively shorter reaction time and has little toxic side products. Mohanty and Berry firstly used GO as sensing material in SGGTs [25], and this material is still popularly used in SGGT until now. So GO could be produced at low cost, easily used in various devices, and most importantly, have plenty of oxygen functional groups such as carboxylic acid, epoxy and alcohol groups that could be used for modifying biorecognition molecules in biosensors. However, GO has a significant shortcoming compared with pristine graphene and CVD graphene. The oxidation process could induce defects that can scatter charge carriers, decrease the carrier mobility and increase the overall noise of the device.

Many method of removing the functional groups on GO through chemical reduction, thermal, photothermal, or electrochemcial reduction has been developed to produce rGO with conjugated structure and much higher electrical conductivity [26]. However, typical chemical reduction cannot completely remove all oxygen in GO. The electronic parameters such as mobility and conductivity are still lower than those of pristine graphene, whereas, on the other hand, rGO-based SGGTs may benefit from

the enhanced interaction or chemical reaction between the remaining functional groups and the analytes.

2.2.4. Graphene Modification

To improve the selectivity, sensitivity, and stability of the SGGT-based sensors, surface modifications on the graphene layers are normally needed in many cases. For example, pristine graphene is chemically inert and it cannot be used for any specific detection without surface modification. For GO and rGO, oxygen-containning chemical groups such as carboxylic, hydroxyl groups is naturely existing. Besides, different kinds of chemical moieties, such as amino, hydroxyl, alkyl, sulfonate groups, and so on, could be introduced by chemical reactions [27]. The chemical moieties can be used to graft functional molecules through covalent bonding. For example, carboxylic groups can react with proteins via amide or ester linkages, leading to high sensitivity and selectivity [28]. The covalent strategies can thus effectively introduce various functionalities; however, they unavoidably alter the electronic structure and the physical properties of graphene in the devices.

For mechanically exfoliated or CVD-grown graphene, improvement of the performance of graphene sensors requires more effort because graphene is almost inert in many chemical reactions. In some sensing applications, graphene needs to be functionalized to enhance its specificity, sensitivity, loading capacity, biocompatibility, and so on. Graphene could be modified through covalent and

noncovalent approaches. However, it is relatively difficult to modify mechanically exfoliated or CVD-grown graphene by covalent attachment and the disrupted sp^2 structure after the modification may induce dramatic changes in its electronic properties. Thus, noncovalent modifications have been employed in order to preserve the intrinstic proper- ties of the original graphene materials. As shown in Figure 2.2d, functional molecules can noncovalently bind to the graphene surface through van der Waals interaction, or electrostatic interactions [18]. Graphene materials also can be noncovalently decorated with nanoparticle through in situ reduction, electrospray, or electrochemical deposition [29]. For example, thiol-ssDNA probes can be anchored on graphene via gold nanoparticles modified on the graphene surface and used for sensing target DNA and Pb^{2+} ions [30, 31].

2.3 Structure of SGGTs

Figure 2.1 shows the structure of a typical SGGT consisting of a graphene channel between source and drain electrodes and a gate electrode immersed in an electrolyte. In a transistor, the direct conduction current between the gate electrode and the source or the drain electrode is prohibited. According to our experience, the source and drain electrode cannot be exposed to the electrolyte. A direct contact of the source and the drain electrodes with the electrolyte can induce high gate leakage current and unstable performance of the device when a gate voltage is applied. Because the electrolyte is conductive, the gate voltage is thus actually applied on the two interfaces, including gate/electrolyte and electrolyte/graphene interfaces, as shown in Figure 2.3. Each

interface has an electric double layer (EDL) that can be regarded as capacitor. [20] Similar to a field-effect transistor, the channel conductance of the SGGT can be modulated by the gate voltage due to field-effect doping. The device performance of a SGGT can be presented by a transfer curve, which is the channel current I_{DS} between source and drain as a function of gate voltage V_G at a fixed drain voltage V_{DS}. Because graphene has zero bandgap, SGGTs exhibit ambipolar transfer characteristics, which means the device exhibits either p-channel (hole conduction) at negative gate voltage side or n-channel (electron conduction) at positive gate voltage side, as shown in Figure 2.3. No off current can be observed in the transfer curve of a SGGT. The channel current I_{DS} for both p-channel and n-channel of a SGGT is given by[14]:

$$I_{DS} \approx \frac{W}{L} \mu C_i |V_G - V_{Dirac}| V_{DS}, \text{ for } |V_G - V_{Dirac}| >> |V_{DS}| \qquad (2.1)$$

where V_{DS} and V_G are the voltages applied on the drain and the gate electrodes, respectively; W and L are the width and length of the channel, respectively; μ is the carrier (electron or hole) mobility in graphene; C_i is the gate capacitance. It is worth noting that C_i is not a constant value and is dependent on V_G. V_{Dirac} is the gate voltage when the Fermi level in graphene channel is modulated to the charge neutrality point (Dirac point). This gate voltage is called the Dirac point voltage of the device.

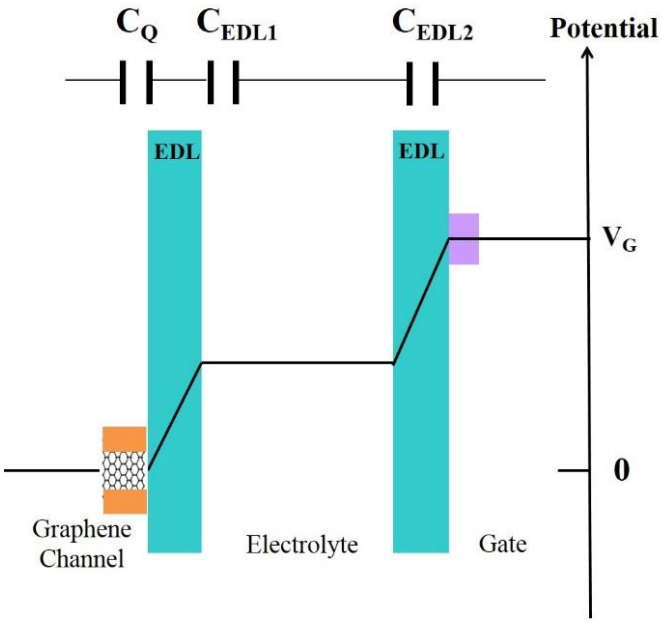

Figure 2.3 Potential drop in a SGGT device under a gate voltage V_G. The blue region represent electric double layer (EDL).

As shown in Figure 2.3, the gate capacitance of a SGGT is related to the two EDL capacitors (C_{EDL1} and C_{EDL2}) connected in series. The capacitance of an EDL is about 10–40 F cm^{-2}, [32] which is largely dependent on ion concentrations in the electrolyte and the applied bias voltage. In addition, the quantum capacitance of graphene channel due to the change of Fermi level when it is charged should be considered. The quantum capacitance C_Q is given by: [33]

$$C_Q = \partial Q / \partial V_{ch} = q^2 \frac{2}{\pi} \frac{qV_{ch}}{(\hbar v_F)^2} \qquad (2.2)$$

where Q is the charge density in graphene channel, q is electron charge, V_{ch} is the channel electrostatic potential, $v_F \approx 108$ cm/s is the Fermi velocity of carriers in graphene, and ħ is the reduced Planck's constant. The quantum capacitance of graphene is dependent on V_{ch} and changes from zero to tens of μF/cm^2, which is lower than or even comparable to double-layer capacitance. [33] Therefore, the gate capacitance of the graphene transistor consists of the two double-layer capacitors and the quantum capacitance connected in series, as shown in Figure 1b. Nevertheless, the total gate capacitance (tens of μF/cm^2) of a SGGT is much bigger than that of a typical field-effect transistor with a thermal oxide gate insulator.For example, the capacitance for a 100 nm-thick SiO_2 layer is only ≈345 nF/cm^2. [34] According to Equation (2.1), if C_i is very high, a low gate voltage can induce a substantial change of channel current. Therefore, the operational voltage of a SGGT is normally less than 1 V, which is much lower than that of a typical field-effect transistor.

The sensitivity of an electronic sensor is the minimum magnitude of input signal that can produce an output signal with a specified signal-to-noise ratio. In analytical chemistry, detection limit, which is the minimum concentration or quantity of a substance that can be distinguished from a suitable blank value, [35]actually has the similar meaning and is normally used to describe the sensitivity of a chemical or biological sensor. An electronic sensor may have a signal even when a blank sample is analyzed, which is referred to as the noise level. So the detection limit is normally defined as the concentration of analyte that can generate output signal three times

higher than the standard deviation of the noise level. Noise in typical graphene filed-effect transistors has been found to be inversely proportional to frequency (f) at low-frequency region (f < 100 Hz) and related to the quality of graphene and the device fabrication conditions. [36] However, the noise level of SGGTs has not been systematically studied until now and further work is needed.

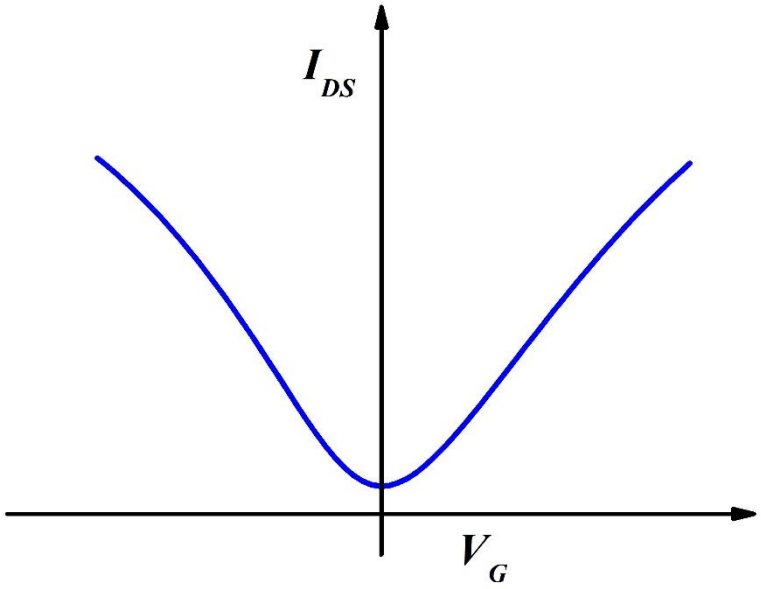

Figure 2.4 A typical transfer curve (channel current I_{DS} *vs.* gate voltage V_G) of a SGGT characterized at a constant drain voltage V_{DS}, I_{DS} could be modulated by VG with a balliastic shape.

The current responses of SGGTs to analytes are important for their sensing applications. Because the SGGT-based sensors are sensitive to potential changes at interfaces as explained in the following section in more details, the current responses

of the devices are proportional to the transconductance of the devices. The change in I_{DS} for a given change in V_G is called the transconductance (g_m) of a transistor. [34] According to Equation (2.1), the transconductance of the device is given by: [34]

$$I_{DS} \approx \frac{W}{L} \mu C_i |V_G - V_{Dirac}| V_{DS} \qquad (2.3)$$

So the channel current response of a SGGT is proportional to the carrier mobility and the gate capacitance (C_i).

2.4 Principles for SGGTs sensing applications

When SGGTs are used as chemical or biological sensors, there are several different sensing mechanisms as reported in literature. In general, analytes can change one or several parameters in Equation (2.1). The possible sensing mechanisms are as follows.

1. Potential drops at interfaces. SGGTs are sensitive to potential changes at the gate electrodes or the graphene channels, which are similar to other types of transistor-based sensors.[13] In this case, the Dirac point voltages (V_{Dirac}) of the devices can be changed by the analytes, which lead to horizontal shifts of the transfer curves. Almost all pH and ion-sensitive SGGT sensors are based on this mechanism. [20] Some biosensors, such as bacterial and DNA sensors, [28, 30] also operate with the same principle. It is notable that most of the researchers were focusing on the potential change on the graphene active layer, whereas few noticed that the potential drop on

the gate electrode is equally important to the sensing applications. Our group recently demonstrated that a KCl ion sensor could be realized by using a SGGT with an Ag/AgCl gate electrode based on the changes of the potential drop at the gate electrode with the variation of ion concentrations. [20] So many other types of chemical and biological sensors with functional gate electrodes are expected to be realized in the future although few works have been reported until now.

2. Changes of carrier mobility or doping level in graphene. The interactions between analytes and graphene channel may dramatically change the graphene properties, especially the carrier mobility and the Fermi level, which all influence the performance of the SGGTs. Many biosensors, such as DNA, [37] cell, [38] and bacteria sensors, [25] have been realized based on this mechanism. The selectivity of this type of devices would be a major problem if pristine graphene was used in the active layer, so surface modification on the graphene layer is needed in specific detections.

3. Change of contact resistance. Contact resistance in a transistor is an important factor for the device performance, although it is not included in Equation 2.1. The contact resistance is normally due to the nonohmic contact near the source and/or drain electrodes induced by energy level mismatch between the metal contact and the semiconductor layer. Therefore, the modulation of the work function of the metal electrode can change the device performance, including the calculated field-effect carrier mobility and the Dirac point voltage. [39] Although this mechanism in the SGGT sensors has not yet been confirmed, [40] biosensors based on other types of

transistors, including carbon nanotube transistors [41] and organic thin film transistors[42], were reported to operate with this mechanism. Similar effect is expected in some SGGT-based sensors especially short channel devices. It is notable that some researchers may not realize this effect in analyzing their data as the effect is rather difficult to be clarified and separated from other possible factors.

4. Potential change in electrolyte. Electrolytes are conductive and are thus equipotential in the bulk. However, in some special cases, there is a potential drop in the electrolyte between the gate and the channel, which will also influence the performance of a SGGT device. For example, our group reported the SGGT-based flow velocity sensor, [20] which was based on measuring the variation of streaming potential in the electrolyte due to the change of flow velocity. In biological systems, especially living organisms, potential drops maybe induced by fluids or the diffusion of ions, which all may change the performance of a SGGT device when it was used for in vitro or in vivo tests.

5. Gate capacitance change. The EDL capacitance (C_{EDL1} and C_{EDL2} in Figure 2.2) is related to ion concentrations, impurities, or distribution of charges near the graphene layer or the gate electrode. [15] Therefore, the device performance can be influenced by this factor at certain measurement conditions. separated gate and channel regions, as shown in Figure 2.1. The source, drain, and gate electrodes can be deposited and patterned with typical microfabrication techniques directly on substrates. [20] The graphene active layer can be fabricated by using printing or transfer techniques. The

metal (e.g., Au) source and drain electrodes can be isolated from the electrolyte by the graphene layer above them because high-quality graphene film is impermeable to water. However, if the metal electrodes are deposited on top of the graphene layer, packaging of the metal contacts is needed to ensure low gate leakage currents. [20]

The major concern in the fabrication of SGGTs is the quality of graphene used in the devices. Producing high-quality graphene in scalable, economical processes is a very important step for the fabrication of graphene devices. Three major kinds of graphene have been used in the fabrication of SGGTs, including graphene flakes prepared by mechanical exfoliation, [9] CVD-grown graphene, [43] and solution-based and chemically reduced graphene oxide (rGO) prepared by chemical exfoliation of graphite. [6, 25] Each method has its own advantages, draw- backs, and unique features in terms of economic cost, quality, and processability.

2.5 Chemical sensors based on SGGTs

A chemical sensor is a transducer that can convert chemical information, ranging from the concentration of a specific sample component to total composition analysis (like gas or ion concentrations), into signals that can be read out by an observer or by an (mostly electronic) instrument. Chemical sensors may be classified according to the operating principle of the transducer, including optical, electrochemical, electrical, mass sensitive, magnetic, and thermometric devices. [44] Most of the SGGT-based chemical sensors are electrochemical or electrical ones, in which the interaction

between the analyte and the sensitive layer induces a potential change that is then transformed into a change of the channel current. SGGTs have been successfully used as pH sensors and ion (i.e., K^+, Na^+, Ca^{2+}, Hg^{2+},Mg^{2+}, Pb^{2+}, etc.) sensors that are described as follows.

Table 1 chemical sensors based on SGGT

Sensor type	Analyte	Active layer	Detection limit or sensing region	Reference & year
pH sensor	H_3O+, OH-	Epitexal graphene	pH 14-2, 99 mV/pH	[45]2008
	pH	Exfoliated graphene	pH 4.0-8.2, 25 mV/pH	[40]2009; [46]2010
	pH	Suspended graphene	pH 6-9, 20 mV/pH	[47] 2010
	pH	CVD-grown graphene	Insensitive, 6-0 mv/pH	[48]2011
Ion sensor	NaF	Exfoliated graphene	10×10^{-3} M to 1 M	[49]2009
	NaCl, KCl	CVD-grown graphene	1.0×10^{-9} M to 1.0×10^{-3}M	[50]2010
	Na^+	Exfoliated graphene		[51],2011
	Ca^{2+}, Mg^{2+}, Hg^{2+}, Cd^{2+}	rGO	Ca^{2+} 1×10^{-6}M, Mg^{2+} 1×10^{-9}M, Hg^{2+} 1×10^{-9}M, Cd^{2+} 1×10^{-9}M	[52]2011
	KCl	CVD-grown graphene	1×10^{-6}M	[20]2012
	NaCl	CVD-grown graphene	40×10^{-9}M	[53]2012
	Pb^{2+}	CVD-grown graphene	20×10^{-12}M	[54]2012

2.5.1 pH sensors

pH sensors have many applications because pH is an important parameter for lots of chemical and biological reactions. The first transistor-based pH sensor is the ion-sensitive field-effect transistors (ISFET) fabricated on silicon chips in 1970 by P. Bergveld. [55] An ISFET normally shows a gate voltage shift V_G as a function of pH value of the aqueous solution given by[55]:

$$\Delta V_G = 2.3\frac{kT}{q}\alpha\Delta pH \qquad (2.4)$$

where k is the Boltzmann constant, T is the temperature of system, q is the electronic charge, α is a constant less than 1, ΔpH is the pH relative change of solutions. Only in ideal conditions, α is equal to 1 and in this case Equation (4) is called Nernstian relationship. At room temperature (T = 300 K), the gate voltage shift is about 59 mV pH^{-1} when the constant $\alpha = 1$.

Then many different types of transistors, including polysilicon thin film transistors, [55] carbon nanotube transistors, [56] oxide nanowire transistors, [57] and organic thin film transistors [58] were successfully used in pH sensors. SGGTs has been used and studied as pH sensors since 2008. [45] Although the sensing mechanism in some devices remains unclear, large variation of pH sensitivities ranging from zero to a value of 99 mV pH^{-1} (larger than the ideal value given by Nernstian relation) has been reported. Recent research indicated that this variation could be attributed to different

graphene quality and a clean graphene device actually had minor sensitivity toward pH.

In 2008, Ang et al. firstly fabricated SGGTs using epitaxial graphene grown on SiC substrates by thermal deposition and patterned by photolithography. [45] Because the insulating substrate is very thick, only top gate transistor can be fabricated on the epitaxial graphene via "solution gating." The transfer curve exhibited ambipolar behavior with the maximum hole and electron mobilities of about 3600 and 2100 cm^2 /V s, respectively. By applying a gate potential from an Ag/AgCl reference electrode placed on top of the channel, the channel conductance was modulated for only about 30%, which is much lower than those of the SGGTs reported later. [20, 52, 53] So the graphene used in the device may have high density of traps. The transfer curves of the devices shifted to more positive gate voltage with the increase of pH and showed a supra-Nernstian response of 99 mV/pH, indicating great potential for pH sensing applications. The mechanism may be attributed to the interplay between surface potential modulation by ion adsorption and the attached amphoteric OH^- groups on the graphene surface. They also investigated the electrochemical properties of the EDL on graphene using cyclic voltammetry (CV) and frequency dependent impedance methods and found that the graphene/electrolyte interface was very sensitive to pH, which further confirmed that the pH-sensitive behavior of the SGGTs is due to the graphene/electrolyte interface.

Ohno et al. fabricated SGGTs with mechanically exfoliated pristine graphene for electrical detecting pH as well as protein adsorption. [40, 46] The transfer characteristics were measured in buffer solutions with different pH ranged from 4.0 to 8.2. The dependence of the channel conductance at fixed gate and drain voltages on the pH value was also characterized. It was reasonable to find that the Dirac point of the SGGT shifted to a positive direction with increasing pH, similar to the previous report. [45] However, the transfer curve only shifted for about 25 mV/pH, which is much lower than the above result reported by Ang et al. [45]

Cheng et al. reported performance improvement of SGGTs by suspending them in aqueous solution through a novel in situ etching technique. [47] The transconductance of the device was increased for about two times after the suspension of graphene from the substrate, whereas the low-frequency noise was decreased for about one order of magnitude. Therefore, the sensitivity of a sensor based on the suspended device can be improved. The devices were demonstrated as real-time and sensitive pH sensors in testing solutions with pH values varied from 6 to 9. The Dirac point voltage of the transfer curve shifted positively with the increase of pH while the shift was only about 20 mV/pH.

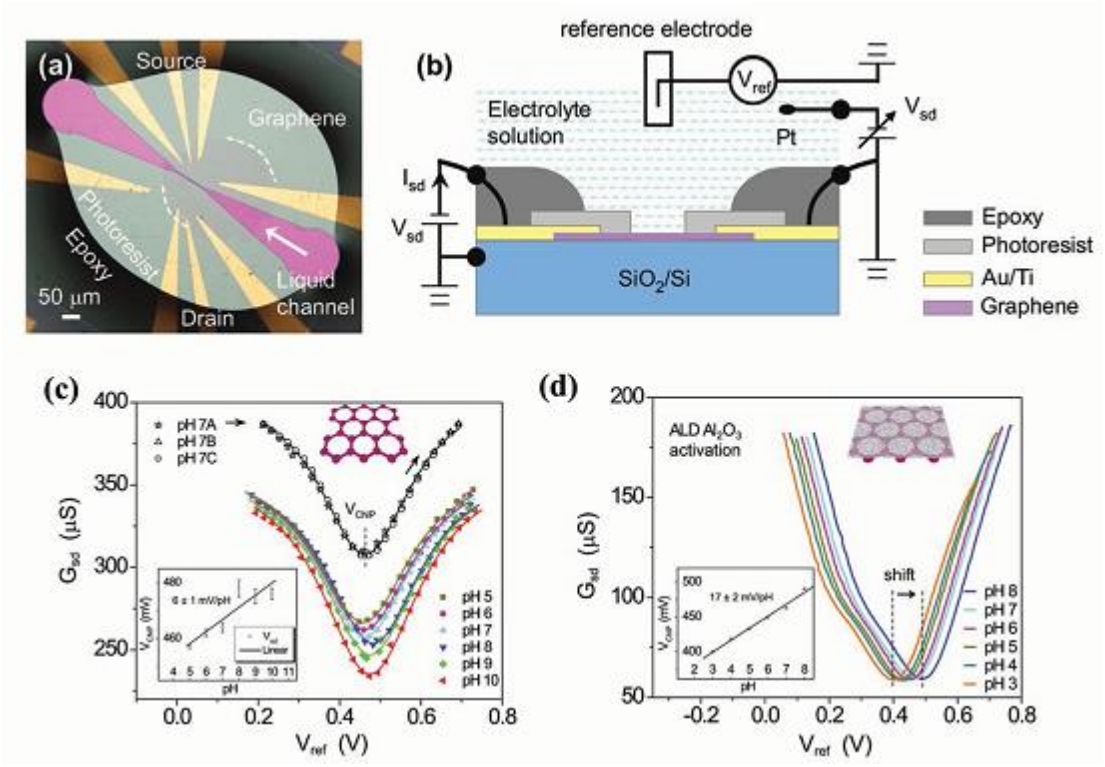

Figure 2.5 a) Optical image of a graphene transistor beneath a liquid channel. b) Schematics of the experimental setup and the electrical circuitry of the SGGT. c) Source-drain conductance as a function of gate voltage applied by the reference electrode measured in different pH buffer solutions for an as-prepared SGGT and d) a SGGT with a thin Al_2O_3 film coated on graphene channel. [48]

Fu et al. found that SGGTs with high-quality graphene were insensitive to the pH values of solutions.[48] As shown in Figure 2.5, they fabricated devices with CVD-grown graphene and observed little gate voltage shift (6±1 mV/pH) in the transfer characteristic of a SGGT when the pH of the solutions were varied from 4 to 10. The voltage-shift of the SGGT can be further reduced when the device was covered by a

hydrophobic fluorobenzene layer on the graphene. But the voltage shift was increased to 17±2 mV/pH when a thin Al_2O_3 layer was coated on the graphene, as shown in Figure 2.5. It is notable that Al_2O_3 is a pH-sensitive material that has been used in ion-sensitive field-effect transistors before.[55] So, the results suggested that clean graphene was not sensitive to the concentration of proton or pH in solutions, which is a consequence of its ideal hydrophobic surface with few dangling bonds. They believed that the gate voltage shifts induced by pH change reported in the previous literature reflected the quality of graphene. So, it is reasonable to conclude that defective graphene, where free bonds exist on the surface, is sensitive to the pH value of the solution, whereas high-quality graphene with no dangling bonds is not.

These studies indicated that pH sensors can be realized by using SGGTs only in some special conditions. Compared with typical silicon-based ISFETs that showed pH-dependent gate voltage shifts close to Nernstian relationship, [42, 55] the pH sensors based on graphene transistors exhibited responses diverged greatly from this relationship. Supra-Nernstian response was even observed in the devices with high-density defects in the graphene layers. [45] Therefore, to realize the high-performance pH sensors, it is necessary to know the underline mechanism that can induce the big shift of Dirac point voltage, [45] which is unclear until now. Further work is needed to better understand this effect.

2.5.2 Ion sensors

Ion sensors have many important applications, such as environment monitoring, food safety inspections, and so on. On the other hand, the interactions between ions and graphene are important to all types of SGGT-based chemical or biological sensors since the devices operate in aqueous solutions. Besides the pH sensors, various ion sensors based on SGGTs, including Na^+, K^+, Ca^{2+}, Mg^{2+}, Hg^{2+}, and Pb^{2+} sensors, have also aroused great attentions in recent years.

Chen et al. prepared SGGTs with mechanically exfoliated graphene on SiO_2 substrates. [49] Ag wires or Ag/AgCl reference electrodes were used as gate electrodes. They studied the influence of ionic concentrations in NaF solutions on the device performance and observed the shift of the transfer curve to lower gate voltage with the increase of ionic concentration. Assuming that the potential drop across the electrolyte/SiO_2 interface was induced by the impurity charges and partially counteracted by the ions in solution, the influence of ionic concentrations on the shift was then simulated with an analytical model successfully. In addition, they found that the charged impurity on the SiO_2 substrates was another important factor that can influence charge transport in graphene layer. By fitting the device performance, the concentrations of charged impurities in different devices were extracted. A clear relationship between the minimum conductivity at the Dirac point and the impurity

concentration was obtained. The minimum conductivity decreased exponentially with the impurity density, which was attributed to the impurity scattering of the carriers.

Heller et al. investigated SGGTs composed of single-layer graphene flakes and Cr/Au source and drain electrodes on SiO_2 substrates. [50] An Ag/AgCl reference electrode was used as the gate. The device performance was sensitive to the ionic concentrations and pH values of the electrolytes. The transfer curve shifted to positive gate voltage with the increase of pH, similar to the pH-sensitive SGGTs reported before. [45] At the same pH condition, the transfer curve shifted with the change of ionic concentrations. When pH is 7, the shift is −42.7 mV per decade for both LiCl and KCl solutions, whereas for pH of 3, the shift is +18.9 mV per decade. So the shift of the transfer curve was sensitive to different ions without selectivity. They believed that the response to ions in electrolytes could be affected by a high density of ionizable groups on both the underlying substrate and the graphene surfaces. These effects should be considered in many other sensing applications of SGGTs, in which the electrical signal can be affected by charged target molecules as well as electrolyte ions. Therefore, careful control of electrolyte properties is needed in some experiments.

Sofue et al. used mechanically exfoliated graphene to fabricate SGGTs for ion sensors and demonstrated sensitive electrical detection of NaCl of various concentrations in Tris–HCl buffer solution. [51] Sodium ion in electrolytes was found to affect the electrical potential of graphene channels. As a result, the transfer curves shifted toward negative voltages with increasing Na^+ concentration. The voltage shift of the SGGT

can be used to accurately detect the concentrations from 1.0×10^{-9} M to 1.0×10^{-3} M. The device was also demonstrated for real-time detection of Na^+ concentrations with high sensitivity.

In practical applications, device packaging of SGGTs is important to achieving stable performance. SGGTs can be integrated in microfluidic systems with only small active areas exposed to electrolyte while all contacts are well packaged. More importantly, microfluidic chips can be easily fabricated in clean room to achieve low cost, highly sensitivity, and high-throughput detections. Our group fabricated and integrated SGGTs into microfluidic channels on both glass and flexible substrates (PET), [20] as shown in the Figure 2.6. The transfer curve of a SGGT with Ag/AgCl gate electrode shifted toward the negative voltage direction with the increase of KCl concentration in the microfluidic channel, as shown in Figure 2.6b. But the device was insensitive to ionic concentration when the Ag/AgCl gate electrode was replaced with an Au wire, indicating that the gate electrode was responsible for the ion-sensitive performance. As shown in Figure 2.6, the voltage shift in the former case was about 61.9 mV per decade close to the ideal value (59 mV per decade) given by Nernst equation at room temperature. So the response was caused by the variation of the potential drop at the Ag/AgCl gate electrode.

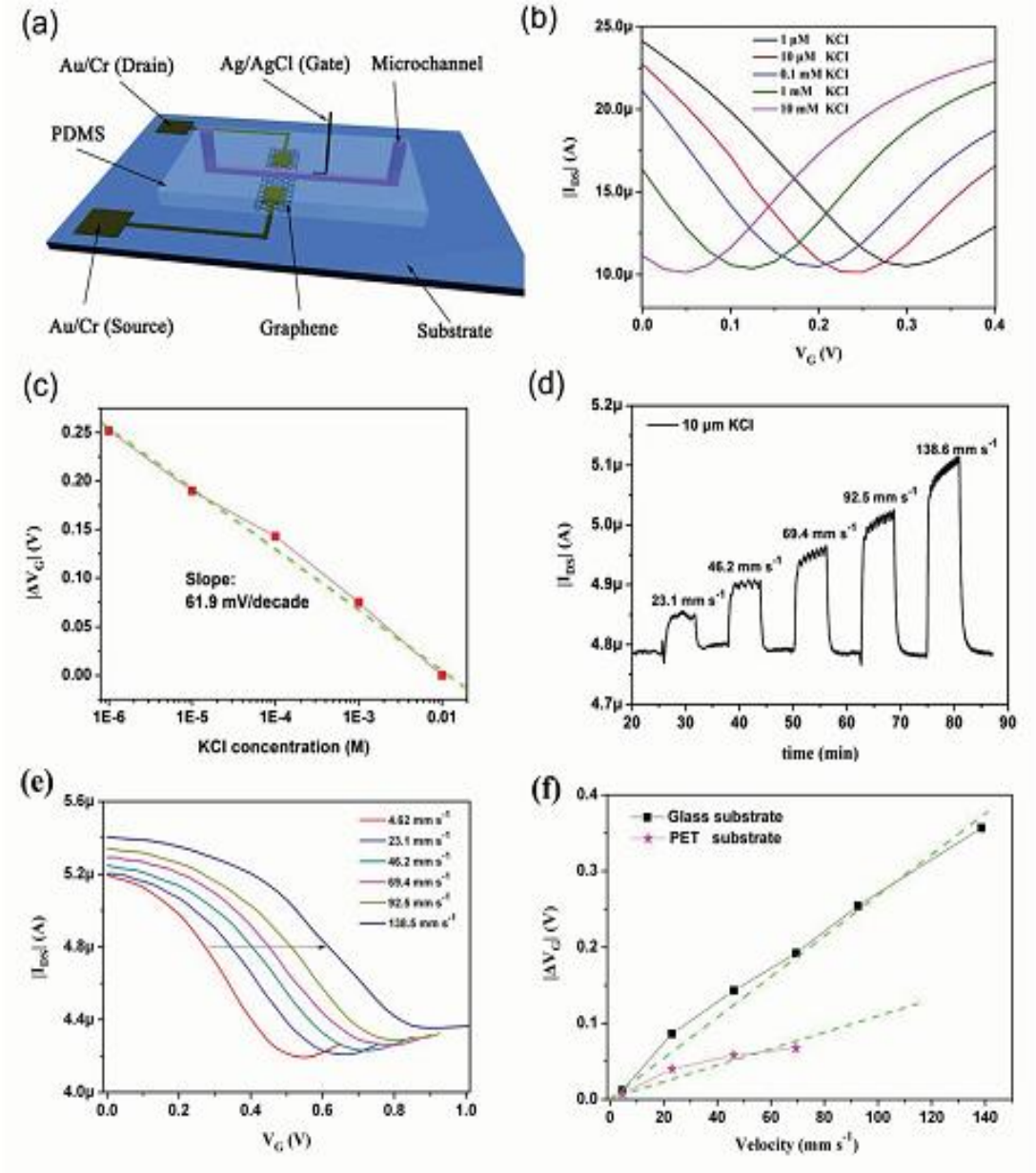

Figure 2.6. a) Schematic diagram of a SGGT with an Ag/AgCl gate electrode integrated in microfluidic channel; b) transfer curves of a SGGT measured in KCl aqueous solutions with different concentrations; c) the shift of Dirac point voltage as a function of KCl concentration. d) Time-dependent channel current of the SGGT

characterized in flowing KCl solution with different velocities; e) transfer curves of the SGGT characterized at different flow velocities; f) the shift of Dirac point voltage (ΔV_G) of SGGTs on glass or plastic substrates at different flow velocities. [20]

The SGGT could also be used to detect flow velocities in the microfluidic channel. As shown in Figure 2.6 d, the channel current I_{DS} changes with the variation of flow velocity. We also observed that the transfer curve of the device shifted horizontally with the change of flow velocity shown in Figure 2.6 e. The voltage shift can be fitted with the following equation for the streaming potential (V_{str}) generated by the moving counterions inside the EDL: [59]

$$V_{str} = \frac{\varepsilon_0 \varepsilon_r \zeta \omega h R}{\eta e (\mathrm{C} + \lambda) \mu} \upsilon \qquad (2.5)$$

Where ζ is the zeta potential on the surface of the micro-chip channel, ε_0 is the vacuum permittivity, ε_r is the relative dielectric constant of the electrolyte solution, ω, h, and R are the width, height, and flow resistance of the microchannel, respectively; η is the dynamic viscosity of the electrolyte solution, e is the electron charge, C is the ionic concentration, λ is an offset concentration that arises from the background concentration of ions, μ is the effective ionic mobility, and υ is the flow velocity in the microchannel.

Because the streaming potential in Equation (2.5) is dependent on three physical quantities, including the flow velocity υ, the ionic strength of the fluid C, and the zeta potential of the substrate ζ, the device could be adopted for sensing any one of the three quantities when the other two were known. As shown in Figure 2.6 f, the SGGTs on different substrates (glass or plastic) exhibited different sensing behavior, which further confirmed the sensing mechanism of the devices. This flexible, multifunctional, and miniaturized SGGT-based sensor might have great potential for applications in lab-on-a-chip platforms, biological systems, or medical devices.

Recently, Newaz et al. investigated the influence of fluid flow on the performance of a SGGT in a microfluidic channel.[75] Because the change of flow velocity or the concentration of ions (NaCl) would induce transfer characteristic shift due to the change of streaming potential given by Equation (2.5), they developed a graphene-based mass flow and ionic strength sensors. The flow sensitivity of SGGTs reached about 70 nL/min, which was about 300 times higher than the reported flow sensitivity of a carbon nanotubes device, and about four times higher compared with a device based on Si nanowire. Their SGGTs could also detect changes in the ionic strength of a moving liquid with the sensitivity of about 40×10^{-9} M. So the devices sensitive to liquid flow and ionic strength may find some applications as mentioned above.

After surface modification on graphene, SGGTs could achieve high sensitivity and specificity to certain kind of ions. Wen et al. reported Pb^{2+} ion sensors using gold nanoparticle and DNAzyme-functionalized SGGTs. [60] As shown in Figure 2.7,

CVD-grown graphene was decorated with gold nanoparticles that serve as the anchoring sites to covalently immobilize thiolated Pb^{2+}-dependent DNAzyme molecules. Upon binding with Pb^{2+} ion, the enzymatic strand cleaved the substrate strand and induced the diffusion of enzymatic strand and the unthiolated portion of the substrate strand from the graphene active layer, which altered the original electronic coupling between the charged DNAzyme complex and the graphene. It is found that the transfer curve shifted to positive gate voltage after adding Pb^{2+} ion, indicating the alleviation of n-doping by DNA molecules. So the Dirac point shift was caused by the interaction between DNAzyme molecules and graphene surface rather than between Pb^{2+} ions and graphene. The detection limit of the devices to Pb^{2+} was about 20×10^{-12} M, which was several orders of magnitude lower than that of other approaches, such as optical methods. [61] Moreover, the selectivity of the devices was very high because Pb^{2+}-dependent DNAzyme was used as the recognition element.

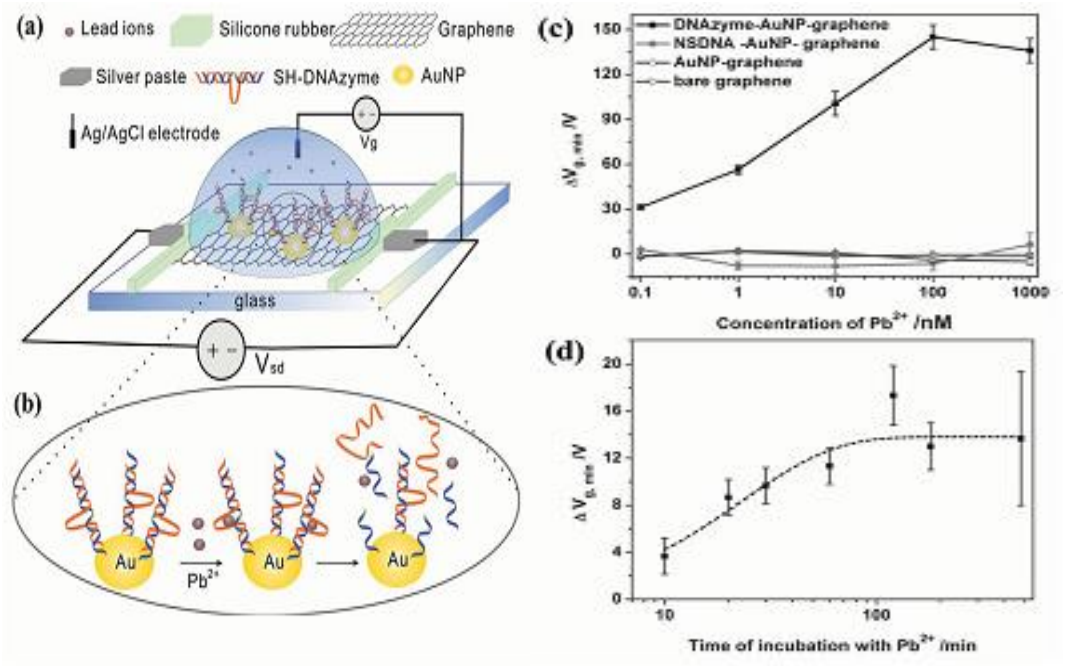

Figure 2.7 Schematic illustration of the SGGT functionalized with Au nanoparticles (AuNPs) and DNAzyme molecules. b) Schematic of Pb^{2+} -induced self-cleavage of the DNAzyme. c) The Dirac point shifts of SGGTs based on bare graphene, AuNP-decorated graphene, nonspecific DNA–AuNP complex decorated graphene, and DNAzyme–AuNP complex decorated graphene, to various Pb^{2+} concentrations. d) The averaged Dirac point shift of DNAzyme–AuNP complex decorated SGGTs in the presence of 20×10^{-12} M Pb^{2+} ion for different incubation time. [61]

Sudibya et al. used micropatterned rGO films to fabricate SGGTs as ion sensors. [52] rGO is the desirable alternative to the pristine graphene due to its low cost, solution processable, and scalable production. [62, 63] After the modification of specific proteins, the devices can be used to effectively detect Ca^{2+}, Mg^{2+}, Hg^{2+}, and Cd^{2+} ions

with high specificity and the detection limit down to 1.0×10^{-9} M, which is comparable to those of conventional methods. [61] By applying different gate voltages, both the p-type and n-type detection can be easily realized in the same rGO-based SGGT. The simple rGO devices could be readily patterned and fabricated by solution process on various substrates and utilized to detect various metal ions in solutions rapidly and label-freely with high sensitivity and specificity. The devices could be easily integrated in lab-on-a-chip systems as microarrays for parallel recording multiple targets.

2.6 Biosensors based on SGGTs

A biosensor is an analytical device combining functional materials or biological components with a physicochemical detector for sensing a biological analyte. The device can convert the biological information into another signal that can be more easily quantified. Graphene has shown great biocompatibility, environmental sensitivity, and stability in biosystems, which is important to either point-of-care or real-time sensing applications. Recently, SGGTs has been fabricated and developed as many kinds of biosensing applications such as biomolecule and bacteria sensing, cell activity monitoring, and so on. After certain modifications, SGGTs could achieve similar or higher sensitivities to bacteria, DNA, protein, and so on compared with other sensing techniques. [64, 65] SGGTs can be easily miniaturized and integrated into microfluidic systems, exhibiting great potential for high-throughput, ultrasensitive, and highly selective biosensors for broad applications.

Table 2.2 Biosensors based on SGGT

Sensor type	Analyte	Active layer	Detection limit or sensing region	Reference & year
Cell based sensor	Chicken cardiomyocyte	Exfoliated graphene		[38],2010
	Cardiomyocyte-like HL-1	CVD-grown graphene		[66],2011
	Malaria-infected red blood cells	CVD-grown graphene		[67],2011
Bacteria sensor	Gram-positive Bacillus cereus cells	GO and GA	A single bacterium	[25],2008
	E. coli, P.aeruginosa	CVD-grown graphene	10 cfu/mL	[68],2011
DNA sensor	DNA	GO		[25],2008
	DNA	CVD-grown graphene	10×10^{-12}M	[30],2010
	DNA	rGO	10×10^{-9}M	[69],2010
	DNA	CVD-grown graphene	1×10^{-9}M	[70],2011
	DNA	rGO	2.4×10^{-9}M	[71],2012
	DNA	CVD-grown graphene	1×10^{-12}M	[72],2013
	DNA	CVD-grown graphene	1×10^{-12}M	[37],2013
Glucose sensor	Glucose	CVD-grown graphene	0.1×10^{-3}M	[28];2010
	Glucose	CVD-grown graphene	$3.3\text{-}10.9\times10^{-3}$M	[73];2012
Protein	BSA	Exfoliated	0.3×10^{-9}M	[40]; 2009

sensor		graphene		
	IgE	Exfoliated graphene	0.29×10^{-9}M	[74];2010
	Fibronectin; avidin	rGO	0.5×10^{-9}M; 80×10^{-9}M	[75];2010
	Immunoglobulin G	rGO	0.2 ng/mL	[26];2011
	PSA-ACT complex	rGO	1.1×10^{-15}M	[76];2013
Dopamine sensor	Dopamine	rGO	$1\text{-}60\times10^{-3}$M	[75];2010
Bioelectronic nose	Amylbutyrate	CVD-grown graphene	0.04×10^{-15}M	[77]; 2012

2.6.1 cell and bacteria sensors

Because of the good biocompatibility of graphene, [78] SGGTs can be integrated with cells for sensing applications. Cohen-Karni et al. reported the first application of SGGTs in cell-based biosensors, in which electrogenic cells were integrated with the graphene channel. [38] Single-layer graphene flakes prepared by mechanical exfoliation were transferred to SiO_2 substrates and Cr/Au/Cr source and drain contacts were then patterned on the graphene layers by electron beam lithography. Spontaneously beating embryonic chicken cardiomyocytes were brought to have direct contact with graphene channels. The devices could yield well-defined extracellular conductance signals with signal to noise ratio higher than 4. By adjusting

the solution gate potential V_G, the amplitude of the signal could be tuned nearly one order of magnitude. Both n- and p-type recording could be easily achieved from the same device by changing V_G. They also studied the relative resolution of SGGTs with different sizes. The peak-to-peak width of the signal increased with the device area, indicating that the devices presented an averaged signal from different points across the outer membrane of the beating cells. The study demonstrated that SGGTs showed better performance than other planar devices, such as microelectrode arrays and other field-effect transistors and offered the unique capability of recording signals as both n- and p-type devices by simply changing the gate voltage.

Hess et al. recently developed a system including arrays of SGGTs using CVD-grown graphene for the detection of electrical activities of electrogenic cells, [66] as shown in Figure 2.8. Compared with exfoliated graphene used by Cohen-Karni et al., [38] CVD-grown graphene can be utilized to prepare large-area devices or arrays, which offers a more suitable platform allowing mass production at low cost. Cardiomyocyte-like HL-1 cells were seeded and cultured on these arrays and exhibited a healthy growth. The action potentials of these cells were detected and resolved by the working SGGTs under the cells, similar to other types of cell-based biosensors. [79] Using the whole transistor array, the propagation of the cell signals across the cell was also tracked and recorded, as shown in Figure 2.6 b and c. The propagation speed was observed to be 12–28m/ms, which is similar to that observed by microelectrode arrays. [80] As shown in Figure 2.8 d, the SGGT arrays were capable of detecting single

voltage spikes as low as 100 μV with a signal-to-noise ratio better than 10, exhibiting a similar performance to that of microelectrode arrays and better signal to noise ratio than that of the solution-gated Si transistors. This study suggests that the outstanding performance of SGGTs together with the promising applications of graphene in flexible electronics imply innovative technologies that can be developed in the field of bioelectronics, [20] such as electrically functional neural prostheses.

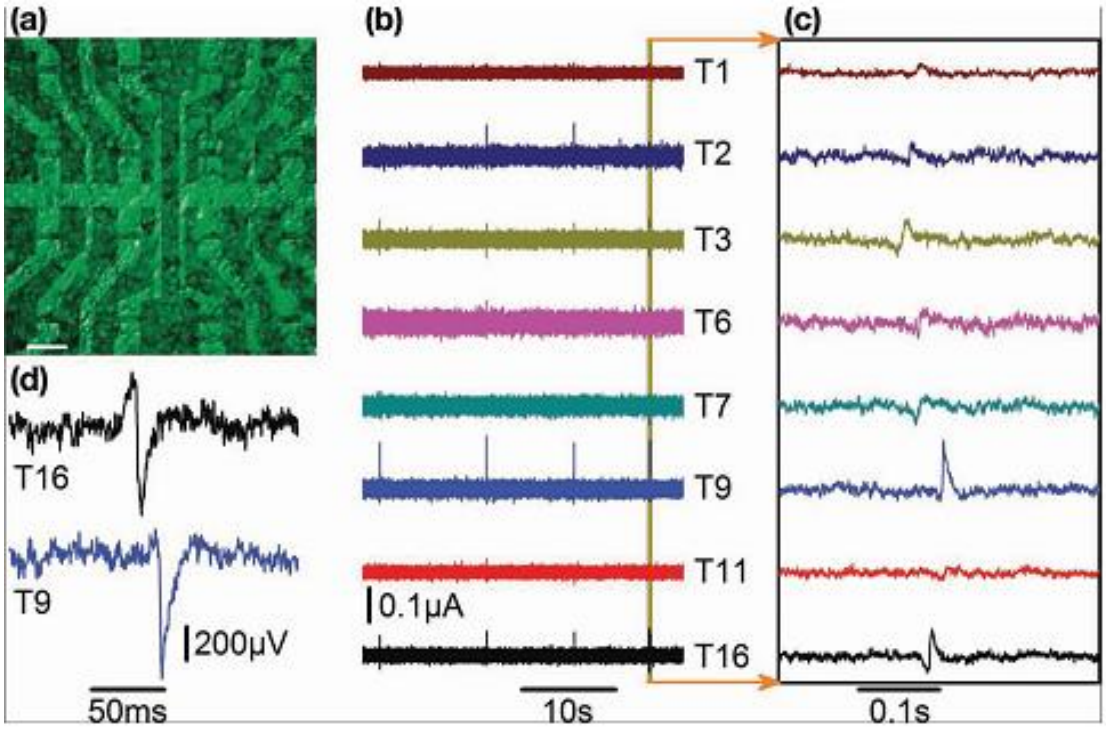

Figure 2.8 a) A SGGT array with calcein-stained cells (fluorescence image) on the top. The scale bar is 100 μ m. b,c) Time dependent current of eight transistors in one FET array measured simultaneously. d) Exemplary single spikes of two transistors. The current response has been converted to an extracellular voltage signal. [66]

Ang et al. integrated SGGTs with microfluidic systems for the “flow-catch release” sensing of malaria-infected red blood cells at the single-cell level, [67] as shown in Figure 2.9. Graphene was functionalized with the endothelial CD36 receptors for the selective capture of the malaria-infected cells when the diseased blood flows through the microfluidic channel. Coulomb-impurity potential exerted by charged protrusions on cell surfaces induced local doping in graphene channel and led to conduct- ance changes between source and drain electrodes. Therefore, the SGGT sensor is able to generate dynamic disease diagnostic patterns in term of conductance changes and characteristic dwell time, showing great potential in clinical diagnostic applications.

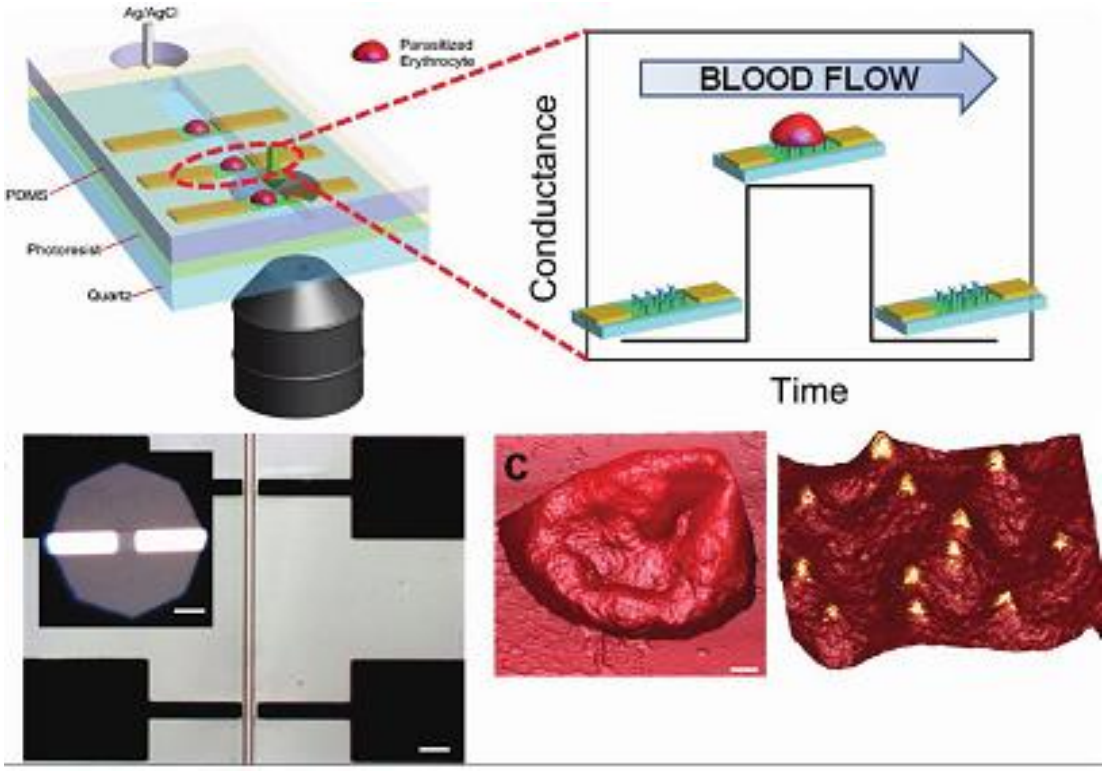

Figure 2.9 Graphene-based detection of single plasmodium falciparum-infected erythrocyte (PE). a) Left: schematic illustration of an array of graphene transistors on quartz. Right: specific binding between ligands located on positively charged membrane knobs of parasitized erythro-cyte and graphene channel induces a conductance change. b) Image of SGGTs integrated with a microfluidic channel. Scale bar in the inset is 30 μm. c) Three-dimensional AFM images of (left) parasitized erythrocyte14 (scale bar is 1μm) and (right) 3D height plot of the surface of parasitized erythrocyte with Protruding knobs. [67]

SGGTs also showed great promise in sensing bacteria because the graphene layer can be easily functionalized with biomaterials. Mohanty and Berry integrated chemically modified graphene (CMG) nanostructure (GO and plasma-modified graphene-amine) with bacteria and DNA.[25]The Gram-positive Bacillus cereus cells possessing a highly negative-charged surface were employed in the study. The CMG device exhibited a sharp increase in conductivity upon the attachment of a single bacterial cell on the surface. The increase in graphene conductance is due to the increased hole density induced by bacterial surface. This detection relied on nonspecific electrostatic adhesion of bacteria without discrimination of bacterial species. They also fabricated a novel bacterial DNA/protein and polyelectrolyte chemical transistor based on graphene-amine for the first time. Electrostatic adsorption of a mixture of negatively charged bacterial, DNA, and proteins extracted from Bacillus cereus cells on the device led to a sharp 2 orders of magnitude decrease in resistance due to the negative charge gating effect.

Huang et al. recently developed a type of bacterium sensors based on SGGTs with high sensitivity (10 cfu mL^{-1}). [68] The SGGTs were fabricated using CVD-grown graphene modified with anti-E. coli antibody on the surface. When the device was exposed to different concentrations of E. coli, it showed the increase in channel conductance with the increase of the bacterial concentration from 10 cfu mL^{-1}. Meanwhile, different bacteria, such as P.aeruginosa with the concentration of 105 cfu mL^{-1}, did not cause significant response of the anti-E. coli antibody functionalized

SGGT, indicating the high specificity of the detections. Furthermore, this device was employed to detect the glucose-induced metabolic activities of the bound E. coli bacteria in real time, providing a platform for screening antibacterial drugs.

2.6.2 DNA sensors

DNA diagnostics has shown great scientific and economic importance in many areas. It has significant applications in gene expression monitoring, clinical medicine, viral and bacterial identification, biowarfare and bioterrorism agents detecting, and so on.[10]However, it is challenging to detect the nucleic acid molecules especially short DNA strands without the use of time-consuming radioactive labelling assays and the unportable confocal fluorescence microscope. Many studies focusing on the application of SGGTs in label-free DNA sensors have been reported. In these devices, graphene channels were functionalized with DNA probes and nanomaterials, which led to highly sensitive and selective DNA detections.

Mohanty and Berry firstly studied DNA hybridization by characterizing the conductance change of amino-modified GO active layer. [25] The hybridization process can lead to large increase in hole density due to the electrostatic gating effect by the negatively charged DNA molecules. However, the detection sensitivity of this kind of device was strongly dependent on the size and the shape of GO sheets, the presence of wrinkles on GO surface and the degree of oxidation in GO.

Dong et al. reported electrical detection of DNA hybridization with high specificity using SGGTs based on CVD-grown multilayer graphene as an alternative of low conductive GO[30]. After preimmobilizing probe-DNAs on graphene surface via nonspecific binding due to the nonelectrostatic stacking interaction, the devices were capable of detecting the hybridization of target DNAs with the concentration down to 0.01×10^{-9} M and distinguishing single base mismatch, which are similar to some other transistor-based DNA sensors. [10, 13] Being different from the above GO-based DNA sensors, the sensing mechanism of the SGGTs was attributed to electron transfer from the electron-rich, aromatic nucleotide to graphene. The gate voltage at the Dirac point was identified from the transfer curve and used to monitor the electron doping state of the graphene film. They observed that the Dirac point shifted to negative voltage with the addition of complimentary DNA targets in the solution. The upper limit of the DNA detection could be extended from 10 to 500×10^{-9} M by decorating Au nanoparticles on graphene sheets because more DNA molecules were immobilized on the graphene surface. In addition to the voltage shift, the minimum channel current at the Dirac point was also decreased obviously with increasing DNA concentration, which might be attributed to nonspecific binding of charged molecules or ions on the graphene surface that can influence carrier transport in graphene by scattering. [81] This study demonstrates the great potential of SGGTs in sensitive and selective detections of DNA.

Guo et al. developed label-free DNA sensors based on graphene field-effect transistors with CVD-grown graphene. [70]The devices were patterned by conventional photolithography and modified by 1-pyrenebutanoic acid succinimdyl ester. Probe DNA molecules were immobilized on graphene surface by the ester and used for detecting complimentary target DNA with the detection limit of about 1×10^{-9} M, which is inferior to the above DNA sensors reported by Dong et al. [30]

Chen et al. reported the SGGT fabricated with CVD-grown monolayer graphene. [72] Operational conditions were optimized to achieve the DNA detection as low as 1×10^{-12} M, which was more sensitive than the aforementioned SGGTs with few-layer graphene. They also demonstrated that the gold-transfer technique is better than the typical PMMA-transfer in the fabrication of SGGTs for sensing applications. Recently, Lin et al. from the same group studied the underline sensing mechanism of the SGGT-based DNA sensors by measuring Hall effect of the graphene channels. [37] The Hall effect is the production of a voltage difference (called Hall voltage) across an electrical conductor or a semiconductor, transverse to an electric current in the material and a magnetic field perpendicular to the current. The Hall effect measurement is very useful as a means to characterize the carrier density and mobility of a semiconductor. They observed that the addition of either complementary or one-base mismatched DNA on the devices could increase the sheet resistance and decrease the hole carrier mobility and thus one-base mismatched DNA could not be differentiated by the conductance change. Fortunately, they found that the hole carrier concentration in graphene

increased significantly with the addition of complementary DNA while it was less affected by one-base mismatched DNA, as shown in Figure 2.10. So they concluded that the increase in hole carrier density, evidenced by n-doping in graphene, is better correlated with the DNA hybridization. However, the underline mechanism is still unclear since both complementary DNA and one-base mismatched DNA strands are negatively charged, which are expected to induce n-type doping in the graphene channel as shown in other types of sensors based on graphene transistors reported before. [82]

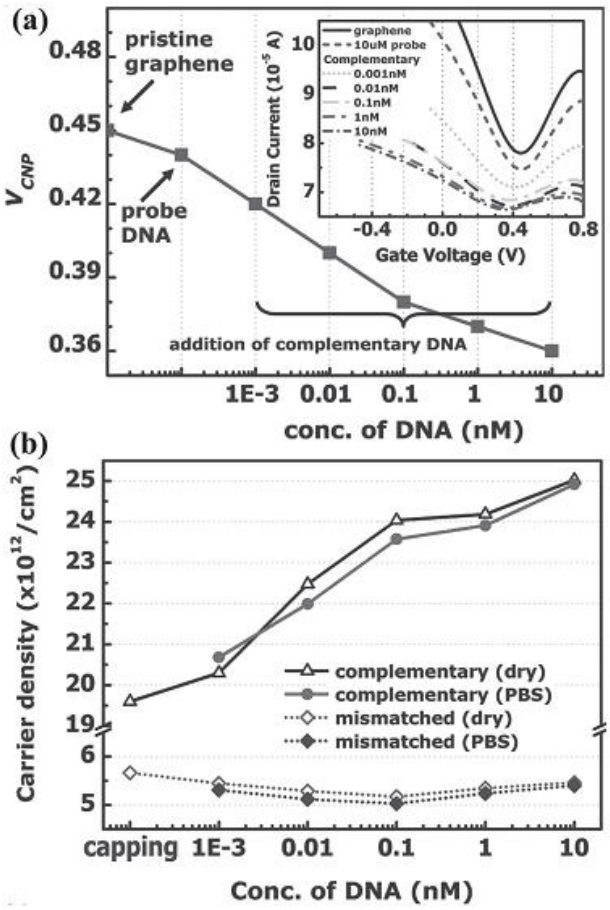

Figure 2.10. a) The Dirac point voltage (V_{CNP}) as a function of complementary DNA concentration added in the solution. Inset: the transfer curves for the graphene devices before and after each DNA addition step. b) The carrier concentration of graphene as a function of the concentration of added complementary and one base mismatched DNA. Two curves were measured separately in dry (without PBS) and wet (in PBS) states by the Hall effect measurement. [82]

Stine et al. fabricated SGGTs utilizing rGO for real-time and label-free DNA detection. [69] An amino-silane film was formed on the substrate before GO deposition and reduction, which could stabilize the rGO layer on the surface in aqueous solutions. Then a flow cell contained a Pt wire inside the flow region was attached to the device to isolate the active rGO areas for solution exposure. The DNA sensors could reach the detection limits as low as 10×10^{-9} M, which is not as good as the devices based on CVD-grown graphene. [30] However, rGO films could be easily deposited and etched to form device arrays, this technique might offer a simple and low-cost approach for high-throughput DNA detection with good specificity and sensitivity.

Yin et al. reported Pt nanoparticle-decorated rGO-based SGGTs for real-time DNA detection. [71] Large-area rGO thin film was fabricated on a Si/SiO_2 wafer using the Langmuir–Blodgett method followed by thermal reduction. Then Pt nanoparticles were directly synthesized onto rGO sheets by photochemical reduction. The resulting composite was used as the channel material of the SGGTs. Pt electrodes were employed as the gate in the devices. The decoration of probe DNA on the devices was achieved by Pt-S covalent bonding. The devices were used to detect and analyze the hybridization process of target DNA in real time through continuously monitoring channel current. The hybridization of target DNA caused a decrease of channel current, which can be explained by the increased n-doping effect by DNA. The detection limit of the read time detection was estimated to be 2.4×10^{-9} M, being similar to other rGO-based devices. [69]

Cai ect. reported ultrasensitive label-free detection of DNA via peptide nuclei acid (PNA)-DNA hybridization based on rGO solution-gated transistor. PNA modified on rGO take the place of probe DNA used in others work. Firstly, PASE (the linker molecule) is fixed on the rGO surface through π-π stacking interaction，then PNA probe was linked on PASE end by convalent bond. The PNA-DNA hybridization induced lower detection limit of DNA reaching 100 fM, which is 1 orders of magnitude lower than SGGTs adopted DNA-DNA hybridization as probe mechanism. Furthermore, the rGO solution-gated transistor could distingush DNA mismatch at one base level.

Therefore, DNA sensors based on SGGTs has been successfully realized by several research groups with the similar sensing mechanism. The interaction between DNA and graphene can induce n-doping in graphene due to the negative charge on the DNA molecules in solution. In addition, many experiments demonstrated the decrease of channel conductance at the Dirac point of a SGGT induced by DNA immobilization or hybridization, indicating that the carrier mobility was decreased by charge scattering from DNA. This effect was also confirmed by Hall effect measurement recently.[37]So the SGGT-based DNA sensors show the performance comparable to that of other types of transistor-based counterparts and better than conventional techniques for DNA analysis accomplished by fluorescence observation. [64]

2.6.3 Protein sensors

Proteins, large biological molecules consisting of one or more chains of amino acids, perform a vast number of functions within living organisms. They are the center of most pathological conditions and have been regarded as most disease biomarkers. Besides the studies of DNA, they are perhaps the subject most intensely researched. Protein sensors have emerged as the most promising platforms for the study of proteins, which will be more and more important in the diagnoses of diseases. [83]Similar to the mentioned DNA sensors in Section 2.3.4., the SGGT-based protein sensors are label free, sensitive, and potentially low cost.

Ohno et al. firstly reported SGGTs for the detection of protein adsorption in electrolytes. [40]The devices were fabricated with mechanically exfoliated pristine single-layer graphene with the channel length of only several micrometers. This device was used for label-free protein detection without any modification on the graphene surface. A negatively charged phosphate serum albumin (BSA) was tested in a phosphate buffer solution with a pH of 6.8. When the adsorption of BSA onto the graphene surface occurred, the conductance of the channel at a fixed gate voltage (−0.1 V) was increased. This change of conductance with BSA concentration was fitted with the Langmuir adsorption isotherm. In this work, the conductance change due to BSA adsorption was quite small, which might be induced by three possible reasons including: 1) the change of electrode-graphene contact resistance; 2) the desorption of

BSA molecules; 3) the relatively small difference between isoelectric point of BSA and the solution pH, which may lead to some uncharged amino acid of BSA molecules.

In another work of Ohno et al., they demonstrated a label- free immunsensor based on an aptamer-modified graphene transistor.[74]Immunoglobulin E (IgE) aptamers were successfully immobilized on a graphene surface, the benefit of using aptamers is that they are smaller than the Debye length of an EDL. This aptamer-modified SGGT × exhibited selective detection of IgE protein to 0.29 × 10−9 M. The drain current was dependent on IgE concentration, due to the reaction between negatively charged IgE aptamers and positively charged IgE protein. By fitting the drain current change with IgE concentration, the dissociation constant was estimated to be 47×10^{-9} M. Meanwhile, nonspecific sensing of BSA and SA protein was also investigated. The results showed that the effects from the nontarget proteins were successfully suppressed in the aptamer-modified SGGTs.

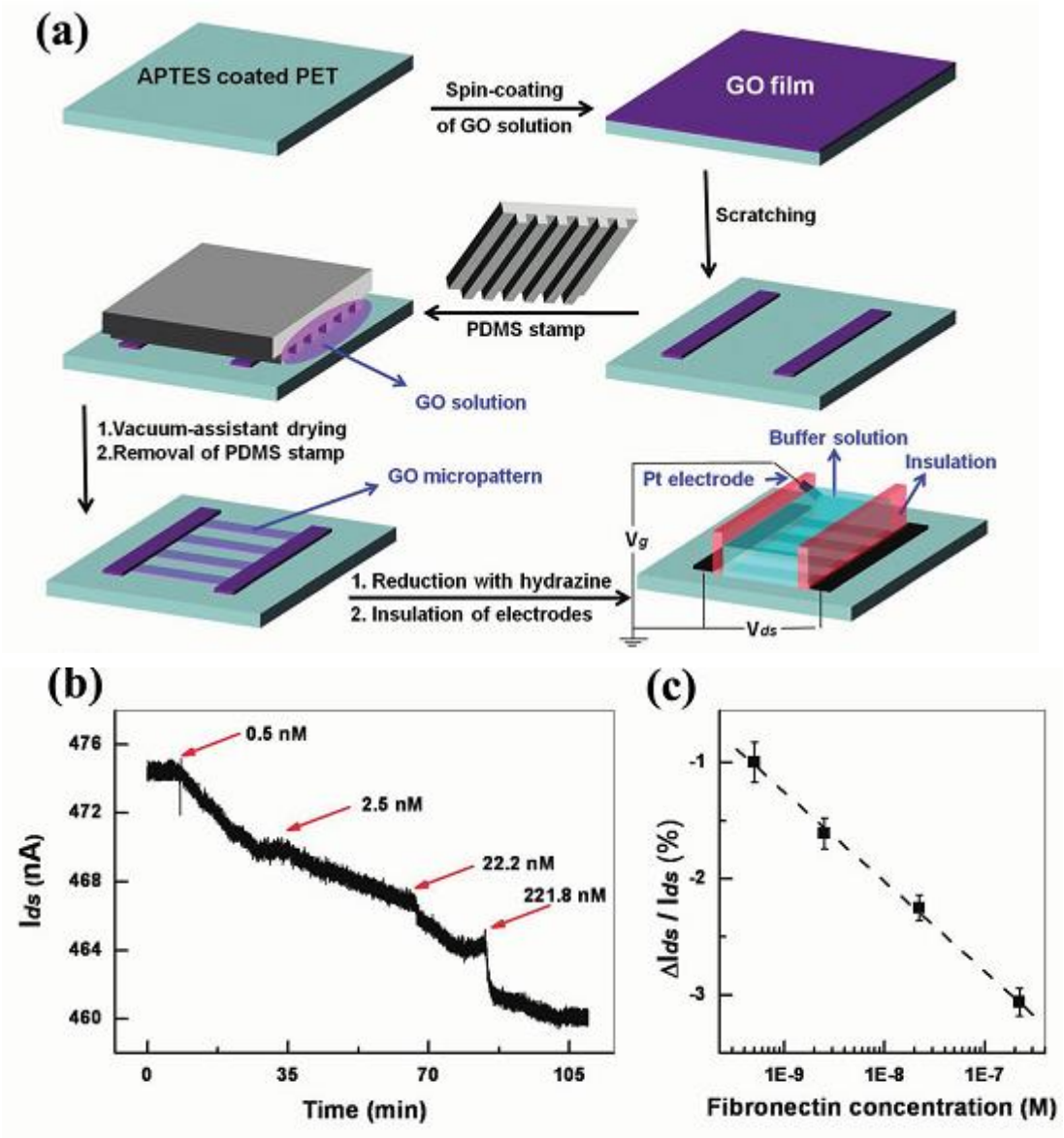

Figure 2.11 a) Schematic illustration for the fabrication of all-rGO SGGT. b) Real-time detection of fi bronection in PBS buffer using the pyrene-functionalized SGGT. c) Channel current changes at different fibronectin concentrations.

He et al. reported the fabrication of transparent, flexible, all rGO-based SGGTs by the combination of solution-processed rGO electrodes with micropatterned rGO channels, as shown in Figure 2.11a, and their applications in detecting proteins. [75] After being functionalized with 1-pyrenebutanoic acid succinimidyl ester (PASE), which served as linker molecules to catch proteins in buffer solution, the device was used to detect fibronectin. The cross-linking of fibronectin onto the functionalized rGO channel resulted in the decrease of channel current. As shown in Figure 2.11b,c, the devices successfully detected the concentration of fibronectin down to 0.5×10^{-9} M with a signal-to-noise ratio of 16. They further linked biotin and coated PEG on the rGO channel to prevent nonspecific binding of proteins, detected the lowest avidin concentration of 80×10^{-9} M through avidin–biotin binding, whereas the introduction of BSA caused no current change. Therefore the all-rGO SGGTs can be used in flexible electronics for biosensors with high sensitivity and selectivity.

Mao et al. reported antibody–antigen protein biosensors based on a thermally reduced GO transistor decorated with Au nanoparticle–antibody conjugates. [26] Probe antibody was labeled on the surface of rGO sheets through the Au nanocrystals to catch target protein. The channel current change induced by protein binding process (Immunoglobulin G/IgG and anti-Immunoglobulin G/anti-IgG) on the device was observed. The detection limit of the protein sensor was about 0.2 ng mL^{-1}, which was among the best of the reported carbon-based protein sensors at that time.

Kim et al. reported rGO-based SGGTs for label-free detection of a prostate cancer biomarker, prostate specific antigen/alantichymotrypsin (PSA–ACT) complex. [76] Immunoreaction of PSA–ACT complexes with PSA monoclonal antibodies on the rGO channel surface caused a linear response in the shift of the gate voltage at Dirac point. The SGGT can detect protein-protein interaction down to femtomolar level (1.1×10^{-15} M) with a dynamic range over 6 orders of magnitude. The ultralow detection limit is very similar to those of the protein sensors based on silicon nanowire transistors and better than those based on carbon nanotube transistors. [84, 85] This sensor showed a high specificity to other cancer biomarker in both the phosphate-buffered saline solutions as well as in the human serum.

2.6.4 Glucose sensors, neurotransmitter sensors and others

Glucose is an indispensable part of metabolic activities. Glucose sensing is important to human health, especially in the diagnosis of diabetes mellitus. [86, 87] Currently, glucose biosensors account for about 85% of the entire biosensor market. Electrochemical glucose sensors have been studied for more than 50 years.[87] Recently, glucose sensors based on SGGTs have been reported by several groups.

Huang et al. demonstrated the use of CVD-grown graphene film in SGGTs for real-time biomolecular sensing.[28] Glucose or glutamate molecules were detected by measuring the conductance change of the graphene channel because the molecules can be oxidized by the specify redox enzyme (glucose oxidase (GOD) or glutamic

dehydrogenase) functionalized onto the graphene film. The detection limits of the glucose sensor (0.1×10^{-3} M) and glutamate sensor (5×10^{-3} M) are comparable to the commonly used electrochemical sensors, yet inferior to some electrochemical sensors integrated with functional nanomaterials. Kwak et al. reported a flexible glucose SGGT sensor using CVD-grown graphene on a PET flexible substrate.[106] The graphene surface was functionalized with linker molecules (PASE) in purpose of better immobilizing GOD enzyme that induce the catalytic response of glucose. By measuring the Dirac point shift and drain-source current variation, the SGGT sensor could detect gluose levels in the range of $3.3–10.9 \times 10^{-3}$ M. In addition, the SGGTs could provide continuous real-time monitoring. However, the detection limit of the above glucose sensors are much worse than other types of transistor-based glucose sensors reported before.[86] Therefore, further work is needed to improve the performance of SGGT-based glucose sensors.

Dopamine, a neurotransmitter produced in brain, plays an important role in the regulation of neuronal transmission and is related to many diseases such as Parkinson's and schizophrenia. [88] Normal level dopamine in human plasma is quite low, only around several 10^{-9} M. [89]Thus, it is necessary to find dopamine sensors with low detection limit and high sensitivity. He et al. described the fabrication of SGGTs by large-scale direct patterning of rGO on flexible substrate. [75] As a proof of concept, the SGGTs were used for sensing both the manually titrated dopamine in the concentration region of $1–60 \times 10^{-3}$ M and the vescular released catecholamines

from living meuroendocrine PC12 cells. Although, the device only showed the detection limit to dopamine at 10^{-3} M level, which is much worse than that of other transistor-based dopamine sensors,[88] the methodology demonstrated by them indicated the potential use of SGGTs in neurochemistry measurement. Further work is needed to optimize the performance of the devices.

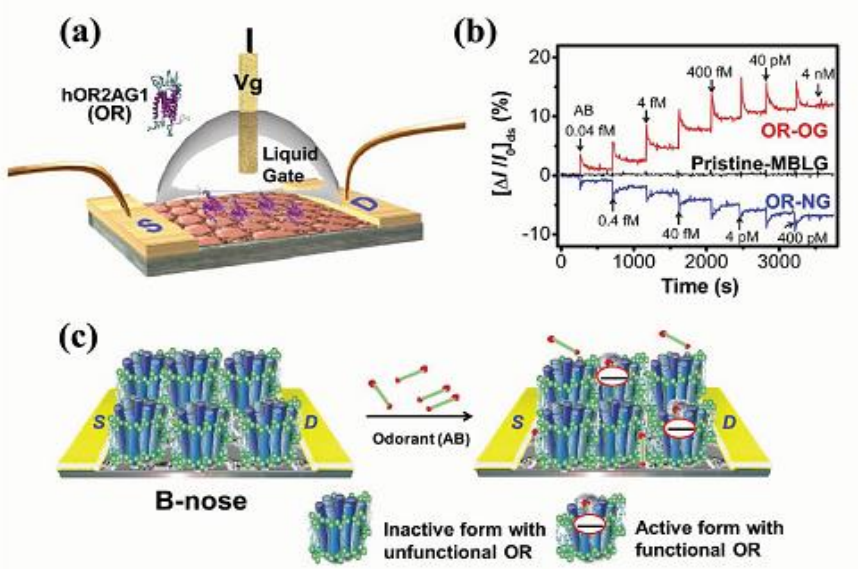

Figure 2.12 a) Schematic diagram of a B-nose based on a SGGT with OR-modifi ed bilayer graphene (MBLG). b) Real-time responses of SGGT B-noses based on OR-conjugated oxygen plasma-treated graphene (OR-OG) and ammonia plasma-treated graphene (OR-NG) measured at V_{DS}=10 mV (V_G =0 V) to different AB concentrations (0.04×10^{-15} to 4×10^{-9} M). Pristine MBLG without OR was a control sample. c) Schematic for plausible binding mechanism of B-nose through active and inactive OR forms. The addition of odorant (AB) leads to the active form with functional OR with negative charges. [77]

Recently, Park et al. reported flexible ultrasensitive bioelectronic nose (B-nose) based on SGGTs, [77] in which graphene was conjugated with human olfactory receptors 2AG1 (hOR2AG1: OR). As shown in Figure 2.12, the ORs can selectively bind to the particular odorant amyl butyrate (AB), so the device can detect AB with unprecedented sensitivity and good selectivity. The minimum detection limit was as low as 0.04 × 10−15 M, which was 2–5 orders of magnitude more sensitive than other odorant sensors reported before.[90] In addition, the B-noses were stable for more than 10 d and showed excellent bending stability. Therefore, this methodology offers a new direction for the highly sensitive and selective recognition of odorants and could be expanded to a broader range of applications in flexible and wearable electronics.

2.7 Measurements and characterizations

In this thesis, several equipments are used for device measurements and materials characterizations, including semiconductor parameter analyzer (4156C, Agilent Technology), general model sourcemeter (Keithley, 2400), electrochemical workstation (Princeton Co. Ltd), atomic force microscopy (Digital Instruments, nanoscope 3100), Raman spectroscopy, etc.

2.7.1 Semiconductor parameter analyzer and general model source meter

Two Keithley 2400 general model sourcemeters are connected and cooperated to measure the transfer characteristic of SGGT devices in chapter 3, 5. The equipments

are controlled by Labview program. The setup devices are also used for real time channel current monitoring in chapter 3, 5.

Semiconductor parameter analyzer (4156C, Agilent Technology) is used to measure the transfer curve (I_{DS} vs V_G) and real time channel current of the SGGTs fabricated in chapter 4 (I_{DS} vs time).

2.7.2 Electrochemical workstation

Electrochemical workstation (Princeton Co. Ltd and EG&G PAR 2273) is used to measure the cyclic voltemmetry as well as the potential step of Pt electrodes, graphene electrodes in chapter 3. Also, the electrochemical workstation is used to measure the cyclic voltemmetry of graphene electrode and PtNP/graphene electrode in chapter 4.

2.7.3 Atomic Force Microscopy

The atomic force microscopy is used to characterize the morphology and roughness of the CVD-grown graphene adopted in chapter 3, chapter 4, and chapter 5. The type of the AFM used is NanoScope 8 (Digital Instruments Ltd. Co.). The materials are characterized by tapping mode in all the research, because tapping mode have the least influence to the surfaces. The surface morphology of the graphene film after wet transferring procedure in chapter 3 and chapter 5 is characterized and shown in Figure 2.13. As exhibited on the figure, graphene film have little roughness (~0.39 nm) after transfering to Si/SiO_2 substrate. Meanwhile, the CVD graphene film and CVD

graphene modified with PtNPs used in chapter 4 is characterized and shown in Figure 4.2 (a, b).

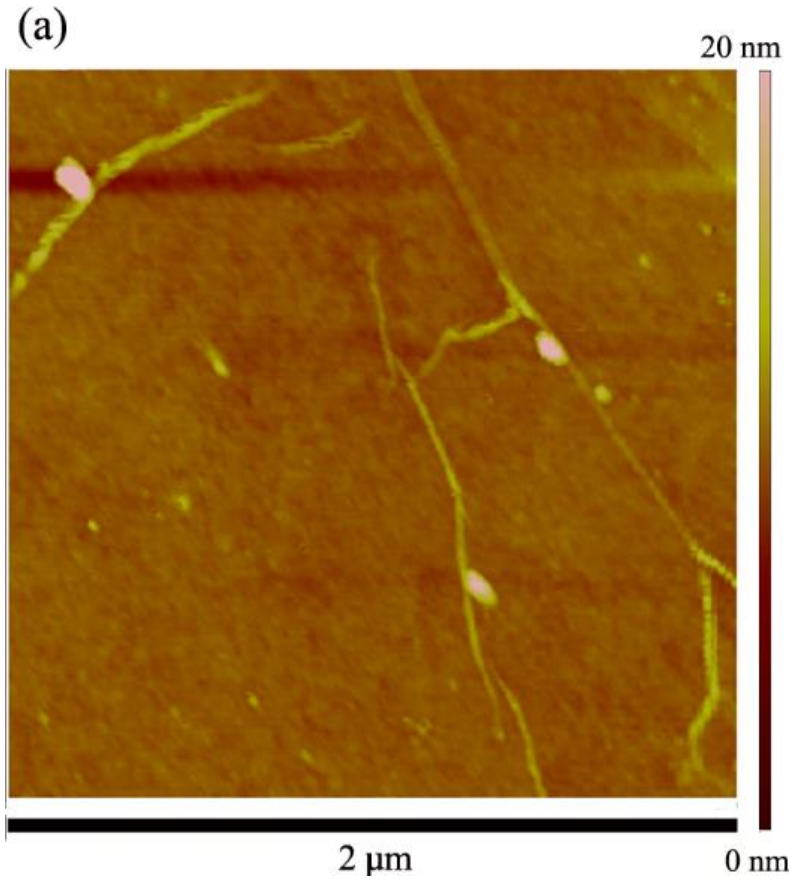

Figure 2.13 AFM image of a single-layer graphene film (roughness (rms): 0.39 nm).

2.7.4 Raman spectroscopy

In chapter 3, 4, 5, Raman spectra of the CVD-grown graphene after wet transferring working flow are measured to examine the material quality. The type of the equipment used is Horiba Jobin Yvon LabRAM HR800 Raman spectrometer (Horiba Jobin Yvon Ltd. Co.) A laser excitation source with 488 nm wavelength were used for material

characterization. The CVD graphene film used in chapter 3, 4, and 5 was characterized under the Raman spectroscopy, as shown in figure 2. 14. Characteristic G band (1592.3 cm^{-1}), D (1356 cm^{-1}) band and 2D band (2702.5 cm^{-1}) were observed in Raman spectrum [142], indicated CVD-grown graphene film has 2-D nanocarbon structure. [143].

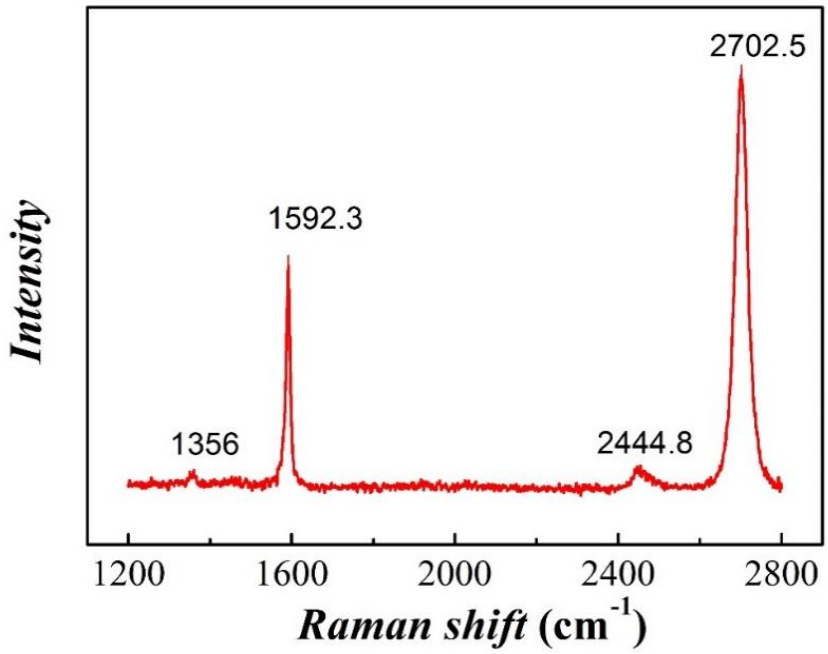

Figure 2.14 Raman spectrum of a single layer graphene on SiO_2/Si.

2.8 Summary

Graphene, the 2D material with high carrier mobilities, excellent mechanical flexibility, and good chemistry stability, has been viewed as one of the most promising materials for the fabrication of rapid, highly sensitive, and low-cost chemical and biological sensors. Viable approaches for synthesizing high-quality and low-cost

graphene have been developed very fast in the past few years, which paved the way for the development of many different graphene-based sensors. SGGTs have been successfully used in various types of chemical or biological sensors, including pH, ion, glucose, DNA, cell, bacterial, and protein sensors. Compared with conventional counterparts, the SGGT-based sensors are more sensitive in many applications due to the strong interactions between analytes and graphene or the high transconductance of the devices for the high carrier mobilities. Some reported sensors exhibited outstanding performance and great potential for many important applications, such as single-molecule detection or single-cell monitoring.[86] However, these techniques are still far from real applications due to the difficulties in fabricating devices with good uniformity and reproducibility. Moreover, the complicated interactions between graphene and organic or inorganic materials may lead to uncertainties in the future applications.

Therefore, challenges still exist and more effort needs to be paid on the following aspects of this field. Firstly, specific detection of the chemical or biological sensors are of critical importance to their practical applications. The reported devices are normally tested in strictly controlled conditions while many interference factors widely existing in real environment have not been considered. So, the selectivity and stability of the SGGT-based sensors need to be characterized and optimized. Secondly, miniaturization and functionalization of SGGTs should be investigated to facilitate the fabrication of SGGT arrays that can be used in multifunctional microchips for highly

sensitive, selective, and high-throughput sensing. One advantage of using the transistor-based sensors is the feasibility for miniaturization and multiplexing. Some conventional micro fabrication techniques, such as metal deposition, photolithography, and so on, can be used in the fabrication of device arrays, whereas some key techniques for graphene transfer, interface treatment, and surface modification should be developed SGGT-based sensors are more sensitive in many applications due to the strong interactions between analytes and graphene or the high transconductance of the devices for the high carrier mobilities. Some reported sensors exhibited outstanding performance and great potential for many important applications, such as single-molecule detection or single-cell monitoring.[86] However, these techniques are still far from real applications due to the difficulties in fabricating devices with good uniformity and reproducibility. Moreover, the complicated interactions between graphene and organic or inorganic materials may lead to uncertainties in the future applications.

Chapter 3 High Performance Dopamine Sensors Based on Whole Graphene Solution-Gated Transistors

Neurotransmitters are endogenous chemicals that transmit signals across a synapse from one neuron to the target neuron. Precise detection the concentration of neurotranmitter in body fluids have obviously importance for clinical applications. [91]In the chapter 3, I will fabricate a whole graphene solution-gated transistors for highly senstive and selective sensing of one type of neurotransmitters - dopamine.

3.1 Introduction

Dopamine being a neurotransmitter has been extensively studied since 1950s.[92]. Because dopamine plays an important role in the functions of central nervous system, renal, hormonal, and cardiovascular system, etc., [93, 94] abnormal dopaminergic neuron process may lead to various neurological diseases. [95] Therefore, rapid detection of dopamine in biological system is very important for the routine analysis and diagnosis of neurological disorders[96].Various analytical methods for measuring dopamine, including high performance liquid chromatography (HPLC) [97], mass spectroscopy[98], electrochemical detection, [99, 100] and transistor-based sensing, [37] have been developed. However, these methods have some limitations in practical

applications. HPLC and mass spectroscopy are not suitable for portable and low-cost analytical measurement. Electrochemical analytical technique for dopamine determination is an attractive method due to low cost, easy operation and fast response while the detection limit is relatively high (normally ~ 1 μM). [54, 101] Si nanowire transistors showed ultrahigh sensitivity to dopamine being attributed to their small size and large surface-to-volume ratio while the selectivity of the devices was not characterized [37]. Actually, graphene shows higher surface-to-volume ratio than Si nanowires.As mentioned in chapter 2, He *et al.* firstly reported dopamine sensors based on SGGTs[75]. The sensing mechanism of the device is attributed to the π-π interaction between dopamine and graphene channel. Unfortunately, the devices showed the detection limit of only about 1mM, which is much worse than typical analytical techniques and the Si nanowire transistors.

In this chapter, we present a whole-graphene SGGT-based dopamine sensor with a novel sensing mechanism. [75] The gate electrodes used in SGGTs reported before are Ag/AgCl electrodes or metal wires[20, 28, 30, 40, 45, 68, 75, 102]. Considering graphene being a semimetal with zero bandgap, [29, 82] we fabricated SGGTs with graphene as both channel and gate electrodes for the first time. So the device is mainly made of graphene, which is potentially low-cost and convenient for high-density integration. The device shows stable performance, high sensitivity and the low detection limit down to 1nM to dopamine, which is sensitive enough for characterizing dopamine levels in many biological systems. [89]We also find that conventional

electrochemical measurements with the same graphene electrode only show the detection limit to dopamine of ~3 μM , which further indicates the advantage of using SGGTs in biosensors. The selectivity of the dopamine sensor is improved by modifying the gate electrode with the biocompatible polymer Nafion. [103] The sensing mechanism can be attributed to the electrochemical reaction of dopamine at the gate electrode, which leads to the change of effective gate voltage applied on the transistor. [20] It indicates that the SGGTs with suitable surface modification on the graphene gate electrode can be used as many other types of biosensors with high sensitivity.

3.2 Fabrication of device

3.2.1 Preparation of SGGTs

The device design is shown in Figure 3.1a. Source, drain and gate Cr/Au electrodes were deposited on glass substrates by thermal evaporation through a shadow mask. Single-layer graphene was synthesized on copper foils by CVD method, as shown in Figure 3.2 [20, 29] A thin poly(methyl methacrylate) (PMMA) film (~500nm) was spin coated on graphene and then annealed at about 100^{o}C for 30 min. Then, it was immersed in an aqueous solution of iron chloride to etch the Cu substrate and washed by distilled water. The graphene/PMMA film was then transferred on the target substrate with Cr/Au electrodes. The PMMA layer was dissolved and removed from graphene by toluene. The graphene layer was then patterned on the susbtrates. The

patterning procedures were described in Figure 3.3. [20] In the end, the Au electrodes were packaged with silicone layer.

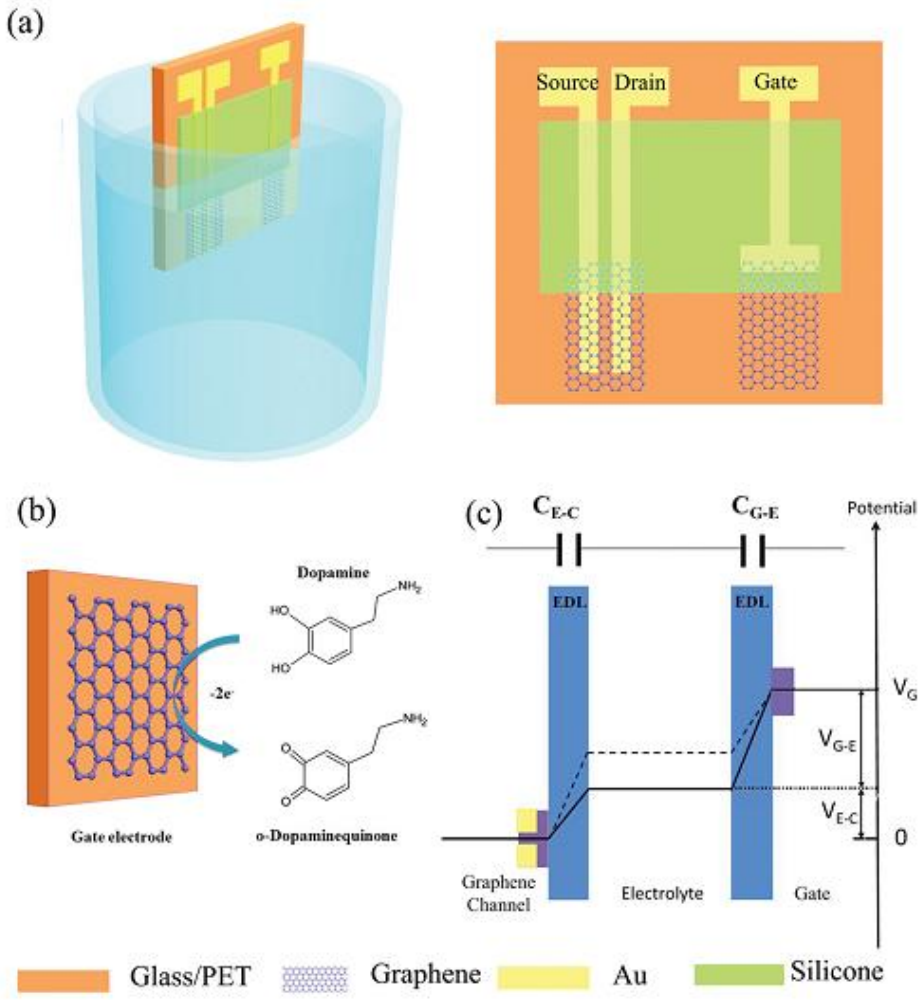

Figure 3.1 a) Schematic diagram of a SGGT with graphene channel and a graphene gate electrode characterized in electrolyte. b) Electrochemical reaction of dopamine on the graphene gate electrode. c) Potential distribution between the gate and the channel of a SGGT in electrolyte.

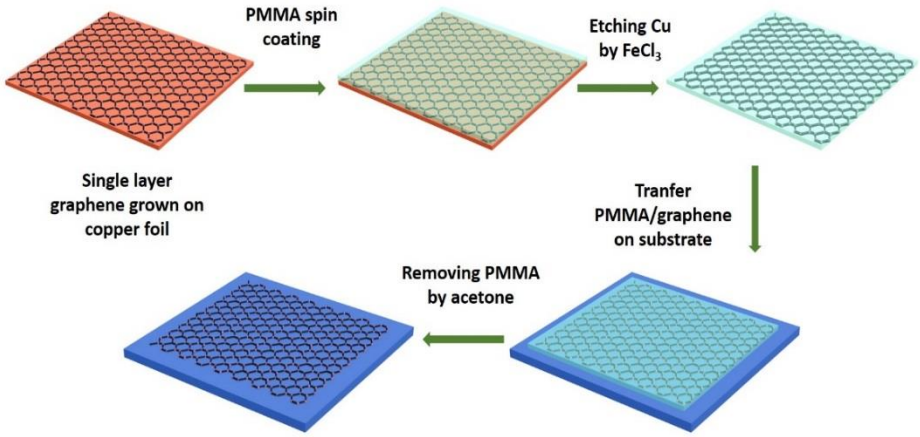

Figure 3.2 procedures of graphene wet tranferring. i. PMMA spin coating; ii.etching copper foil with $FeCl_3$ solution; iii. Transfer PMMA/graphene film on substrate; iv. Romoving PMMA by acetone.

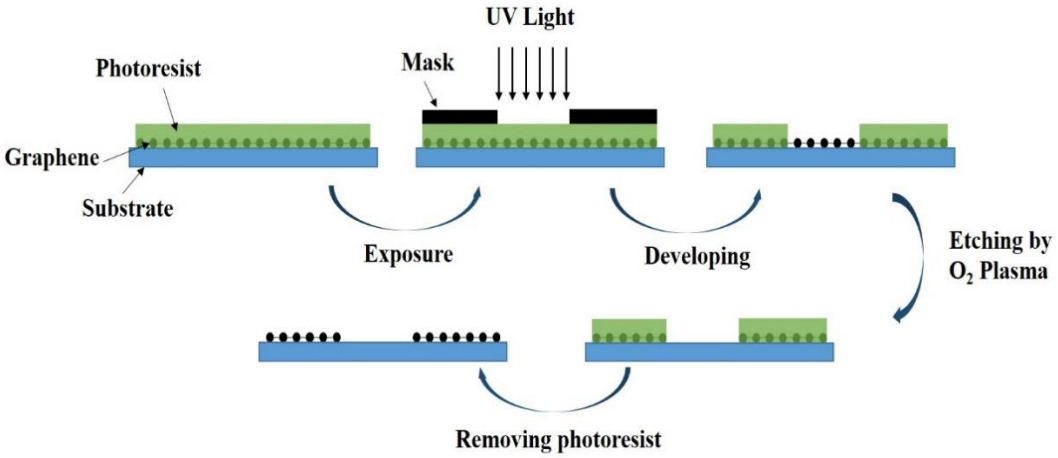

Figure 3.3 Photolithography procedures. i. spin-coating; ii. Exposure by UV light; iii. Developing; iv. Etching by O_2 plasma; v. removing photoresist.

Nafion® solution (5% in a mixture of lower aliphatic alcohols and water) was purchased from Sigma-Aldrich Company. The solution was mixed with 2-propanol with volume ratio 1:1. For the SGGTs with Nafion modified on the gate electrode, 5 μL of the mixture was drop coated onto graphene gate electrode and kept at 4°C for 4h to get solvent completely evaporated. The formed Nafion film was rinsed by DI water and dried for future use.

3.3 Electrical characterization

3.3.1Device Characterization

Before measurements, all of the as-prepared electrodes were immersed in PBS (pH 7.4) for 15 min to remove the residual. The SGGTs were tested at a fixed V_D = 0.05 V at different gate voltages (V_G: 0 ~ 0.8 V) and PBS was used as the electrolyte for all measurements. The device performance, including transfer curves (I_{DS} vs V_G) and time-dependent channel currents (I_{DS} vs time) , was characterized by using two Keithley 2400 source meters controlled by a computer with a Labview program.

3.3.2 Electrochemical measurements

Additionally, EG&G PAR2273 Potentiostats-Electrochemistry Workstation was used to characterize the electrochemical properties of the different gate electrodes. The electrochemical responses of the graphene or Pt electrodes to dopamine in PBS solutions were investigated by cyclic voltammetry (CV) with a scan rate of 50mV/s.

Amperometric measurement of a graphene electrode was carried out in a stirred PBS solution by adding dopamine with different concentrations. The applied potential is fixed (+0.7 V) relative to an Ag/AgCl reference electrode.

3.4 Dopamine detection by SGGTs

3.4.1 Using pure graphene electrode as gate

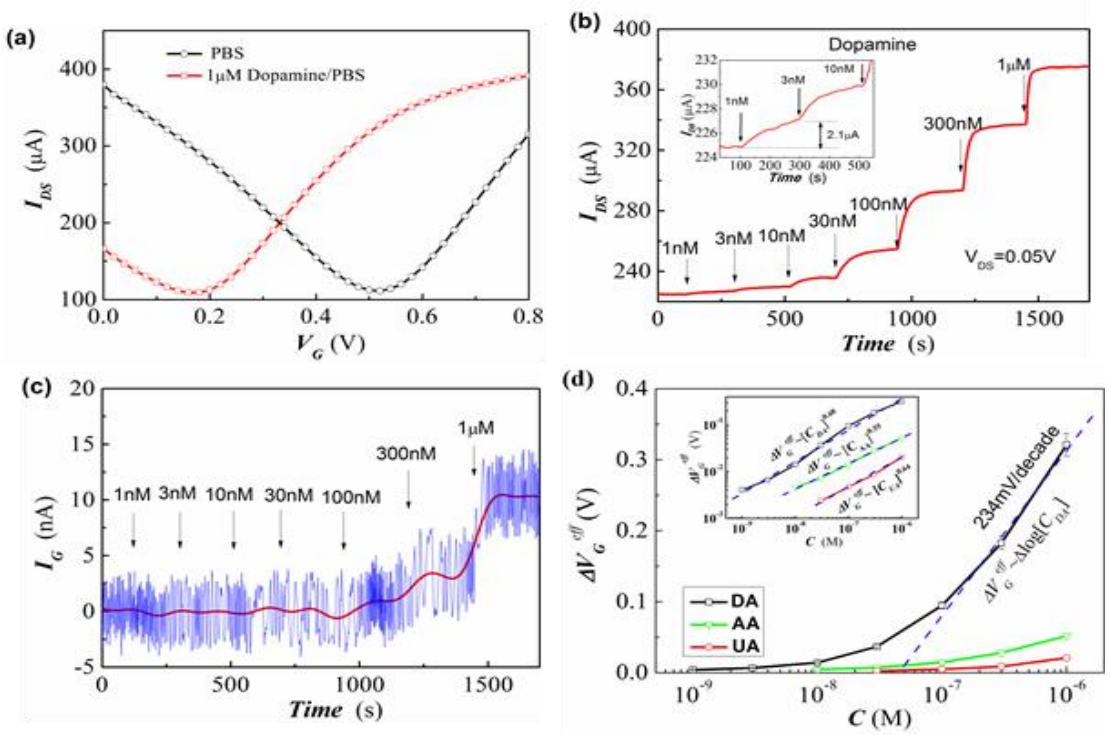

Figure 3.4 a) Transfer characteristics (I_{DS} vs. V_G, V_{DS} = 0.05V) of a SGGT measured in PBS solution (pH = 7.4) before and after the addition of dopamine with the concentration of 1μM. b) Channel current response of the SGGT to additions of dopamine with different concentrations. V_{DS} = 0.05V, V_G = 0.7V. c) Gate current of

the SGGT during the additions of dopamine with different concentrations. Blue curve: measured gate current. Red curve: average current. d) The change of effective gate voltage (ΔV_G^{eff}) as functions of the concentrations of dopamine (DA), ascorbic acid (AA) and uric acid (UA). Inset: the results fitted with Equation (3.8).

Figure 3.4a shows the transfer characteristic (I_{DS} versus V_G) of a SGGT with V_{DS} = 0.05V. The device shows a typical ambipolar behavior with the Dirac point at about 0.4V~0.5V. It is reasonable to find the positive voltage of the Dirac point because graphene is p-type doped in air and water. Then the device was characterized in 1μM dopamine PBS solution at the same voltages. It is interesting to find that the transfer curve shows a horizontal shift of about 0.3V to lower gate voltage. To better understand the effect, we fabricated another SGGT device with an Ag/AgCl (sat. KCl) gate electrode (control sample) and characterized it in PBS solution before and after the additions of 1μM and 10μM dopamine. However, the control device showed little change after the addition of dopamine as shown in Figure 3.5.

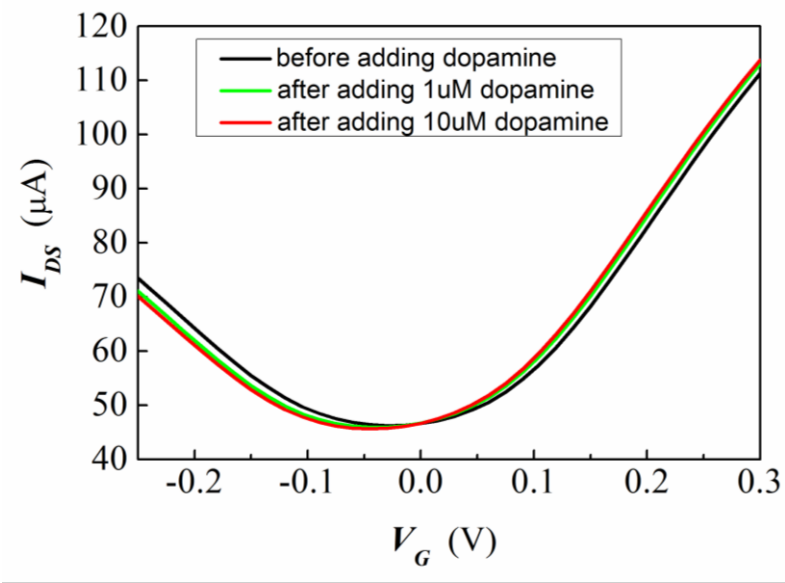

Figure 3.5 Transfer characteristics of a SGGT with an Ag/AgCl gate electrode measured in PBS solution before and after the additions of dopamine with the concentrations of 1μM and 10μM.

So the response of the device with graphene gate electrode was due to the electrochemical reaction of dopamine at the gate as shown in Figure 3.1b. Because the transfer curve of the device was characterized at positive gate voltages, the graphene gate can be regarded as an anode. So dopamine is electro-oxidized to *o*-dopaminequinone at the surface of the gate and generates faradic current. [13, 79, 86, 104, 105] To confirm the electrochemical reaction of dopamine, the graphene gate electrode was characterized in 1mM dopamine PBS solution by cyclic voltammetry (CV) measurements. A redox peak current at about 0.65 V vs. Ag/AgCl was observed

as shown in Figure 3.6, which corresponds to the electro-oxidation of dopamine at the graphene electrode.

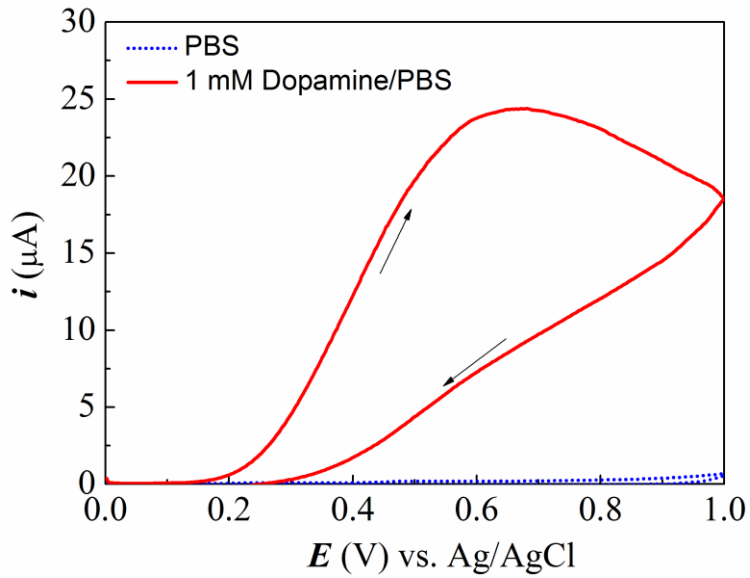

Figure 3.6 The Cyclic Voltammograms (CV) of a graphene gate electrode measured in blank and 1 mM dopamine PBS solutions. CV scan rate: 50 mV s^{-1}.

In blank PBS solution, the potential drop between the gate and the channel under a gate voltage V_G is shown as the solid lines in Figure 3.1c. The gate voltage was actually applied on the gate/electrolyte and electrolyte/channel interfaces. [65] Assuming $V_{G\text{-}E}$ and $V_{E\text{-}C}$ are the voltages applied on the gate/electrolyte and electrolyte/channel interfaces, respectively, the gate voltage applied on the transistor is given by: $V_G = V_{G-E} + V_{E-C}$. Similar to the equivalent circuit in other solution-gated transistors,

[13, 79, 86, 104, 105] the two interfaces can be regarded as two capacitors and thus the gate voltage is given by:

$$V_G = (\frac{C_{E-C}}{C_{G-E}} + 1)V_{E-C} = (\gamma + 1)V_{E-C}, \qquad (3.1)$$

where $\gamma = \frac{C_{E-C}}{C_{G-E}}$, $C_{G\text{-}E}$ and $C_{E\text{-}C}$ are the capacitances of the electrolyte/gate and electrolyte/channel interfaces, respectively. [106, 107] Each interface capacitance contains the two series connected capacitors, including electric double layer capacitance and graphene quantum capacitance. [32, 33] The capacitance of an electric double layer (10 to 40 μF/cm^2) is dependent on the ion concentrations in the electrolyte and the applied bias voltage. [32] The quantum capacitance of graphene is between zero to tens of μF/cm^2, which is lower than or comparable to double-layer capacitance. [33]

After the addition of dopamine, the electrochemical reaction of dopamine at the gate electrode decreases the potential drop at the electrolyte/gate interface because of the faradic current. Consequently, the voltage applied on the electrolyte/channel interface is increased, as indicated by the dash line in Figure 1c, which leads to the increase of the effective gate voltage applied on the transistor and the shift of the transfer curve of the SGGT to a lower gate voltage.

In sensing applications, it is more convenient to measure the channel current response of the SGGT at fixed gate and drain voltages. [20] Figure 3.4b shows the response of

the channel current (V_{DS}=0.05V and V_G=0.7V) to different concentrations of dopamine. According to the I-V curve that when V_G=0.7V, it has the largest slope, it is predicable that the device would have the largest amplification effect. It is notable that the device can measure dopamine concentrations down to 1nM (signal/noise ratio >3). Some devices even show the detection limit down to 0.1nM as shown in Figure 3.7.

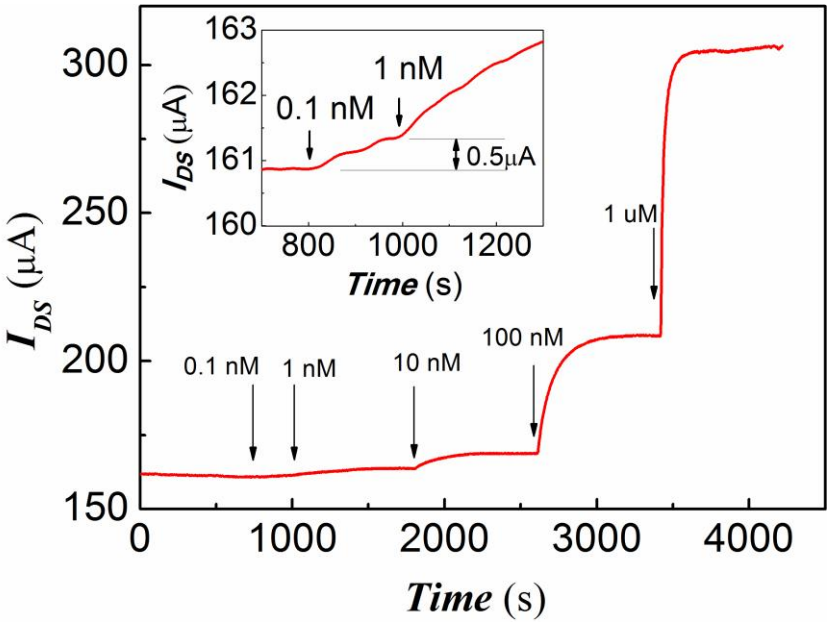

Figure 3.7. Current response of a whole-graphene SGGT to additions of dopamine with concentrations changed from 0.1nM to 1 μM.

On the other hand, as shown in Fig. 3.4c, the gate leakage current measured simultaneously is only about 10 nA, which is four orders of magnitude lower than the channel current of the device. So the channel current response is different from the

faradic current due to dopamine reaction at the gate electrode, indicating that the SGGT-based dopamine sensor has a different working principle from the typical electrochemical methods. [99, 100]

The voltage applied on the electrolyte/gate interface $V_{E\text{-}G}$ is given by the Nernst equation and an overpotential due to the faradic current: [32]

$$V_{E-G} = E_0 + \eta - 2.30\frac{kT}{ne}\log C_{DA}, \qquad (3.2)$$

where E_0 is a constant; k is the Boltzmann's constant; T is temperature, e is electron charge; n (=2) is the number of electrons transferred during the electro-oxidation of dopamine; C_{DA} is the concentration of dopamine in the PBS solution, η is the overpotential on the gate related to the faradic current. So the voltage applied on the electrolyte/channel interface is:

$$V_{E-C} = V_G - V_{E-G} = V_G - E_0 - \eta + 2.30\frac{kT}{ne}\log C_{DA}. \qquad (3.3)$$

In the above experiments, the gate voltage (V_G) applied on the transistor is constant. So the increase of channel current can be regarded as the increase of the effective gate voltage V_G^{eff} applied on the transistor. According to equation (3.1), we assume $V_G^{eff} = (\gamma + 1)V_{E-C}$ and thus the effective gate voltage corresponding to a channel current can be decided from the transfer curve of the WGSGT characterized in blank

PBS solution. The increase of $V_{E\text{-}C}$ will lead to the increase of effective gate voltage V_G^{eff} given by:

$$V_G^{eff} = 2.30(\gamma+1)\frac{kT}{ne}\log C_{DA} - (\gamma+1)\eta + \text{constant}. \qquad (3.4)$$

Considering the SGGT being a potentiometric transducer that has very low faradic current at the gate as show in Figure 3.4c, the overpotential η is very low[32], which is similar to other types of transistor-based biosensors. The relationship between the faradic current density j and the overpotential η at low current is given by Butler-Volmer equation: [32]

$$j = j_0(e^{-\alpha ne\eta/kT} - e^{(1-\alpha)ne\eta/kT}), \qquad (3.5)$$

where j_0 is the exchange current density; α is called standard rate constant, which is normally between 0.3 and 0.7. Figure 3.4c shows that the faradic current on the gate (area: 0.9 cm^2) is about 10 nA when dopamine concentration is 1 μM, so the current density is about 1×10^{-7} A/cm^2. The exchange current is given by: [32]

$$j_0 = nFk^0C, \qquad (3.6)$$

where C is the dopamine concentration, k^0 is the standard rate constant, $F = 9.63\times10^4$ C/mole. k^0 was measured to be 1.34×10^{-3} cm s^{-1} (Figure 3.9).

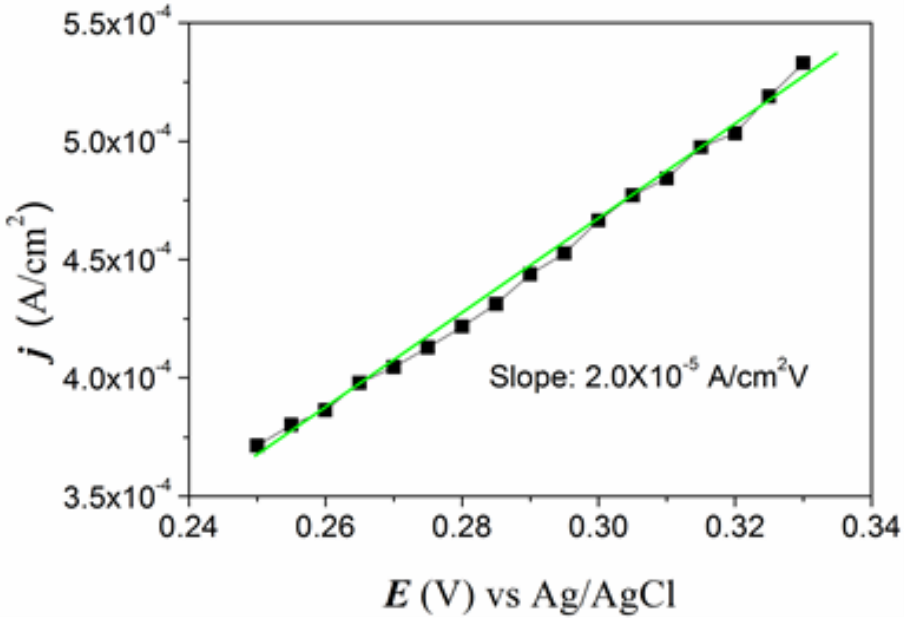

Figure 3.8. Plot of initial polarized current density *j* against potential *E* obtained from a series of potential step measurements of a graphene electrode in PBS solution containing 0.1mM dopamine.

So the exchange current is $j_0 \approx 2.6\times10^{-7}$A/cm^2 when dopamine concentration is 1 μM[32, 108]. Assuming $\alpha = 0.5$, the overpotential is estimated to be about $\eta \approx 5$ mV, which is negligible compared with the effective gate voltage change (~300 mV). So the effective gate voltage can be approximately given by:

$$V_G^{eff} \approx 2.30(\gamma+1)\frac{kT}{ne}\log C_{DA} + \text{constant}, \qquad (3.7)$$

Figure 3.4d shows the change of effective gate voltage ΔV_G^{eff} as a function of dopamine concentration C_{DA}. Equation (3.7) can be used to fit the curve when dopamine concentration is higher than 0.1μM. However, the curve in the lower concentration region cannot be fitted with this equation for the very weak reaction of dopamine on the graphene gate.

As shown in the inset of Figure 3.3d, we find that the relationship can be fitted very well with the following equation:

$$\Delta V_G^{eff} = AC_{DA}{}^{\alpha}, \qquad (3.8)$$

where A and α are constants. Such power function has been successfully used in many other transistor-based sensors such as photo sensitive transistors, although it is difficult to be derived analytically. [82, 109-111]

In practical dopamine analysis, the main interference comes from ascorbic acid (AA), uric acid (UA), ions and glucose. [112, 113] The device did not show any response to glucose when the concentration of glucose was increased up to 10 mM. Regarding the interference from ions, the SGGT with high quality graphene is not sensitive to ion concentrations as reported in our previous paper. [20] On the other hand, the ion concentrations in body fluids are relatively stable. For example, sodium ion (Na^+) is the major cation in plasma and its concentration is finely maintained within the narrow range of 135-145 mM (less than 10% variation) despite great variations in water and

salt intake of human beings[114]. Our device characterized in NaCl aqueous solutions with the concentrations of 100mM and 300mM shows very little difference in the transfer curves although the ion concentration is increased for 200%. Furthermore, as mentioned in chapter 2 some studies found that only in special conditions SGGTs devices is sensitive to pH changes, so that the influence of pH value is not been viewed as main interferences in this chapter.

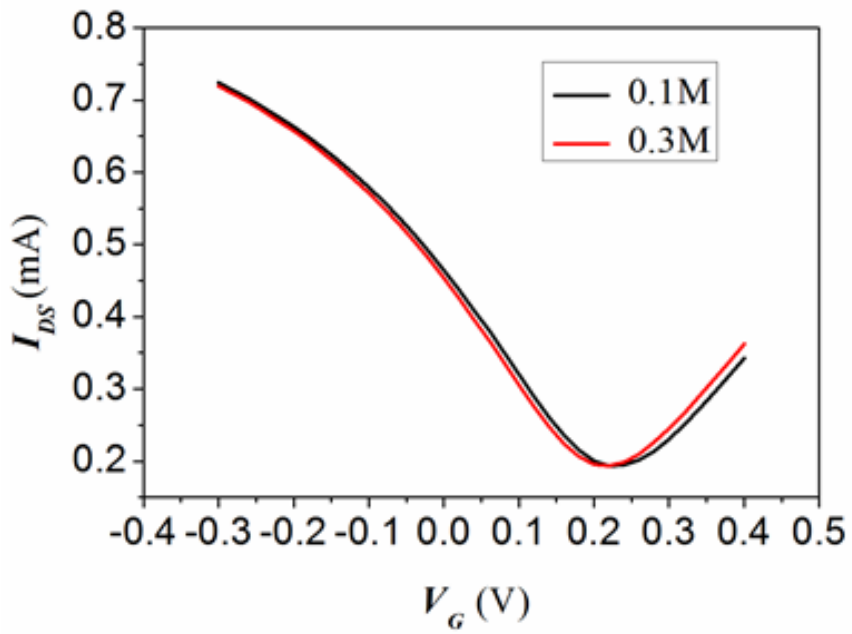

Figure 3.9. Transfer characteristics of a SGGT measured in NaCl aqueous solutions with the concentrations of 100 mM and 300 mM. V_{DS}=0.05V.

It is easy to understand this result. First, even if some SGGTs are sensitive to ion concentrations because of the impurities on the surface of graphene, the shift of transfer curve is normally less than the ideal value given by Nernst equation (59mV

per decade for Na^+). In body fluids, the ion concentrations are relatively stable. It can be estimated that 10% change of ion concentration in body fluid will lead to less than 1mV shift of the transfer curve, which is negligible in the measurements. The second factor is the change of double layer capacitance induced by the change of ion concentrations on the surface of graphene, which can induce slope changes of the transfer curves. It can be found that this effect is negligible in practical applications as shown in Figure 3.9. Therefore, the influence of ion concentrations in practical applications of the SGGT is negligible. [114]

So the selectivity of the device was characterized by adding AA and UA in PBS solution as shown in Figure 3.10.

The detection limits to AA and UA are 10nM and 30nM, respectively. The changes of effective gate voltage as functions of the analyte concentrations are shown in Figure 3.3d. The responses of the SGGT to AA and UA can be attributed to the direct electro-oxidation of AA and UA on the graphene gate electrode. The curves for AA and UA can be fitted with the functions similar to equation (3.7). So the sensitivities of the SGGT to AA and UA are about 1 and 2 orders of magnitude lower than that to dopamine, respectively. However, the concentration of AA is normally two orders of magnitude higher than that of dopamine in human body fluids (e.g. plasma, urine, etc), which severely restricts the effective dopamine determination by using the SGGT.

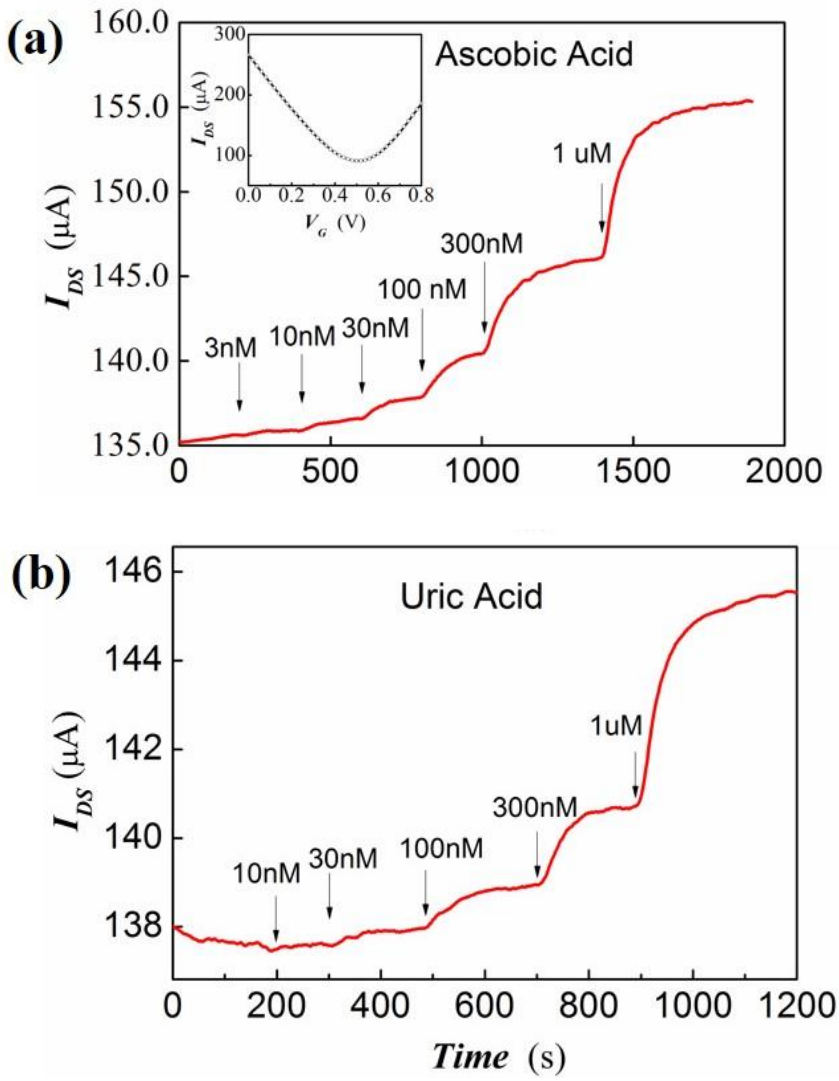

Figure 3.10 a) Current response of a whole-graphene SGGT to additions of AA. V_{DS}=0.05V, V_G=0.7V. Inset: Transfer characteristics (I_{DS} vs. V_G, V_{DS}=0.05V) of the SGGT measured in PBS solution (pH =7.4). b) Current response of a whole-graphene SGGT to additions of UA. V_{DS}=0.05V, V_G=0.7V.

To improve the selectivity of SGGTs to dopamine, the graphene gate electrode was modified with a biocompatible polymer Nafion, which has been used to modify

electrodes in biosensors. Because Nafion is negatively charged in PBS (pH = 7.4) solution, it could effectively alleviate the interference from other substances in negatively charged states, e.g. UA and AA, by electrostatic interaction. Figure 3.4a-c shows the channel current response of the SGGT to additions of dopamine, AA and UA, respectively. The device exhibited detection limits of 1nM to dopamine, 1μM to AA and 10 μM to UA, indicating the improved selectivity of the device to dopamine. The induced changes of effective gate voltages were calculated and shown in Figure 3.4d. The voltage change of the device to dopamine can be fitted very well with Equation (8) down to 5nM as shown in the inset of Figure 3.4d. The sensitivities of the device to AA and UA are about 3 and 4 orders of magnitude lower than that to dopamine, respectively. So the selectivity of the SGGTs to dopamine was dramatically improved by the Nafion modification on the gate electrodes.

We found that the SGGT with a graphene gate electrode is even better than a device with a Pt gate electrode in sensing dopamine although Pt electrodes have been popularly used in the electrochemical detections of dopamine. [88] A SGGT with a Pt gate electrode (size: 3mm×3mm) was characterized in PBS solution. Figure 3.11a shows the transfer curve of the device before and after the addition of 1 μM dopamine in PBS solution, which shifts for about 70mV to lower gate voltage induced by dopamine. Figure 3.11b shows the current responses of the SGGT to additions of dopamine with different concentrations. The device exhibits a detection limit of ~10nM, which is not as good as the device with the graphene gate.

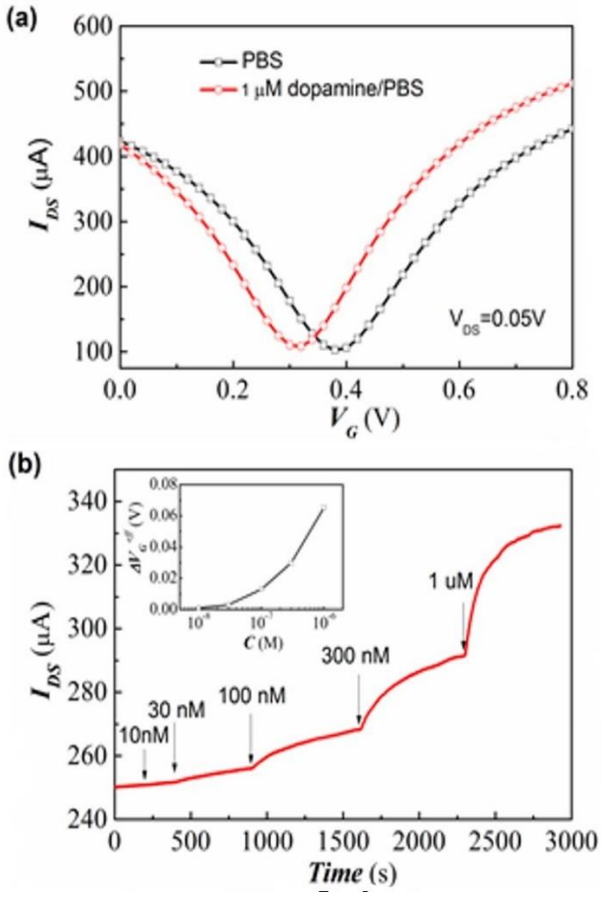

Figure 3.11, a) Transfer characteristics (V_{DS} = 0.05V) of a SGGT with Pt gate electrode measured in PBS solution before and after the addition of dopamine with the concentration of 1μM. b) Channel current response of the SGGT to additions of dopamine with different concentrations. V_{DS} = 0.05V, V_G = 0.7V. Inset: the change of effective gate voltage (ΔV_G^{eff}) for different dopamine concentrations.

The Pt gate electrode was also characterized in pure PBS solution and 1mM dopamine PBS solution by CV measurements (Figure 3.11). The electro-oxidation of dopamine on the Pt electrode can be observed.

It is notable that the current density across the Pt electrode in blank PBS solution is much higher than that of the graphene electrode (Figure 3.7). Therefore, the device with Pt gate electrode shows a high faradic current in PBS solution even without dopamine, which leads to worse selectivity, stability and detection limit of the dopamine sensor.

The changes of effective gate voltage at different dopamine concentrations were calculated and shown in the inset of Figure 3.11b. For the same dopamine concentration, the gate voltage change is lower than that of the devices with the graphene gates as shown in Figure 3.4d and 3.10b. According to equation (3.6), the effective gate voltage change is proportional to the value of γ, which is inversely proportional to the capacitance of the gate/electrolyte interface $C_{G\text{-}E}$. A graphene gate electrode has lower interface capacitance than a Pt gate electrode with the same area due to the quantum capacitance of the graphene layer. Consequently, the device with the graphene gate electrode exhibits a higher value of γ and thus a bigger gate voltage change to dopamine than the device with a Pt gate electrode.

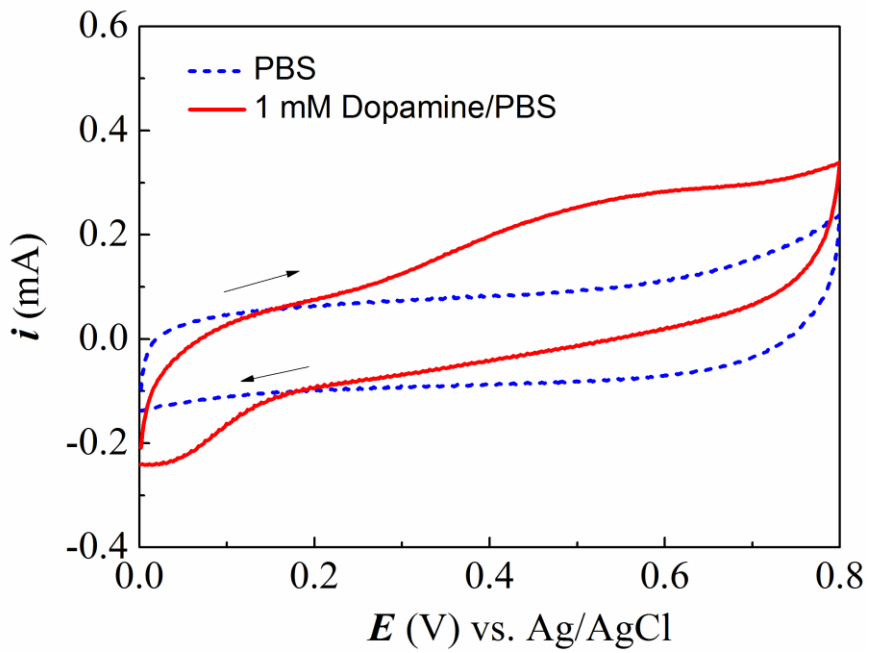

Figure 3.12. CV of the Pt gate electrode in blank and 1 mM dopamine PBS solutions. Voltage scan rate: 50 mV s^{-1}.

3.4.2 Using Nafion/graphene electrode as gate electrode

To further indicate the advantage of the SGGT-based dopamine sensor, the Nafion modified graphene gate electrode was characterize in PBS solution with a typical electrochemical method. Amperometric responses of the electrode to additions of dopamine are shown in Figure 3.13 and exhibit a detection limit of about 3μM (signal to noise ratio >3), being similar to the reported results. So the SGGT-based dopamine sensor shows much higher sensitivity than the conventional electrochemical measurements, which is consistent with various transistor-based biosensors has been reported [64, 88, 104, 105].

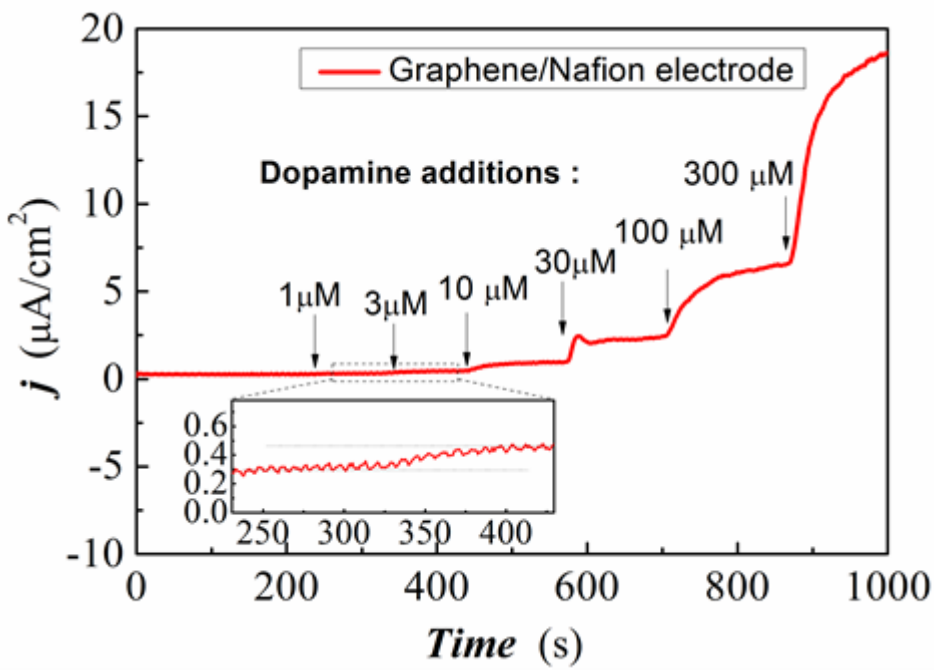

Figure 3.13**,** Amperometric response of a Nafion modified graphene electrode (area: 3 mm×3 mm) to additions of dopamine with different concentrations. The applied potential is fixed at 0.7 V vs. Ag/AgCl. Inset: the detection limit is about 3μM (signal/noise >3).

The SGGTs with graphene gate electrodes are much more sensitive to dopamine than the graphene transistors reported before due to the different sensing mechanism based on the electrochemical reaction of dopamine at the gate electrode. The detection limit of the SGGTs to dopamine is much better than that of many other electrochemical approaches. For example, Zhao *et al*. reported the electrochemical detection of dopamine with the minimum concentration of 0.55μM by using poly(sulfosalicylic acid) modified glass carbon electrode. [100] Sheng *et al*. fabricated electrochemical

sensors based on nitrogen-doped graphene and successfully detected dopamine down to 0.5 μM. [115] Guo et al. reported electrochemical dopamine sensors using electrodes modified with carboxylated carbonaceous spheres with the detection limit down to 20 nM. [100] Our group recently reported a dopamine sensor based on an organic electrochemical transistor with the detection limit of 5 nM, [88] which is inferior to the SGGT-based dopamine sensors. Considering the dopamine levels in urine and plasma being in the ranges of μM and nM levels, respectively, the SGGTs are potentially useful for clinical applications in the future. [89, 116] The low detection limit of the SGGTs can be attributed to the fact that the devices are sensitive to potential changes given by Equation (3.7) even when faradic currents are too low to be detected.

Electrochemical biosensors presently hold a leading position in many sensing applications, including clinical, healthcare, environmental, food, and national defense detections. One main goal in designing new biosensor systems is to achieve greater sensitivity. [117] Besides dopamine sensors, graphene has shown promising applications in many other electrochemical biosensors for its large surface area, high electrical conductivity, good biocompatibility and electrochemical activity, and has been successfully used in modifying electrochemical electrodes with enhanced sensitivity in the detections of AA, UA, cytochrome c, nicotinamide adenine dinucleotide, hemoglobin, cholesterol, H_2O_2 and so on. [118] Due to the high electrochemical activity of graphene, the whole-graphene SGGT devices consequently

can operate as many other sensors with the sensing mechanism based on the electrochemical reaction of analytes on the graphene gates. Obviously, the gate electrodes of the SGGTs should be modified with suitable functional materials to improve the selectivity of each type of biosensors, which is similar to conventional electrochemical biosensors.

3.5 Summary

In summary, a highly sensitive dopamine sensor was realized by using a SGGT with a graphene gate electrode. The sensing mechanism of the device is attributed to the electrochemical reaction of dopamine at the gate electrode, which changes the potential distribution at the interfaces on the graphene gate electrode and the graphene channel. The device shows excellent selectivity to dopamine after the modification of the graphene gate electrode with a thin layer of Nafion. The interference from AA and UA is 3 to 4 orders of magnitude lower than the response of the device to dopamine. The device shows the detection limit to dopamine down to 1 nM, which is good enough for analyzing dopamine levels in clinical applications. Because the channel and the gate of the device are all made of graphene, it can be fabricated on various substrates including flexible ones at low temperature by convenient techniques. Based on the same mechanisms, many other types of biosensors can be developed in the future. Therefore, the whole-graphene SGGT is a promising candidate for disposable, flexible and highly sensitive biosensor.

Chapter 4 Highly sensitive glucose sensors based on enzyme-modified whole-graphene solution-gated transistors

4.1 Introduction

Glucose plays a key role in human metabolism processes and the detection of glucose levels in blood or body fluid is directly related to diabetes mellitus diagnosis.[119] Therefore, high-performance glucose sensors have promising applications in medical diagnosis and healthcare products. Various types of glucose sensors have been successfully developed by using different functional materials, including carbon-based nanomaterials like carbon nanotubes and graphene. [120, 121] Graphene has been successfully used in glucose sensors with different mechanisms for many remarkable physical properties, such as high conductivity, unique electrochemical activity and chemical stability. [3, 7, 104, 122]

Among various types of graphene-based biosensors, [122, 123] solution-gated graphene transistors (SGGT) have drawn lots of attentions because they are promising for real-time, highly sensitive and high-throughput detections.[102] SGGTs could operate directly in aqueous environment at low voltages, which is essential to

biological sensing. Furthermore, SGGT-based devices can exhibit higher sensitivity compared to conventional electrochemical methods because of the inherent amplification function of transistors.[102] SGGTs have been widely investigated as sensors in the detection of pH and ion, [20, 40, 52] glucose, [28], [73] DNA, [25, 30, 72] dopamine, [124] cells, [38] [67]etc. SGGTs have two interfaces with electrolytes, including electrolyte/channel and electrolyte/gate, and the sensors are generally based on the interactions between the analyte and either one of the interfaces.[102] It is notable that, besides the devices with specifically modified channels, [25, 28, 30, 72, 73] SGGTs with functionalized gate electrodes are also good candidates for high-performance biosensors, in previous chapter we developed neurotransmitter (dopamine) sensors with low detection limits (~ 1 nM) and good selectivity. In recent years, high-quality large-area graphene can be prepared with chemical vapor deposition (CVD) methods, which makes it possible to fabricate SGGT-based chemical and biological sensors that can be used in clinical diagnosis, [40] environmental monitoring and food safety tests,[54] etc.

In 2010, Huang *et al*. firstly reported the glucose sensors based on SGGTs by modifying the graphene layer with the enzyme glucose oxidase (GOx). The device can detect the glucose level down to 0.1mM. They considered that the products from the oxidative reaction of glucose are responsible for the increase of channel current while the detailed mechanism was not investigated. In 2012, Kwak *et al.* reported a similar SGGT glucose sensor with GOx immobilized on the graphene channel. The response

of the device was assumed to be related to H_2O_2 generated in the oxidation of glucose catalyzed by GOx. However, the actual interaction between H_2O_2 and graphene is unclear. The device could detect glucose levels in the range of 3.3-10.9 mM, which is not sensitive in comparison with other types of glucose sensors.[125] It is noteworthy that many transistor-based glucose sensors can detect glucose down to μM levels.[13] Therefore the mechanisms of the SGGT-based glucose sensors should be further studied and novel device designs need to be explored to achieve better sensing performance.

In this chapter, we demonstrate a new type of glucose sensors based on SGGTs, in which both channel and gate are made of CVD grown graphene. Graphene is a semi-metal and can be used as not only the semiconductor channel layers but also the gate electrodes of SGGTs. So the devices can be regarded as whole-graphene transistors. The graphene gate electrode was modified with the enzyme GOx and the biocompatible polymers chitosan (CHIT) and Nafion. [126, 127] To improve its electrocatalytic activity, the graphene gate was modified with Pt nanoparticles (PtNPs) by electrochemical deposition. The optimized SGGT glucose sensor shows the detection limit down to 0.5 μM, which has great potential for non-invasive glucose detection in human body fluids, such as saliva.[128] The sensing mechanism is attributed to the enzyme catalyzed oxidation of glucose that generates H_2O_2 near the gate electrode and the oxidation of H_2O_2 that modulates the effective gate voltages applied on the transistors. As potentiometric transducers, SGGT-based sensors are

extremely sensitive to potential changes due to the high transconductance (~several mS). [129] Therefore, these type of devices are promising candidates for high-performance biosensors for not only glucose detections but also many other types of sensing applications.Glucose play a key role in human metabolism processes, the detection of the level of glucose in blood and body fluid is directly related to diabetes mellitus diagnosis[125]. Kwak [73]etc. have reported the application of glucose sensor based on SGGT by using the mechanism based on channel interaction. In their work, the graphene channel was functionalized with linker molecule and immobilized enzymes to induce the detection of glucose in the range of 3.3-10.9 mM. Pt wires served as gate electrodes in the device without specific modification. In purpose of improving the sensitivity of SGGT based glucose sensor, we develop a gate electrode functionalized SGGT. After the modification of the gate electrode with PtNPs, the sensitivity of SGGT towards H_2O_2 could reach as low as 0.1 μM. For H_2O_2 sensing, PtNPs take the role of catalyst since the pure CVD-grown graphene film have relatively low electrochemical activity due to the lacking of defects. On the basis of ultrasensitive H_2O_2 sensor, we immobilized glucose oxidase on graphene gate electrode by using biocompatible polymer (chitosan, Nafion), the Gox-CHIT/Nafion/PtNPs modified device could achieve a detection limit down to 0.5 μM and response range from 0.5 μM to 1 mM. Nafion and CHIT are employed as matrix for enzyme immobilization. Nafion exhibit suitable wettability with CVD-grown graphene. [131, 132] After pre-deposition of Nafion thin film on the graphene surface, hydrophilic Gox-CHIT layer was located on Nafion layer. Both the two materials are

biocompatible polymer with good stability and exchange ability in aqueous environment. It is feasible to find out that the functionalization processes effectively improve the performance of the SGGT devices for H_2O_2 sensing and glucose sensing.

4.2 Sensing Mechanism of SGGTs based glucose sensor

Figure 4.1 shows the schematic diagram of the device structure and the sensing mechanism. The devices were fabricated on glass substrates and characterized in PBS solutions. As shown in Figure 4.1b, the gate voltage (V_G) is actually applied on the two electric double layers (EDLs) since the electrolyte is ion conductive and $V_G = V_{EDL1} + V_{EDL2}$, where V_{EDL1} and V_{EDL2} are the potential drops on the EDLs of channel and gate, respectively. So the device performance is sensitive to the properties of each EDL. The SGGT is a type of potentiometric transducer that is sensitive to potential drops at interfaces influenced by analytes. In the glucose sensor, the graphene gate electrode was modified with GOx on the surface, which can catalyze the oxidation of glucose in PBS solution and generate H_2O_2 near the gate electrode in the following reaction:

$$\mathrm{D-Glucose} \xrightarrow{GOx} \mathrm{D\text{-}Glucono\text{-}1,5\text{-}lactone} + \mathrm{H_2O_2}.$$

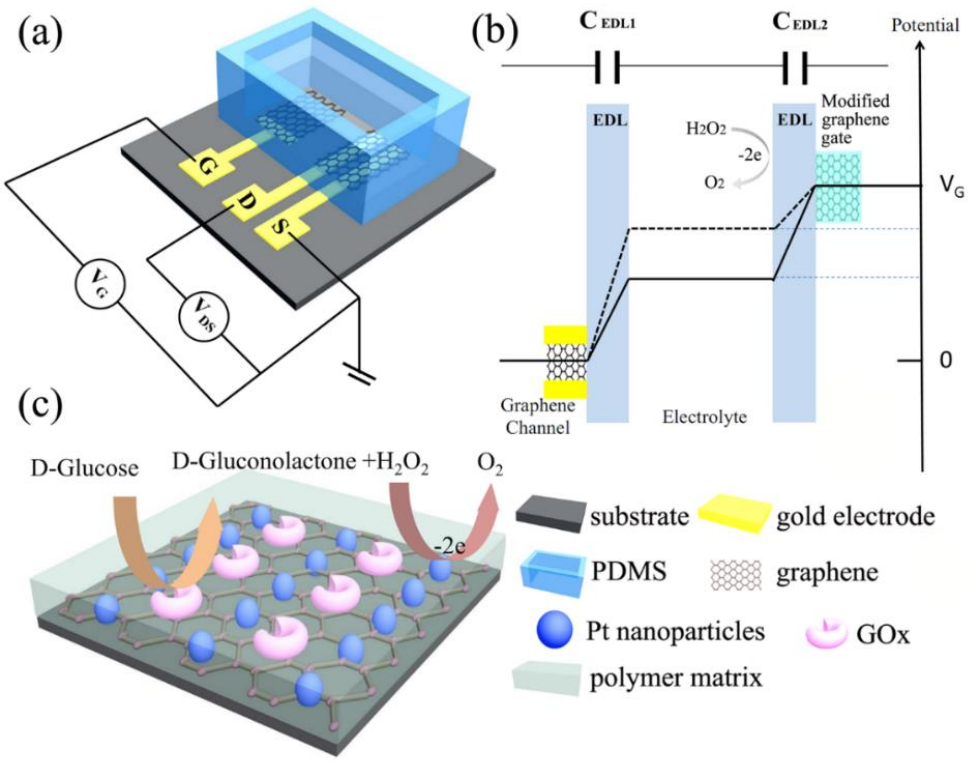

Figure 4.1. a) Schematic diagram of the glucose sensor based on a whole-graphene solution-gated transistor; b) Potential drops at two electric double layers (EDLs) on the surfaces of graphene channel and gate. c) The GOx-catalyzed oxidation of glucose and the oxidation of H_2O_2 cycles on the GOx-CHIT/Nafion/PtNPs/graphene gate electrode of a graphene transistor.

It is notable that the enzymatically produced H_2O_2 will be oxidized on the surface of the graphene under a bias voltage

$$H_2O_2 \rightarrow O_2 + 2H^+ + 2e^-$$

In this reaction, the electrons ($2e^-$) will be transferred to the gate electrode, which will change the potential distribution in the device as indicated by the dash line in Figure 4.1b. For a potentiometric transducer, although the redox current is very low, the reaction of H_2O_2 will change the potential drop on the gate electrode according to the Nernst equation:

$$V_{EDL2} = -\frac{kT}{2q}\ln[H_2O_2] + C, \quad (4.1)$$

where k is Boltzmann constant; T is temperature; q is the electron charge; $[H_2O_2]$ is the concentration of H_2O_2 and C is constant. Consequently, the voltage applied on the channel surface V_{EDL1} will also be modulated by the reaction of H_2O_2 and thus

$$V_{EDL1} = V_G + \frac{kT}{2q}\ln[H_2O_2] - C. \quad (4.2)$$

It is notable that the channel current I_{DS} is dependent on the voltage V_{EDL1} applied on the surface of the channel due to the field effect. Therefore the channel current is sensitive to the concentration of H_2O_2.

4.3 Fabrication of device

4.3.1 Materials

Chloroplatinic acid ($H_2PtCl_6\ 6H_2O$ AR) was purchased from Sinopharm Chemical Reagent Co., Ltd. Glucose oxidase (GOx) (100 kU • g^{-1}) was purchased from Sigma-

Aldrich Reagent Database Inc. and stored at -20℃ for future use. Chitosan (CHIT) and hydrogen peroxide (H_2O_2, 30%, AR) were purchased from Advanced Technology & Industrial Co., Ltd and used as received. Phosphate buffered saline (PBS) solution (pH 7.2) was purchased from Invitrogen Co., Ltd and used as received. Glucose was also purchased from Sigma- Aldrich Co. Deionized water was used throughout in the whole process.

CHIT solution was prepared by dissolving CHIT (0.5g) in acetic acid solution (100 mL, 50 mM, pH 5-6). The solution was electromagnetic stirred overnight and stored in 4 °C refrigerator. GOx stock solution was prepared by dissolving in PBS and stored in 4 °C refrigerator before use. 5%wt Nafion solution was diluted for 10 times by isopropanol before use.

4.3.2 Device Fabrication

The schematic structure of the whole-graphene SGGTs is shown in Figure 4.1a. Au/Cr electrodes were deposited on glass substrates by magnetron sputtering through a shadow mask. Single-layer graphene was grown on Cu foils by CVD method and transferred on the glass substrates with the metal electrodes. Then the graphene films are patterned by the standard lithography method to have the graphene channel and gate. The fabrication procedure is shown in Figure 3.2 and Figure 3.3, chapter 3. The area of the graphene gate electrode is defined to be 3mm×3mm and the channel width and length are 0.2 mm and 3 mm, respectively. A Poly(dimethylsiloxane) (PDMS)

(Sylgard 184, Dow Corning, USA) wall was attached to the substrate to enable the test of the device in liquid (PBS solution).

Graphene gate electrodes were modified with Platinum nanoparticles (PtNPs) to enhance the electrocatalytic activity. PtNPs were eletrodeposited on the graphene electrodes in 5mM H_2PtCl_6/0.1M HCl aqueous solution. [86] A constant voltage of -0.2 V relative to an Ag/AgCl reference electrode was applied on the needed graphene electrode, and the deposition time was controlled to be ~120s. Then the PtNPs/graphene electrodes were rinsed with DI water and used as the gate electrodes of the SGGTs.

For the preparation of GOx-CHIT/Nafion/PtNPs/graphene electrode, 50 uL GOx stock solution was mixed with 0.5%wt CHIT solution and the mixture is sonicated for 15 min before use. The graphene gate electrode was firstly modified with PtNPs as described above, then 10 μL 0.5%wt Nafion was dropped on the surface of the gate and dried at room temperature. After that, 10 μL GOx-CHIT mixture was drop coated on the Nafion/ PtNPs/graphene gate electrode. The as-prepared SGGT was placed in a 4°C refrigerator overnight to dry the GOx-CHIT film. The devices were finally rinsed with DI water to remove unexpected residue and stored in the refrigerator for future use.

4.4 Measurement methods

The SGGT devices were characterized by semiconductor parameter analyzer (4156C, Agilent Technology) in PBS solution at room temperature as shown in Figure 4.1a. The transfer characteristic (channel current I_{DS} versus gate voltage V_G) was tested under a fixed drain voltage V_{DS} = 0.05 V and variable V_G. In the sensing applications, the channel current as a function of time was characterized under the constant voltages of V_{DS} = 0.05 V and V_G = 0.7 V with the additions of analytes (H_2O_2 or glucose). The gate voltage V_G = 0.7V is selected because the device has comparatively large transconductivity at V_G = 0.7V. The transconductance g_m of the device at different gate voltages is calculated with the equation:

$$g_m = \frac{dI_{DS}}{dV_G}. \qquad (4.3)$$

The electrochemical properties of the graphene electrodes were characterized by EG&G PAR2273 electrochemical workstation (Princeton Co. Ltd). During the measurements, Ag/AgCl (sat. KCl) was used as a reference electrode and Pt wire was used as a counter electrode. The graphene and PtNPs/graphene electrodes were studied by cyclic voltammetry (CV) measurements with a scan rate of 50 mV/s.

The surface morphology of graphene electrodes were characterized by Atom force microscopy (AFM, Digital instruments) and Scanning Electron Microscopy (SEM, JEOL JSM-6335F).

4.5 H_2O_2 detection by PtNPs modified SGGTs

Since the glucose sensor is based on the detection of H_2O_2, the first step is to fabricate a highly sensitive H_2O_2 SGGT sensor. We noticed that the electrocatalytic activity of graphene to H_2O_2 can be enhanced by modifying PtNPs on its surface. Figure 4.2a and 4.2b shows the AFM image of the CVD graphene film with and without PtNPs on the surface. The average size of the PtNPs is about 30 nm. Figure 4.2c and 4.2d show the CV curves of a graphene electrode before and after the modification of PtNPs on the surface. It is notable that the electrocatalytic activity to H_2O_2 is dramatically improved by the PtNPs since the redox current is increased for several hundred times after the modification.

Figure 4.3a shows the channel current (I_{DS}) of a SGGT without any modification of PtNPs on the graphene gate measured at V_G=0.7V and V_{DS}=0.05V. The channel current increases with the additions of H_2O_2 and shows the detection limit of about 10μM. The inset of Figure 3a shows the transfer curve of the SGGT characterized in PBS solution, which exhibits a reasonable ambipolar behavior with the Dirac point at about 0.3V. The transfer curve shifts to lower gate voltages in H_2O_2 (1mM) PBS solution, being consistent with the channel current increase with the additions of H_2O_2.

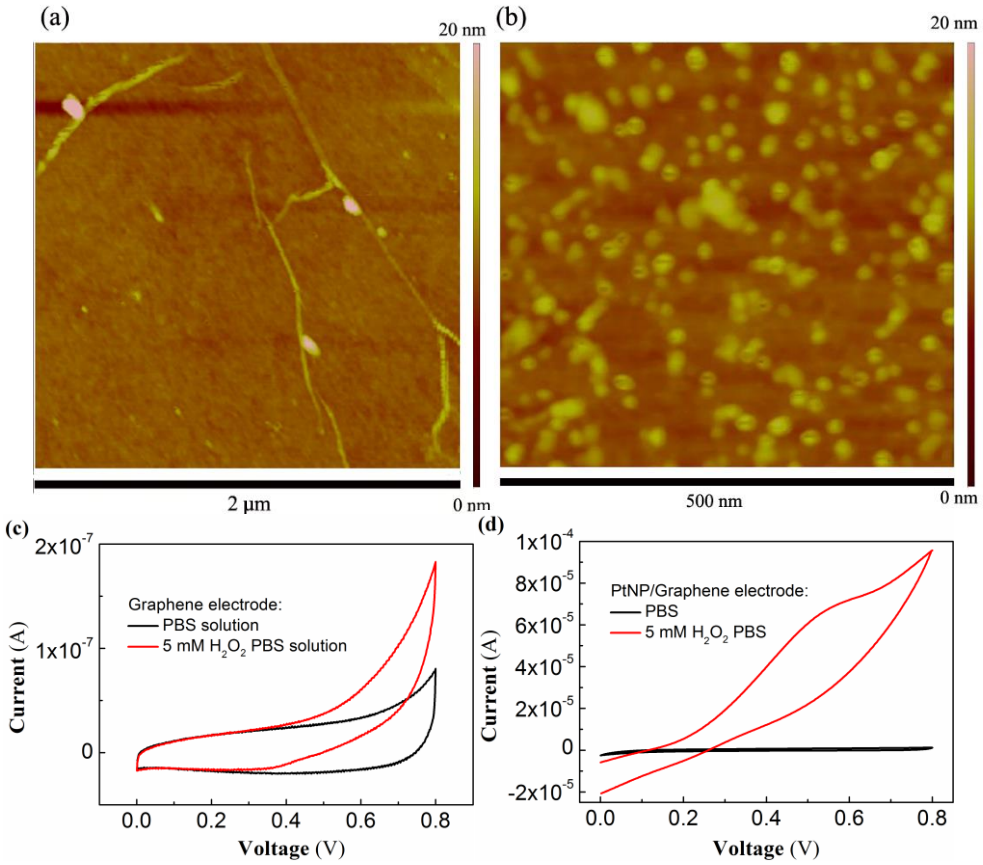

Figure 4.2. AFM images of (a) CVD graphene film and (b) CVD graphene modified with PtNPs. CV curves of (c) graphene electrode and (d) PtNPs/graphene electrode characterized in PBS solution and 5mM H2O2 PBS solution with a scan rate of 50 mV/s.

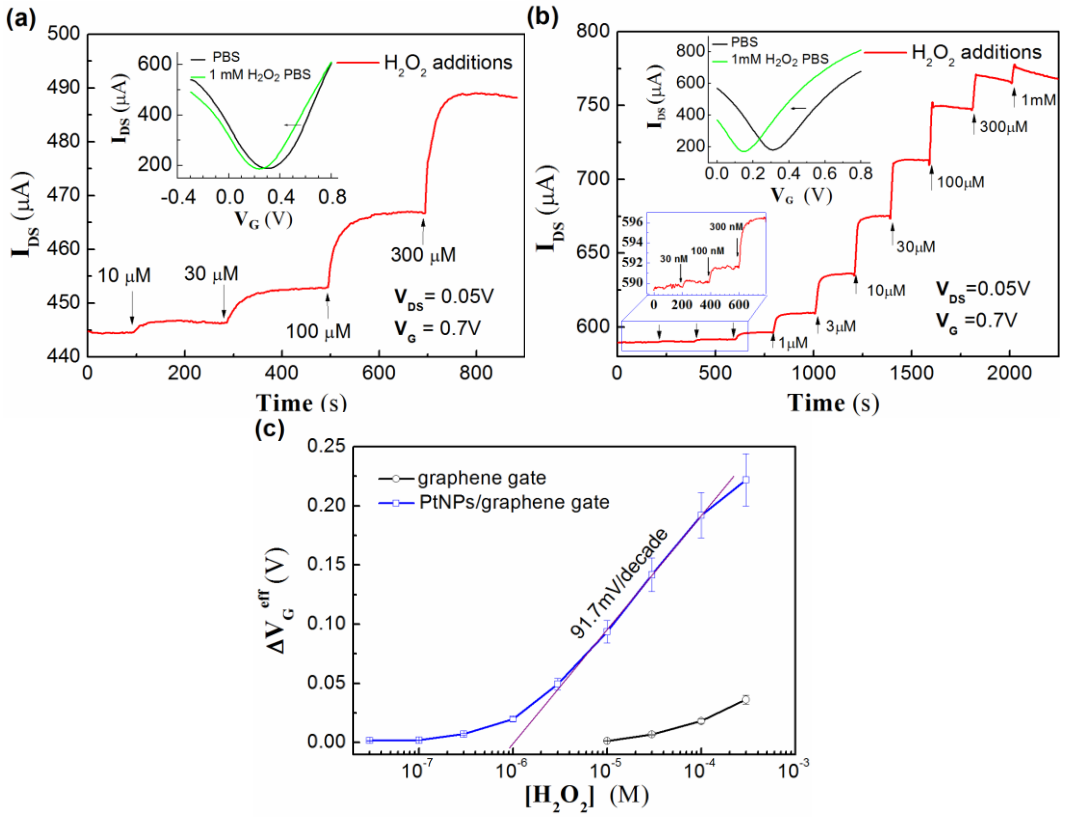

Figure 4.3. a) Channel current (I_{DS}) responses of a SGGT without any modification on the graphene gate to additions of H_2O_2 with different concentrations measured at the fixed voltages of V_G=0.7V and V_{DS}=0.05V. Inset: transfer curves of the SGGT measured in pure PBS and 1mM H_2O_2 PBS solutions. b) Channel current response of a SGGT with PtNP-modifed graphene gate to additions of H_2O_2 with different concentrations measured at the fixed voltages of V_G = 0.7V and V_{DS} = 0.05V. Inset: transfer curves of the device measured in PBS and 1mM H_2O_2 PBS solutions. c) Effective gate voltage (ΔV_G^{eff}) versus H_2O_2 concentration for the SGGTs with or without PtNPs on graphene gate electrodes.

To improve the sensitivity of the device to H_2O_2, the graphene gate electrode of a SGGT was modified with PtNPs by electrodeposition method. Figure 4.3b shows the channel current response of the device to additions of H_2O_2 measured at V_G=0.7V and V_{DS}=0.05V. The detection limit (Signal/Noise ≥ 3) of the device to H_2O_2 is about 30nM, which is much more sensitive than the device without the PtNPs. Similarly, as shown in the inset of Figure 4.3b, the transfer curve of the device shifts horizontally to lower gate voltages when H_2O_2 was added in PBS solution, which is consistent with the increase of channel current measured at the fixed gate voltage. The shift of the transfer curve can be regarded as the change of the effective gate voltage induced by the reaction of H_2O_2 at the gate electrode. Alternatively, the effective gate voltage change (ΔV_G^{eff}) can be calculated according to the change of channel current measured at the fixed gate voltage. The detailed calculation process is as follows. For different channel current value, the corresponding gate voltage can be read out from the transfer curve. The difference between the gate voltages before and after the addition of H_2O_2 is ΔV_G^{eff} for this concentration of H_2O_2. Therefore, effective gate voltage change as a function of H_2O_2 concentration can be obtained, as shown in Figure 4.3c. It is notable that the SGGT with PtNP-modified gate electrode shows much bigger response than the one without the Pt modification.

Assuming the capacitances of EDL1 on the channel and EDL2 on the gate are C_{EDL1} and C_{EDL2}, respectively, the effective gate voltage is given by:

$$V_G^{eff} = (1+\gamma)\frac{kT}{q}\ln[H_2O_2] + \text{constant}$$
$$= 2.30(1+\gamma)\frac{kT}{q}\log[H_2O_2] + \text{constant} \quad (4.4)$$
$$\gamma = \frac{C_{EDL1}}{C_{EDL2}}$$

Therefore, it is reasonable to find that the effective gate voltage changes for 91mV/decade in the linear region (3μM to 300 μM) and we can obtain $\gamma \approx 0.5$ from equation (3) at room temperature (T=300K).

4.6 Glucose detection by functionalized SGGTs

Enzyme-functionalized SGGT glucose sensors were then prepared on the basis of the PtNP-modified devices because H_2O_2 is a major product of glucose oxidation catalyzed by GOx. The gate electrode was coated with a thin layer of Nafion and then the mixture of CHIT and GOx. GOx plays an important role in glucose sensing because the SGGT without the modification of GOx did not show any response to glucose additions with the concentrations up to 3mM as shown in figure 4.4. The Nafion layer has negative charge in PBS (pH=7.2) solution and can dramatically improve the selectivity of the device to the main interferences, including uric acid (UA) and ascobic acid(AA), because UA and AA are negatively charged and are thus difficult to diffuse through the negatively charged Nafion film due to electrostatic interaction. [133] Secondly, we noticed that it is difficult to directly coat GOx and CHIT aqueous solution on graphene for the hydrophobic surface of graphene. [134]

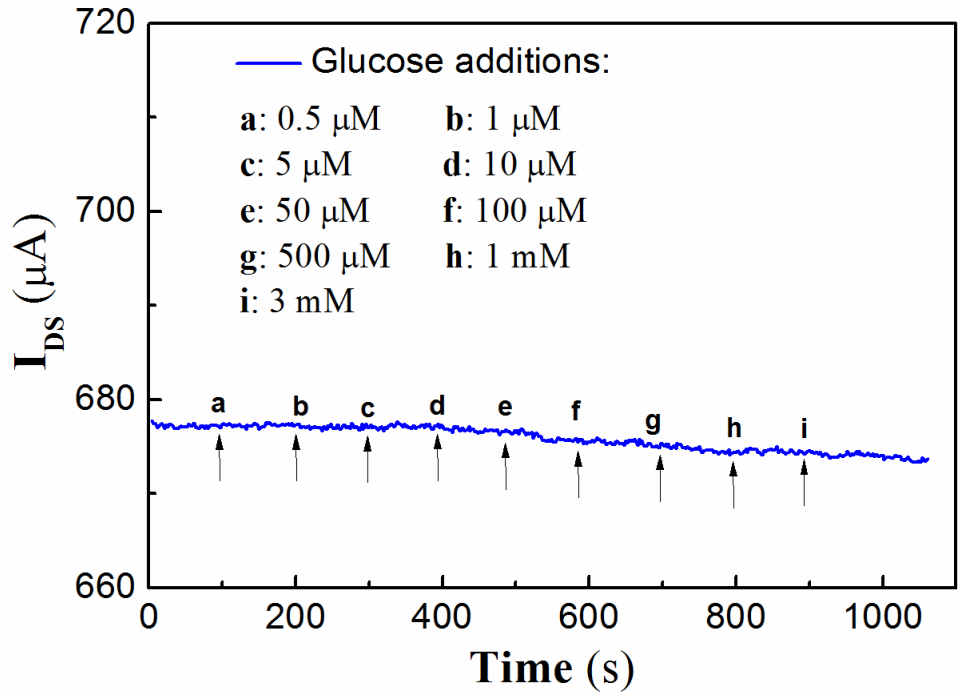

Figure 4.4. The channel current response of a SGGT with PtNPs/graphene gate to additions of glucose. V_{DS}=0.05V, V_G=0.7V.

The Nafion film can be uniformly coated on the graphene film and then used as an interlayer for coating the GOx-CHIT film on the surface. We also noticed that the device with GOx modified on the gate without PtNPs cannot show obvious response to glucose due to the poor electrocatalytic activity of the gate as shown in figure 4.5. So only the devices with GOx-CHIT/Nafion/PtNPs/graphene gate electrodes show high sensitivity to glucose.

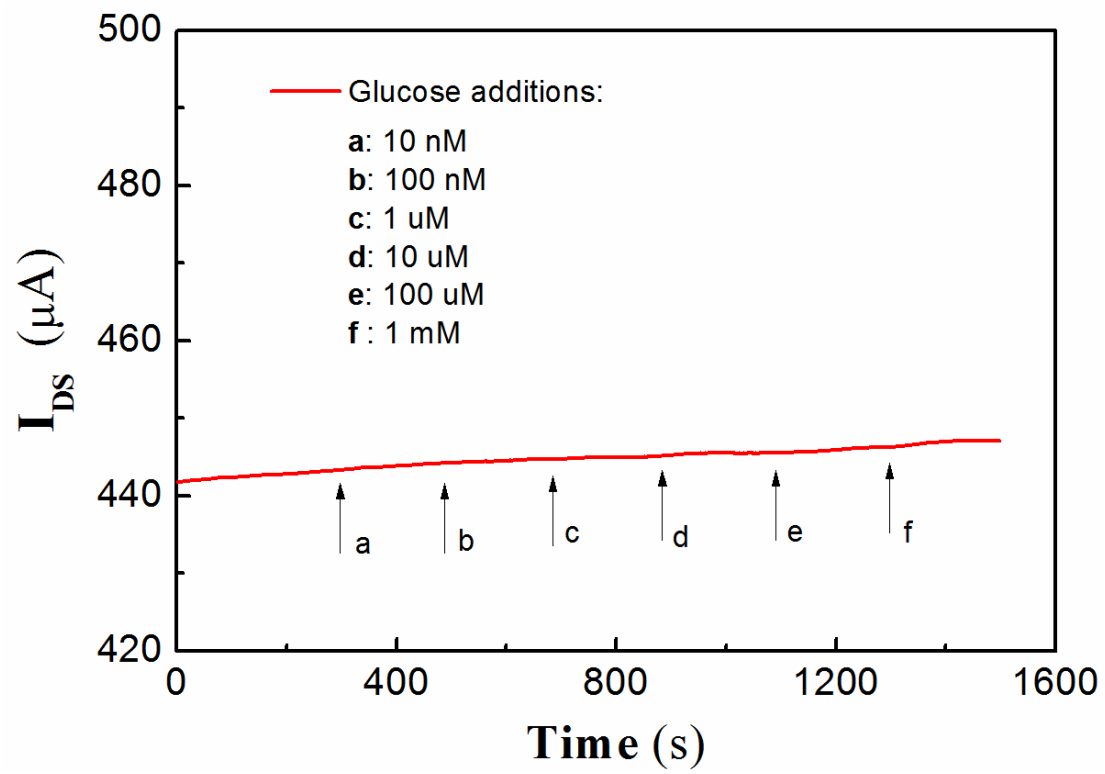

Figure 4.5. The channel current response of a SGGT with Gox-CHIT/Nafion/graphene gate to additions of glucose. V_{DS}=0.05V, V_G=0.7V.

The current change is attributed to the change of effective gate voltage (ΔV_G^{eff}) induced by the reaction of glucose on the gate electrode. Therefore, ΔV_G^{eff} was calculated and was found to change for about 173mV/decade in linear region, as shown in Figure 4.6c. According to equation (3), γ can be calculated to be $\gamma \approx 1.9$. The reason to have higher γ in the glucose sensor is prosumably due to the decreased capacitance of the graphene gate for the modification of the insulating polymers (Nafion and Chitsan) on the surface.

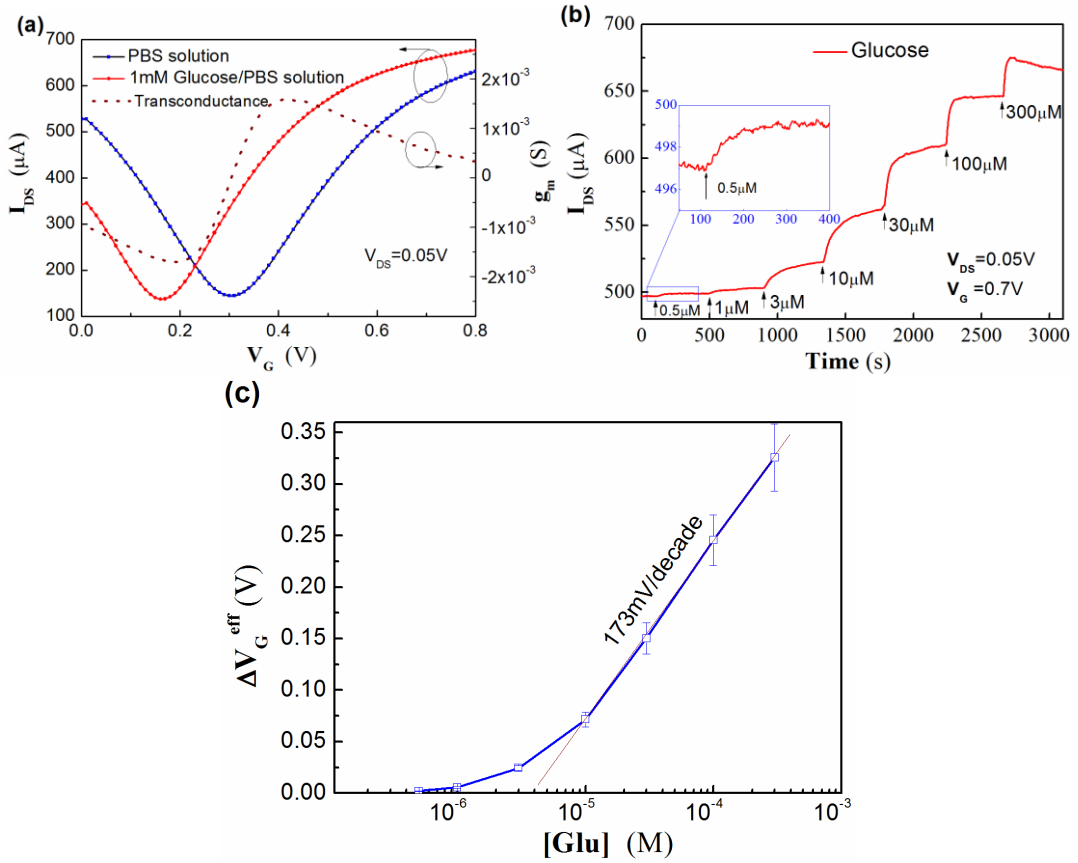

Figure 4.6 a) Transfer characteristics of a SGGT with a GOx-CHIT/Nafion/PtNPs/graphene gate electrode measured in PBS and 1mM glucose PBS solutions. Dash line: Transconductance (g_m) of the SGGT characterized in PBS solution. b) Channel current responses of the SGGT to additions of glucose with different concentrations. c) The corresponding effective gate voltage change (ΔV_G^{eff}) at different glucose concentrations ([Glu]).

The detectable range of the SGGT glucose sensor is from 0.5 μM to 1 mM, which is a suitable range for the detections of glucose in body fluids, such as human saliva.

[135] For blood glucose tests, conventional electrochemical methods are sensitive enough and have been successfully used in commercial products. However, blood glucose tests are painful and not very convenient in clinical diagnosis. Non-invasive detection of glucose level in body fluid has been proposed to be an alternative way since the glucose level in body fluid can reflect the glucose level in plasma. However, glucose level in body fluid is much lower than that in plasma. Therefore, highly sensitive approaches such as the SGGT-based glucose sensor are potentially useful for non-invasive diagnosis of glucose levels in human body.

It is noteworthy that the whole-graphene transistors have many advantages. Firstly, the device structure is very simple and can be prepared with one layer of graphene. So transistor arrays can be easily prepared by patterning high-quality large-area graphene. Besides glucose sensors, many other types of enzyme sensors can be realized based on the detection of H_2O_2. [130] Therefore, multifunctional SGGT arrays for different types of highly sensitive biosensors can be realized by modifying the gate electrodes with specific biomaterials. Secondly, the devices show high transconductance g_m ($g_m = \frac{\Delta I_{DS}}{\Delta V_G}$), which is important for amplifying a potetntial signal into a current signal. As shown in Figure 4a, g_m has the maximum value of about 2mS even at the drain voltage of only 0.05V. It is notable that a typical Si transistor used as a biosensor has a transconductance of only around 20 μS for V_{DS} =0.5V. So the transconductance of a SGGT is two orders of magnitude higher than that of a Si transistor, which is the main reason for the high sensitivity of the SGGT-based biosensor.

4.7 Summary

In conclusion, whole-graphene SGGTs with PtNP-functionalized graphene gate electrodes can be used for highly sensitive detections of H_2O_2 with the detection limit down to 30nM. The device is further demonstrated as a highly sensitive glucose sensor after the immobilization of the enzyme GOx, CHIT and Nafion on the PtNPs/graphene surface and can detect glucose concentrations down to 0.5 μM. The high sensitivity of the SGGT-based sensors is attributed to the inherent amplification function of the transistors and the improved electrocatalytic activity of the graphene gate electrodes after the modification of PtNPs. Since most of enzyme sensors are based on the detection of H_2O_2, this kind of devices are expected to be developed as many other types of enzyme sensors in the future.

Chapter 5 Cell sensing platform integrated with Solution-Gated Graphene Transistors

In this chapter, cell monitoring platform based on solution-gated graphene transistors has been developed for biological process (such as cell adhesion and proliferation) monitoring and studying. Cancer cells (HepG2, HCT116, SAOS2) and fibroblasts (HFF-1) were cultured on the surface of graphene channel of SGGT. The viability, adhesion processes and distribution of these types of cell lines were observed and analyzed.

5.1 Introduction

One of the key issue in the field of biosensor and bioelectronic is developing electrical sensing platform integrated with living cells. Integrated cell sensors offer opportunities to tranfer variations during cell physiological activities into detectable signals, exhibit obvious potential for bimedical applications such as clinical diagnosis [136], drug screening[137], tissue engineering [138], environment monitoring et al [1]. Among these graphene based cell sensors, solution-gated graphene transistors attract growing interest for cell sensing. A SGGT has a typical transistor-based structure while the gate voltage applied directly on the electrolyte. SGGTs has several advantages for cell sensing. 1) It has been found that SGGT have stable performance in electrolyte, which is convenient to detect phenomena happens in aqueous

environment; 2) SGGTs exhibit ballistic transport at room temperature, having both holes and electrons as charge carrier. 3) The transistor-based structure enable amplification of the original signal, imply higher sensitivity rather than conventional electrochemical biosensors [102].

Lieber's group reported the first SGGT based cell sensors in 2010 [38], electrical recording of spontaneously beating of electrogenic cells (embryonic chicken cardiomyocytes) was demonstrated by using SGGT. He etc. reported PC12 cells culturing directly on the channel of SGGTs, by applying high K^+ stimuli to the cells, the corresponding secretion of catecholamine molecules were recorded by their device [75]. Hess etc. fabricated a system containing arrays of SGGTs, after HL-1 cell line culturing on the system, acting potential as well as propagation of cell signals were detected by their device [66]. SGGTs-based cell sensing systems provide an approach for real time detecting cells activities.

In this chapter, we fabricated a SGGT on glass substrate to characterize cancerous cell line (HepG2, SAOS2) and fibroblast cell line (HFF-1) adhesion process on graphene surface. Cell adhesion is one of the fundamental topic for biomedical research because most mamalian cells are anchorage dependent type, thus the interactions between cells and substrates could directly influence the whole life cycle of the cells, including proliferation, differentiation, mirgration, and apoptasis processes [139, 140]. By seeding cells on graphene channel, capacitance change of graphene/electrolyte interface corresponding to cell adhesion process was observed. Meanwhile the channel

current could be monitered, exhibited decreasing value accompany with capacitance variation. [141] Furthermore, it is found out that the density of cell grown along the graphene channel could be modulated by simply applying biased electrical fields on the three electrodes system, forming gradients on graphene surface. This kind of SGGT-based platform provides a powerful tool for electrical detecting and controlling cell adhesion and distribution.

5.2 Experiment for device fabrication and cell culturing

5.2.1 Materials

CVD-grown graphene was purchased from Weijing Co. Hefei. Dulbecco's Modified Eagle Medium (DMEM) (high glucose), 0.05%Trypsin/1.5 mM EDTA, Fetal Bovine Serum, penicillin and T25 flask was purchased from life technology co., Hong Kong. Acetone was purchased from advtech co., Hong Kong. Fluorescence dye Fluorescein Diacectate (FDA) and Propidium Iodide (PI) and anti-cancer drug 5-Fluorouracil (5-FU) was bought from Sigma-adrich co. FDA stock solution is prepared by dissolving 5 mg of FDA in 1 ml acetone. PI stock solution is prepared by dissolving 1 mg of PI in 1ml PBS solution.

5.2.2 Device Fabrication

As shown in the Figure 5.1a, the whole device was fabricated on glass substrate with an area of 2.5 cm×2.5 cm. Firstly, gold electrodes with chromium adhesion layer was thermal evaporated (Edwards Auto306) onto the substrate through a shadow mask. Then, CVD-grown graphene were transffered in direct contact with Au/Cr electrodes following a typical wet tranffer technique as shown in Figure 3.2. After successful graphene tranffer, the graphene channel was patterned by lithography method as shown in figure 3.3. The channel width and length are 2mm and 3mm respectively. Finally, a poly(dimethylsiloxane) (PDMS) well with volumn of 0.7 cm × 1.5 cm × 1 mm was combined with the glass substrate by O_2 plasma treatment. The as-prepared device was used for cell culture and electrical measurements.

5.2.3 Cell culture

Human esophageal squamous epithelial cancer cell line (HepG2), fibroblast cell line (HFF1) and osteoblast cell line (SAOS2) are purchased from American Type of Culture Collection (ATCC). HepG2 cell line, HFF-1 cell line, and SAOS2 cell line were cultured in Dulbecco's Modified Eagle Medium (DMEM) with 4,500 mg/L glucose (Invitrogen) as basic medium supplemented with 15% Fetal Bovine Serum (FBS, Invitrogen) and 1% penicillin (Invitrogen). The cell lines were routinely cultured on a T25 cell culture flask (life technology co) in a cell incubator at the

temperature of 37°C and 5% CO_2/95% air atmosphere. For cell culturing on SGGT devices, the devices were firstly sterilized by UV radiation treatment for 12h in biosafety fume hood before cell seeding. Cells cultured in the flask were treated by standard trypsinization processes (0.05% (w/v) trypsin/ 1.5 mM EDTA, life technologies). Then the cell lines are seeded in the PDMS wall, and cultured in the incubator environment for electrical measurement. For anti-cancer drug testing, 5-FU was solved in 7.4 PBS solution, forming a solution with 500 μg/ml concentration. 10 μL as-prepared 5-FU solution was added into cell culture medium on SGGT devices, and coltured 8 h for further testing.

5.3 Characterization and measurement

The SGGT devices were characterized by keithley 2400 sourcemeter (National instruments) in cell culture medium within cell incubator as shown in Figure 5.1. The I-V characteristic (channel current I_{DS} versus gate voltage V_G) was characterized under a fixed drain voltage V_{DS} = 0.05 V and variable V_G. In the sensing applications, the channel current as a function of time was characterized under the constant voltages of V_{DS}=0.05 V and V_G=0.3 V for 12 h. The microscopy image have been observed by Nikon ECLIPSE 80i fluorescence microscope, the fluorescence microscopy image was taken by Nikon ECLIPSE 80i fluorescence microscope.

Figure 5.1 shows the schematic diagram of the device structure. CVD-grown graphene connected by source and drain electrodes is utilized as the channel of the transistor, Ag/AgCl reference electrode is used as the gate electrode.

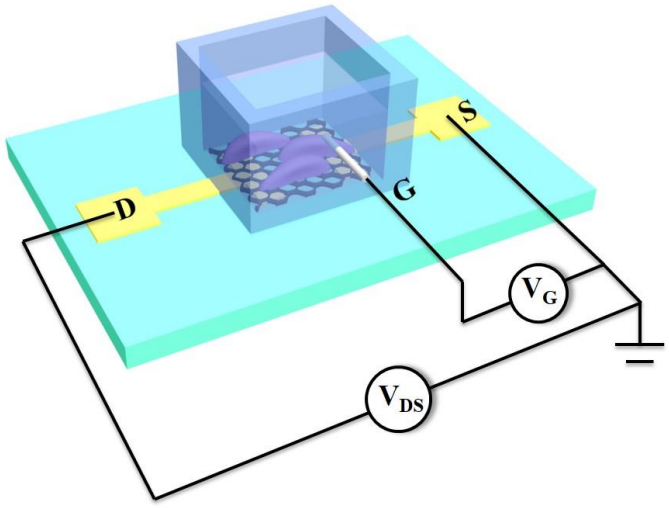

Figure 5.1**.** a) Schematic diagram of cell sensing platform based on solution-gated graphene transistor

5.4 Viability study of cells cultured on SGGTs

Cell was cultured directly on the graphene channel in the PDMS well filled with culture medium. In this work, human Hapatocellular carcinoma cell line(Hep G2), human osteosarcoma cell line (SAOS2), human foreskin fibroblast cell line (HFF-1) were seeded and maintained on the graphene channel as models to study cell adhesion. After 1 day culturing, the cells was labeled with fluoescence stains PI/FDA for " live and dead" assay, in which living cells generating a green fluorescence and dead cells

generating red fluorescence. As shown in Figure 5.2a, b, c, all of the three cell lines cultured on our device exhibited excellent viability(> 99%).Meanwhile, all the three kind of cells exhibited normal morphologies like cells cultured on tissue culturing flasks. Therefore, it is illustrated that SGGTs were a suitable platform for short time cell adhesion detection.

Many methods were developed for cell adhesion sensing at bioelectronic interfaces, such as fluorescence labeling, radiation notation etc [138, 139]. By labeling cells with fluorescence or radiation probe, adhesion activities could be transffered into optical signals. In this chapter, SGGTs were used as transducers for cell activity signaling without specific labeling.

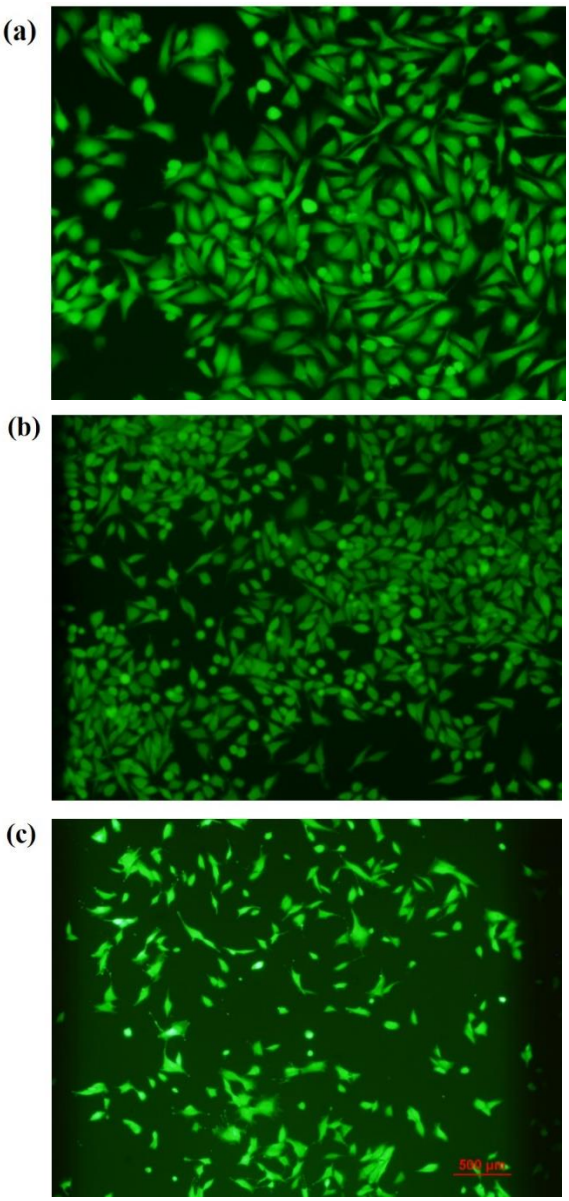

Figure 5.2. a, b, c) Fluorescence image of HepG2 cell, SAOS2 cell, and HFF-1 cell culturing 12 h (staining by FDA/PI), exhibit high viability.

5.5 cell adhesion on SGGTs

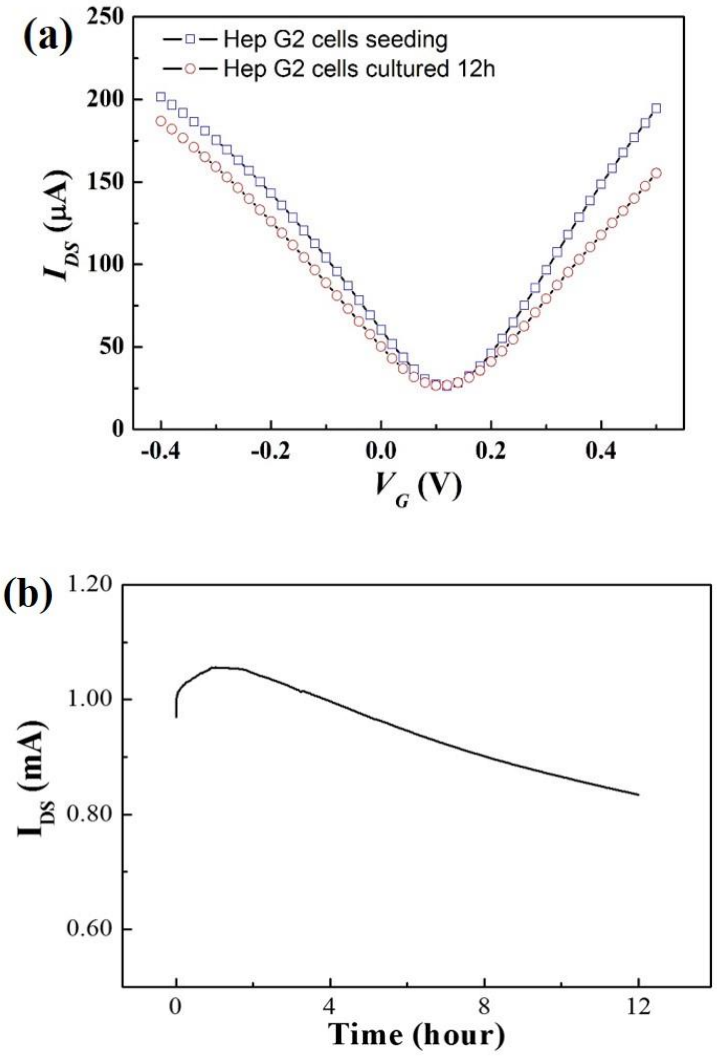

Figure 5.3. a) Channel current (I_{DS}) responses of a SGGT with HepG2 cell seeding voltages of V_G= -0.4 V—0.4 V with 0.02 V as step and V_{DS}=0.05V. b) Channel current (I_{DS}) versus time (h) of a SGGT during HepG2 culturing, measured at voltages of V_G= -0.4 V V_{DS}=0.6V.

Figure 5.3a shows the transfer characteristic of a SGGT with HepG2 cells cultured on the graphene channel and measured at V_{DS}=0.05V, and variable $V_{G,}$ from -0.4 V to 0.4 V. The transfer curve exhibited a typical ambipolar shape due to the electronic structure of graphene [102]. Furthermore, as the cells were seeded and maintained for 12h, it is found that the channel current I_{DS} decreased with time when applying the same V_{DS} and V_G.The channel current of SGGTs is defined by [102]

$$I_{DS} \approx \frac{W}{L}\mu C_i \left|V_G - V_{Dirac}\right| V_{DS} \text{, with } \left|V_G - V_{Dirac}\right| >> \left|V_{DS}\right| \qquad (5.1)$$

The transconductance of SGGT (g_m) is given by

$$g_m = \frac{\Delta I_{DS}}{\Delta V_G} = \frac{W}{L}\mu C_i V_{DS} \qquad (5.2)$$

W and L is the width and length of the channel, μ is the carrier mobiliy. C_i is the gate capacitance. V_{dirac} is the gate voltage corresponding to the carrier neutrality point at which the channel current is minimum. As shown on Figure 5.3a, the Dirac point shift ΔV_{Dirac} is negligible, it is reasonable to speculate that the transconductance decrease is resulted from the gate capacitance decrease during the cell adhesion.

$$\Delta g_m = \frac{W}{L}\mu V_{DS}\Delta C_i \qquad (5.3)$$

Figure 5.4a and 5.5a exhibited similar results when SAOS2 cell and HFF-1 cell cultured on SGGTs channels. The channel current decreases in the first few hours of cell culturing.

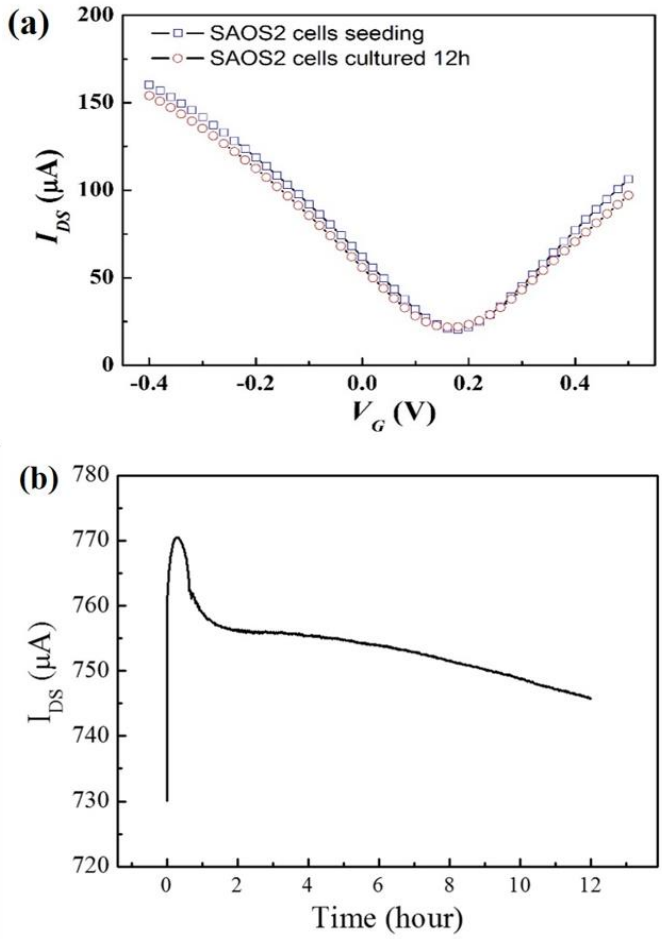

Figure 5.4 a) Channel current response of a SGGT (I_{DS}) with SAOS2 cell culturing 12 h, V_G = 0.3V and V_{DS} = 0.6V. Channel current (I_{DS}) versus time (h) of a SGGT during SAOS2 culturing, voltages of V_G= 0.47 V V_{DS}=0.6V.

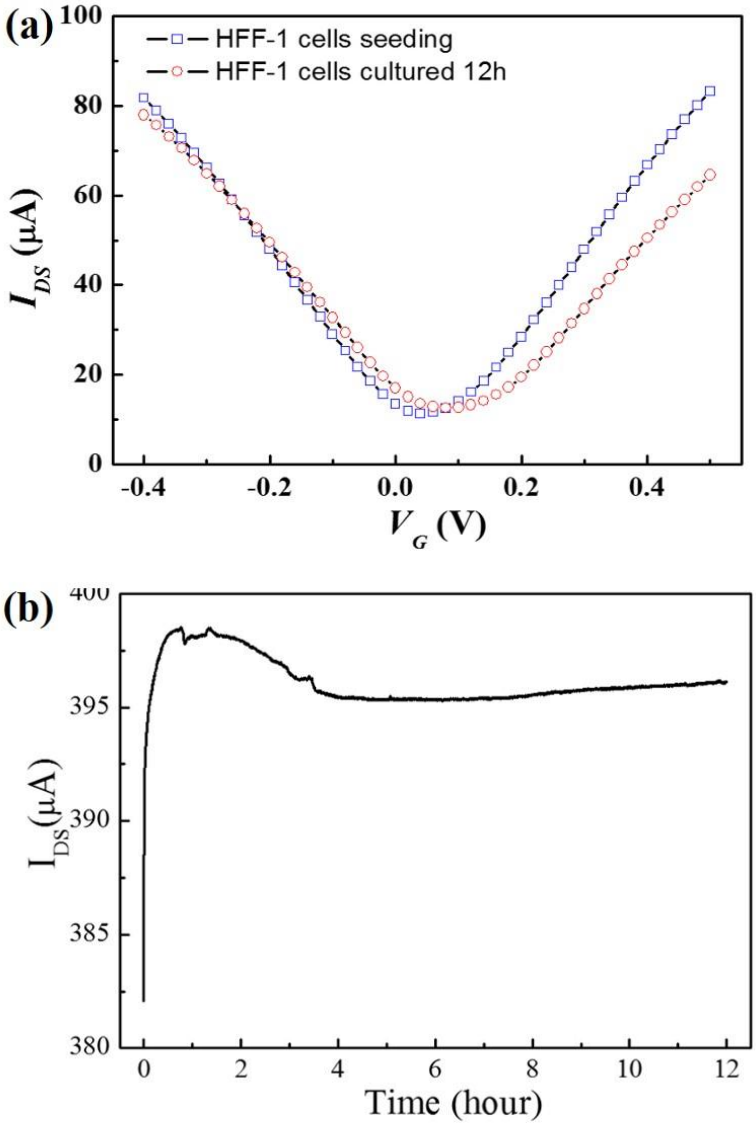

Figure 5.5 a) Channel current response of a SGGT (I_{DS}) with HFF-1 cell culturing 12 h, V_G = 0.3V and V_{DS} = 0.6V. b) Channel current (I_{DS}) versus time (h) of a SGGT during HFF-1 culturing, voltages of V_G= 0.32 V V_{DS}=0.6V

Figure 5.6 describes the sensing mechanism. Before the cell attached on graphene channel, the cells were suspended in the culture medium, the gate voltage is applied on the two electrical double layer (EDL) formed at the graphene/electrolyte, electrolyte/gate electrode interface. The gate capacitance is comprised by double-layer capacitor and the graphene quantum capacitance connected in series [102],

$$\frac{1}{C_i} = \frac{1}{C_{EDL}} + \frac{1}{C_Q} \tag{5.4}$$

$$C_Q = \partial Q / \partial V_{ch} = q^2 \frac{2}{\pi} \frac{qV_{ch}}{(\hbar \upsilon_F)^2}, \text{ when } qV_{ch} << kT \tag{5.5}$$

C_{EDL} is the EDL capacitance, C_Q is the quantum capacitance, Q is the charge density, q is the electron charge, V_{ch} is the channel electrostatic potential, $\upsilon_F = 10^8 cm/\mathrm{s}$ is the Fermi velocity of carriers in graphene, $\hbar$ is the reduced Planck's constant.

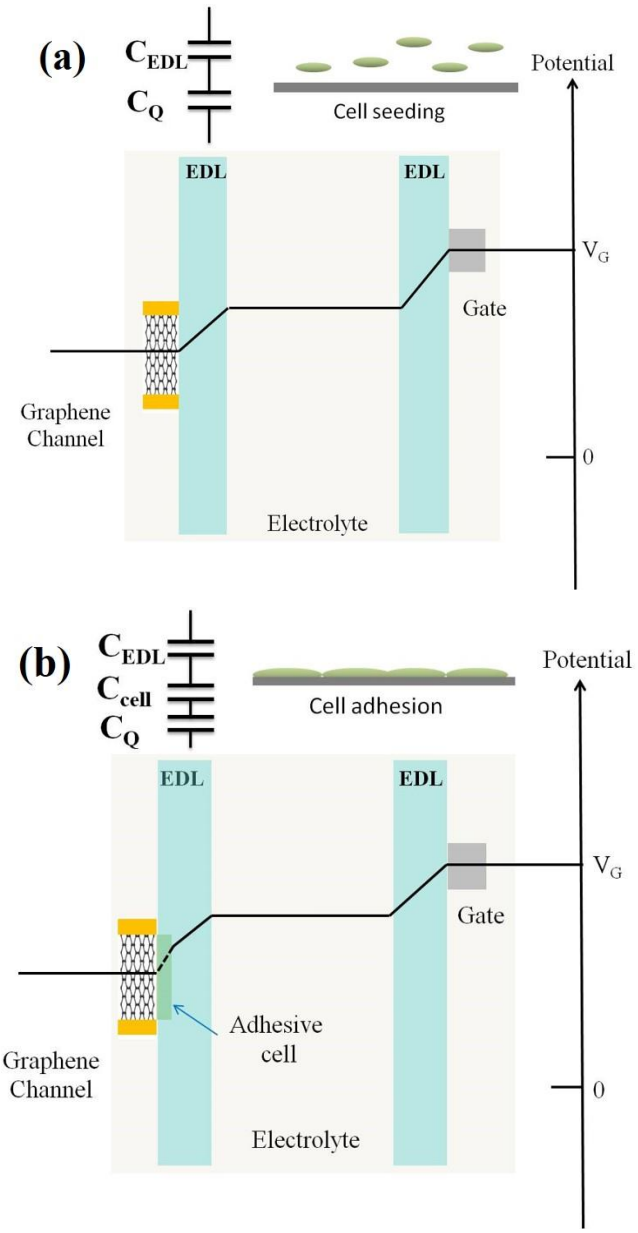

Figure 5.6 cell dielectric layer formation on the graphene channel a), cell seeding on graphene surface, sedimentation phase(top, middle); b) cell adhesion on graphene surface, adhesion phase (bottom).

For HepG2 cell, the cell surface usually carry a negative surface charge, which could induce a counterionic cloud around the cells in culture medium. When the cells were attached on graphene channel, living cells with well formed plasma membrane could form dielectric layer on graphene surface, with electric field applied on cell dielectric layer,the adherent cell could be polarized [144]. In such a situation, the gate capacitance consists cell layer capacitance C_{cell} due to the induced dipole moment besides interface capacitance C_{EDL} and quantum capacitance C_Q. [139]

$$\frac{1}{C_i} = \frac{1}{C_{EDL}} + \frac{1}{C_Q} + \frac{1}{C_{cell}} \qquad (5.6)$$

The cell layer capacitance is influenced by many factors, including adherent cell densities, cell types (as shown in Figure 5.2), membrane integrity, membrane potential, cell morphology, adhesion strength and so on. [140] Figure 5.3b shows the channel current I_{DS} change during cell culturing from 0 h to 12 h, with constant voltages (V_{DS}=0.6V and V_G=0.4V). The channel current decreased continuingly with time, which is in consistant with the results shown in Figure 5.3a. We speculate that, as the density of cells adherent on the graphene channel increases, the channel current decreases due to the cell layer capacitance changes correspondingly, which effects the charge carrier density in the graphene channel. Figure 5.4b and 5.5b exhibited the channel current change in SAOS2 cell and HFF-1 adhesion processes. It is found that the channel current decreased rapidly in the first few hours, and then the channel current came to a comparatively constant stages, which might be attribute to the

adherent of cells suspended previously onto graphene channel. By using this label-free method, cell adhesion processes on graphene interfaces could be detected in real-time, which implies potential future biomedical applications.

5.6 Cancer drug testing on SGGTs

However, when the cells were dead, the cell plasma cannot be kept within the membrane to form induced dipole moments. Based on the mechanism, cell viabilities could also be quantitatively measured on SGGT device. A proof of concept study on anti-cancer drug 5-FU to cancerous cell HepG2 were demonstrated on our device. Firstly, HepG2 cells were cultured on graphene channel for 24h, then 5-FU were added into culture medium. Figure 5.7a shows the transfer characteristic of SGGT before and after drug adding. The capacitance increases after 8 h culturing. Then the cells were stained with PI stain, as shown in Figure 5.7b, most of the cells were dead after coculturing with drug. The red flurescence indicated that the cell membrane was broken by adding anti cancer drug, which induced the capacitance increase. This proof study demonstrated the cell sensing platform has potential biomedical applications needing cell viability measurement like drug screening, environment test et al.

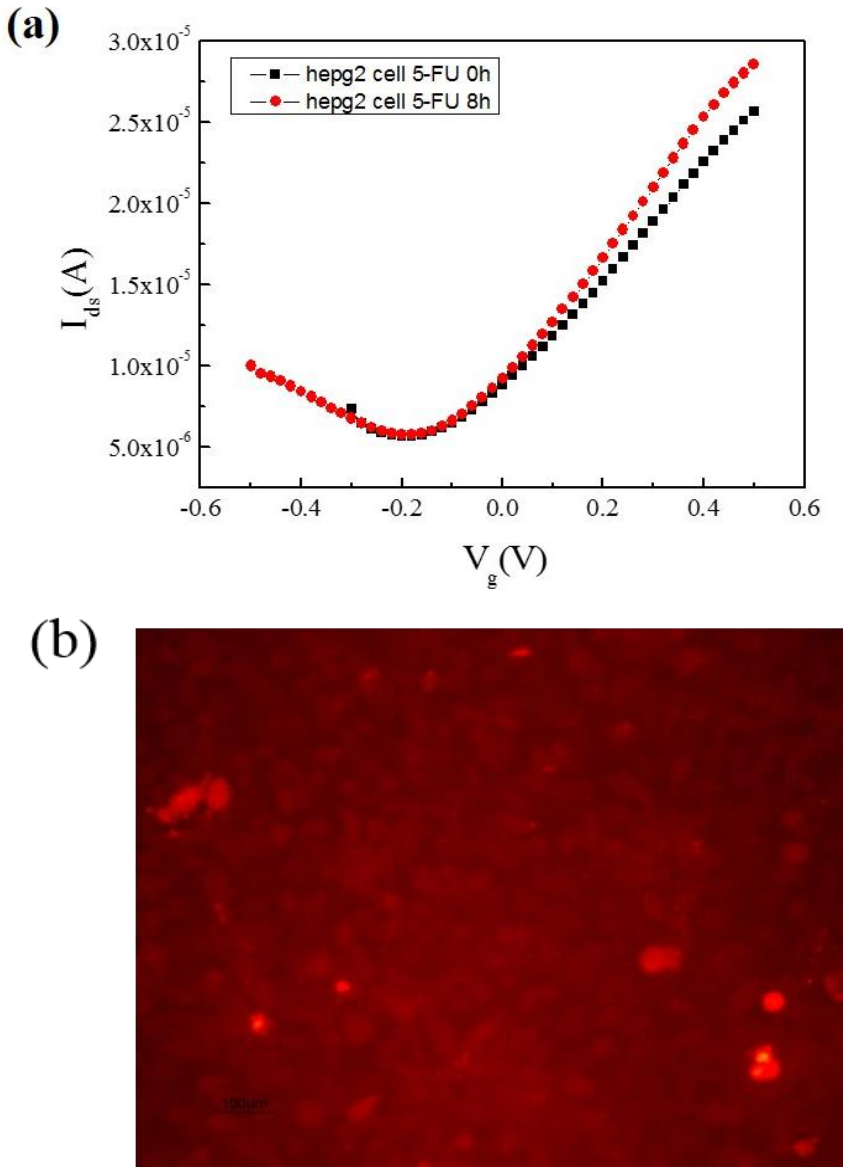

Figure 5.7.a) Channel current (I_{DS}) responses of a SGGT with HepG2 cell culturing voltages of V_G= -0.6 V—0.6 V with V_{DS}=0.05V. The red and black presented channel current with 5-FU cocultured with HepG2 cell 0 h and 8 h. B) fluoescence image of HepG2 cell cultured with 5-FU and stained with PI.

5.7 cell population distribution

An important issue in cell adhesion study is to control the cell density on artificial surfaces, for example bioimplants. Many works focus on modifying the chemistry, texture, and wettability of the surfaces [145]. In this study, the cell sensing platform was used to dynamically controlling the cell adhesion on the channel. As shown in Figure 5.8a, V_{DS}=0.6 V, V_G= V_{DS}-V_{dirac} were applied on the source, drain, and gate electrodes. Considering the graphene channel being a conductive surface, the fermi level in the graphene channel was shifted in a continuous state from the drain electrode to the source electrodes.At the operational voltages, graphene near the drain side induced free electrons as charge carrier, where graphene near the source side induced free holes. The type of the charge carriers were divided by Dirac point, where in our experiments located in the middle of the channel, therefore as shown in Figure 5.8a, left half of the graphene channel has electrons, while the right side has holes. Figure 5.8b exhibited the results of HepG2 cells distribution on graphene channel under the applied electric field. The graphene channel was divided into ten equality area along the channel length. It is obvious that the cell density on area near the drain electrodes is comparatively larger than the area near the source electrodes, exhibited distinct gradient along the channel. Figure 5.8c shows the charge distribution on the drain electrode side, the charge carrier inside graphene is negatively charged, so that the surface of graphene is compensated by positive charge. When HepG2 cells are seeded in the culture medium, because the surface of cell is negatively charged, cells are more

likely to locate on positive surface due to the electrostatic force. The in-situ control of the adhesion of HepG2 cells along the graphene channel is achieved by the cell sensing platform.The experiment demonstrates that the cell adhesion and distribution is heavily influenced by graphene surface charges, which implies a powerful tool for tunable cell adhesion and distribution research.

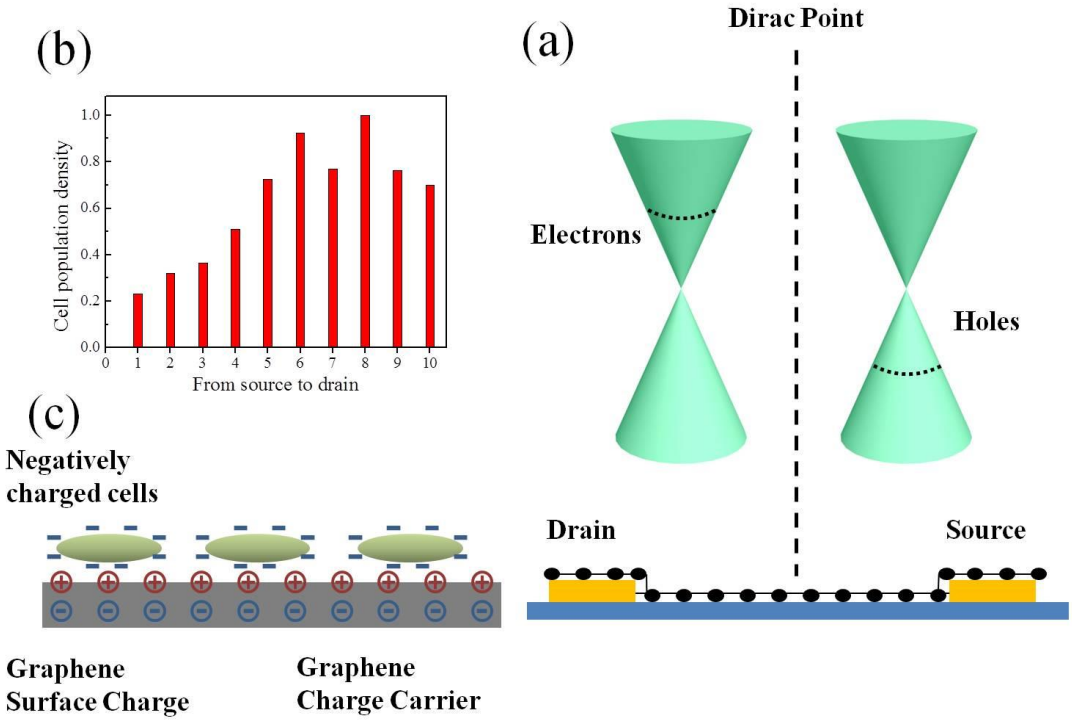

Figure 5.8.a) HepG2 cell population distribution along the graphene channel after culturing 12 h under electric bias $V_G = V_{DS} - V_{Dirac}$ =0.4V and V_{DS} = 0.6V. b) Charge carrier change along the graphene channel with applying $V_G = V_{DS} - V_{Dirac}$ =0.4V and V_{DS} = 0.6V c) mechanism for modulating cell sensing.

5.8 Conclusions

In this chapter, cell sensing platform based on solution-gated graphene transistors (SGGTs) were fabricated to monitor cell adhesion and distribution processes. Cancerous cells (human Hepatocellular carcinoma (HepG2), Human sapien osteosarcoma (SAOS2)) and fibroblasts (Human Foreskin Fibroblast (HFF-1)) were seeded and maintained on the graphene channel of SGGTs. It is found out that during the cell adhesion processes, the channel current changed due to the capacitance variation happened on the cell/graphene channel interface. Based on this phenomenon, the platform were used to monitor anti-cancer drug 5-FU effect to HepG2 cell line. Meanwhile, the cell/SGGT integrated platform were used for controllable cell distribution research. Cell density gradients grown along the channel was modulated by adjusting surface charging state through applying gate voltages. This kind of platform has great potential future biomedical application.

Chapter 6 Conclusions and Future Outlook

6.1 Conclusions

In this thesis, the structure and the mechanism of SGGT based chemical and biological sensors have been introduced and discussed. Present progresses of SGGTs based sensing applications were reviewed in chapter 2. SGGTs have exhibited great potentials for electrical sensing due to its superior electrical, chemical and mechanical properties.

In chapter 3, a highly sensitive dopamine sensor was realized by using a SGGT with a graphene gate electrode. The sensing mechanism of the device is attributed to the electrochemical reaction of dopamine at the gate electrode, which changes the potential distribution at the interfaces on the graphene gate electrode and the graphene channel. The device shows excellent selectivity to dopamine after the modification of the graphene gate electrode with a thin layer of Nafion. The interference from AA and UA is 3 to 4 orders of magnitude lower than the response of the device to dopamine. The device shows the detection limit to dopamine down to 1 nM, which is good enough for analyzing dopamine levels in clinical applications. Because the channel and the gate of the device are all made of graphene, it can be fabricated on various substrates including flexible ones at low temperature by convenient techniques.

In chapter 4, whole-graphene SGGTs with PtNP-functionalized graphene gate electrodes can be used for highly sensitive detections of H_2O_2 with the detection limit down to 30nM. The device is further demonstrated as a highly sensitive glucose sensor after the immobilization of the enzyme GOx, CHIT and Nafion on the PtNPs/graphene surface and can detect glucose concentrations down to 0.5 μM. The high sensitivity of the SGGT-based sensors is attributed to the inherent amplification function of the transistors and the improved electrocatalytic activity of the graphene gate electrodes after the modification of PtNPs.

In chapter 5, cell monitoring platform based on solution-gated graphene transistors were developed for biological process (such as cell adhesion and proliferation) observation and researching. It can be found that the devices exhibited stable performance and excellent biocompatibility in culture medium. Cancer cells (HepG2, SAOS2) and fibroblasts (HFF-1) were successfully grown on the surface of graphene channel of SGGT. We found that the devices were sensitive to the change of surface charge and morphology of adherent cells. The sensing mechanism could be attributed to the capacitance variation between the cells and graphene surface due to the ion polarization within the cellular plasma. The doping level of graphene could be eazily modulated by applying electric fields on the transistor, and thus the surface charge of graphene, which is essential to the cell adhesion on the surface is adjustable on the platform. Cell density gradients grown on the channel is modulated by adjusting surface charging state of graphene in this work.

6.2 Challenges and oppotunities

As mentioned above, graphene has been demonstrated as the most promising candidate nanomaterial for developing electronic biosensors with high speed, high sensitivity, and highthroughput. Many process has been made in recent years. However this research area is still a relatively new and further efforts are needed to make clear some critical issues.

From my point of view, the following issues are still need to be further investigated with a view to realizing high performance sensors that could be used in practical applications. Firstly, most significant task for future work is to minimize the size of the devices for microscale-world detection and to integrate SGGTs into high density for highthroughput sensing. Since large area graphene with uniform properties could be fabricated by CVD method, CVD graphene can be used in microfabrication process to realize SGGT arrays. High density SGGTs imply feasible ways for integretion with complementary digital electronics and show exciting commercial perspective. [69]

Secondly, due to the remarkable mechanical properties of graphene, SGGTs could be incorporated with the concept of flexible electronics. Generally, flexible electronics could impove the conformal interface between biological tissues and the electronics, [66] so that the development of flexible SGGTs would possibly broaden the range of practical applications of SGGTs into environments needing deformation.

Finally, SGGT-based sensors have great potential for complex biosystem research. However, for practical use, SGGT-based devices should be taken into direct contact with real biological samples which inquires the devices has robust performance that can prevent pollutent and provide stable signal. That is still a big challenge we should solve for applications of SGGT biosensors.

References

[1] W. R. Yang, K. R. Ratinac, S. P. Ringer, P. Thordarson, J. J. Gooding, F. Braet, Angew Chem Int Edit 2010, 49, 2114.

[2] M. Pumera, Mater Today 2011, 14, 308.

[3] X. Huang, Z. Yin, S. Wu, X. Qi, Q. He, Q. Zhang, Q. Yan, F. Boey, H. Zhang, Small 2011, 7, 1876.

[4] Y. Liu, X. Dong, P. Chen, Chemical Society Reviews 2012, 41, 2283.

[5] S. Liu, X. Guo, NPG Asia Materials 2012, 4, e23.

[6] Q. He, S. Wu, Z. Yin, H. Zhang, Chem Sci 2012, 3, 1764.

[7] K. S. Novoselov, Science 2004, 306, 666.

[8] X. Du, I. Skachko, A. Barker, E. Y. Andrei, Nature nanotechnology 2008, 3, 491.

[9] K. S. Novoselov, A. K. Geim, S. V. Morozov, D. Jiang, Y. Zhang, S. V. Dubonos, I. V. Grigorieva, A. A. Firsov, Science 2004, 306, 666.

[10] F. Yan, H. Tang, Expert Review of Molecular Diagnostics 2010, 10, 547.

[11] F. Cicoira, M. Sessolo, O. Yaghmazadeh, J. A. DeFranco, S. Y. Yang, G. G. Malliaras, Advanced Materials 2010, 22, 1012.

[12] F. Patolsky, B. P. Timko, G. F. Zheng, C. M. Lieber, Mrs Bull 2007, 32, 142.

[13] P. Lin, F. Yan, Advanced Materials 2012, 24, 34.

[14] F. Chen, Q. Qing, J. L. Xia, N. J. Tao, Chem-Asian J 2010, 5, 2144.

[15] A. K. Geim, Science 2009, 324, 1530.

[16] T. Wu, H. Shen, L. Sun, B. Cheng, B. Liu, J. Shen, New J Chem 2012, 36, 1385.

[17] Y. Si, E. T. Samulski, Nano Lett 2008, 8, 1679.

[18] Y. Cui, S. N. Kim, S. E. Jones, L. L. Wissler, R. R. Naik, M. C. McAlpine, Nano Lett 2010, 10, 4559.

[19] P. W. Sutter, J. I. Flege, E. A. Sutter, Nat Mater 2008, 7, 406.

[20] R. X. He, P. Lin, Z. K. Liu, H. W. Zhu, X. Z. Zhao, H. L. W. Chan, F. Yan, Nano Lett 2012, 12, 1404.

[21] M. Dankerl, M. V. Hauf, A. Lippert, L. H. Hess, S. Birner, I. D. Sharp, A. Mahmood, P. Mallet, J. Y. Veuillen, M. Stutzmann, J. A. Garrido, Advanced Functional Materials 2010, 20, 3117.

[22] C. Mattevi, H. Kim, M. Chhowalla, J Mater Chem 2011, 21, 3324.

[23] E. Rollings, G. H. Gweon, S. Y. Zhou, B. S. Mun, J. L. McChesney, B. S. Hussain, A. V. Fedorov, P. N. First, W. A. de Heer, A. Lanzara, J Phys Chem Solids 2006, 67, 2172.

[24] J. Hass, W. A. d. Heer, E. H. Conrad, Journal of Physics: Condensed Matter 2008, 20, 323202.

[25] N. Mohanty, V. Berry, Nano Lett 2008, 8, 4469.

[26] S. Mao, K. H. Yu, G. H. Lu, J. H. Chen, Nano Res 2011, 4, 921.

[27] S. Park, R. S. Ruoff, Nature Nanotechnology 2009, 4, 217.

[28] Y. X. Huang, X. C. Dong, Y. M. Shi, C. M. Li, L. J. Li, P. Chen, Nanoscale 2010, 2, 1485.

[29] Z. K. Liu, J. H. Li, Z. H. Sun, G. A. Tai, S. P. Lau, F. Yan, Acs Nano 2012, 6, 810.

[30] X. C. Dong, Y. M. Shi, W. Huang, P. Chen, L. J. Li, Advanced Materials 2010, 22, 1649.

[31] Y. Q. Wen, F. B. Y. Li, X. C. Dong, J. Zhang, Q. H. Xiong, P. Chen, Advanced Healthcare Materials 2013, 2, 271.

[32] A. J. Bard, L. R. Faulkner, *Electrochemical methods: fundamentals and applications*, Vol. 2, Wiley New York, 1980.

[33] T. Fang, A. Konar, H. Xing, D. Jena, Appl Phys Lett 2007, 91, 092109.

[34] S. M. Sze, K. K. Ng, *Physics of semiconductor devices*, John Wiley & Sons, 2006.

[35] A. D. McNaught, A. D. McNaught, *Compendium of chemical terminology*, Vol. 1669, Blackwell Science Oxford, 1997.

[36] F. Schedin, A. K. Geim, S. V. Morozov, E. W. Hill, P. Blake, M. I. Katsnelson, K. S. Novoselov, Nat Mater 2007, 6, 652.

[37] C. T. Lin, P. T. K. Loan, T. Y. Chen, K. K. Liu, C. H. Chen, K. H. Wei, L. J. Li, Advanced Functional Materials 2013, 23, 2301.

[38] T. Cohen-Karni, Q. Qing, Q. Li, Y. Fang, C. M. Lieber, Nano Lett 2010, 10, 1098.

[39] D. B. Farmer, R. Golizadeh-Mojarad, V. Perebeinos, Y.-M. Lin, G. S. Tulevski, J. C. Tsang, P. Avouris, Nano Lett 2008, 9, 388.

[40] Y. Ohno, K. Maehashi, Y. Yamashiro, K. Matsumoto, Nano Lett 2009, 9, 3318.

[41] X. W. Tang, S. Bansaruntip, N. Nakayama, E. Yenilmez, Y. L. Chang, Q. Wang, Nano Lett 2006, 6, 1632.

[42] F. Yan, S. M. Mok, J. Yu, H. L. Chan, M. Yang, Biosensors and Bioelectronics 2009, 24, 1241.

[43] S. Bae, H. Kim, Y. Lee, X. F. Xu, J. S. Park, Y. Zheng, J. Balakrishnan, T. Lei, H. R. Kim, Y. I. Song, Y. J. Kim, K. S. Kim, B. Ozyilmaz, J. H. Ahn, B. H. Hong, S. Iijima, Nature Nanotechnology 2010, 5, 574.

[44] A. Hulanicki, S. Glab, F. Ingman, Pure Appl. Chem. 1991, 63, 1247.

[45] P. K. Ang, W. Chen, A. T. S. Wee, K. P. Loh, J Am Chem Soc 2008, 130, 14392.

[46] Y. Ohno, K. Maehashi, K. Matsumoto, Biosensors and Bioelectronics 2010, 26, 1727.

[47] Z. G. Cheng, Q. Li, Z. J. Li, Q. Y. Zhou, Y. Fang, Nano Lett 2010, 10, 1864.

[48] W. Fu, C. Nef, O. Knopfmacher, A. Tarasov, M. Weiss, M. Calame, C. Schönenberger, Nano Lett 2011, 11, 3597.

[49] F. Chen, Q. Qing, J. L. Xia, J. H. Li, N. J. Tao, J Am Chem Soc 2009, 131, 9908.

[50] I. Heller, S. Chatoor, J. Mannik, M. A. G. Zevenbergen, C. Dekker, S. G. Lemay, J Am Chem Soc 2010, 132, 17149.

[51] Y. Sofue, Y. Ohno, K. Maehashi, K. Inoue, K. Matsumoto, Jpn J Appl Phys 2011, 50.

[52] H. G. Sudibya, Q. He, H. Zhang, P. Chen, Acs Nano 2011, 5, 1990.

[53] A. K. M. Newaz, D. A. Markov, D. Prasai, K. I. Bolotin, Nano Lett 2012, 12, 2931.

[54] Y. Wen, F. Y. Li, X. Dong, J. Zhang, Q. Xiong, P. Chen, Advanced Healthcare Materials 2012, 271.

[55] P. Bergveld, Sensor Actuat B-Chem 2003, 88, 1.

[56] A. K. Feldman, M. L. Steigerwald, X. F. Guo, C. Nuckolls, Accounts Chem Res 2008, 41, 1731.

[57] B. S. Kang, F. Ren, Y. W. Heo, L. C. Tien, D. P. Norton, S. J. Pearton, Appl Phys Lett 2005, 86, 3.

[58] U. Lange, N. V. Roznyatouskaya, V. M. Mirsky, Anal Chim Acta 2008, 614, 1.

[59] E. Matijevic, *Surface and colloid science*, Vol. 16, Springer, 2001.

[60] Y. B. Zhang, S. F. Ali, E. Dervishi, Y. Xu, Z. R. Li, D. Casciano, A. S. Biris, Acs Nano 2010, 4, 3181.

[61] J. W. Liu, Z. H. Cao, Y. Lu, Chem Rev 2009, 109, 1948.

[62] H. X. Chang, Z. H. Sun, K. Y. F. Ho, X. M. Tao, F. Yan, W. M. Kwok, Z. J. Zheng, Nanoscale 2011, 3, 258.

[63] H. X. Chang, Z. H. Sun, Q. H. Yuan, F. Ding, X. M. Tao, F. Yan, Z. J. Zheng, Advanced Materials 2010, 22, 4872.

[64] P. Lin, X. Luo, I. M. Hsing, F. Yan, Advanced Materials 2011, n/a.

[65] R.X. He, M. Zhang, F. Tan, P. H. M. Leung, X.-Z. Zhao, H. L. W. Chan, M. Yang, F. Yan, J Mater Chem 2012, 22, 22072.

[66] L. H. Hess, M. Jansen, V. Maybeck, M. V. Hauf, M. Seifert, M. Stutzmann, I. D. Sharp, A. Offenhäusser, J. A. Garrido, Advanced Materials 2011, 23, 5045.

[67] P. K. Ang, A. Li, M. Jaiswal, Y. Wang, H. W. Hou, J. T. L. Thong, C. T. Lim, K. P. Loh, Nano Lett 2011, 11, 5240.

[68] Y. X. Huang, X. C. Dong, Y. X. Liu, L. J. Li, P. Chen, J Mater Chem 2011, 21, 12358.

[69] R. Stine, J. T. Robinson, P. E. Sheehan, C. R. Tamanaha, Advanced Materials 2010, 22, 5297.

[70] S. R. Guo, J. Lin, M. Penchev, E. Yengel, M. Ghazinejad, C. S. Ozkan, M. Ozkan, J Nanosci Nanotechno 2011, 11, 5258.

[71] Z. Y. Yin, Q. Y. He, X. Huang, J. Zhang, S. X. Wu, P. Chen, G. Lu, Q. C. Zhang, Q. Y. Yan, H. Zhang, Nanoscale 2012, 4, 293.

[72] T. Y. Chen, T. K. L. Phan, C. L. Hsu, Y. H. Lee, J. T. W. Wang, K. H. Wei, C. T. Lin, L. J. Li, Biosens Bioelectron 2013, 41, 103.

[73] Y. H. Kwak, D. S. Choi, Y. N. Kim, H. Kim, D. H. Yoon, S.-S. Ahn, J.-W. Yang, W. S. Yang, S. Seo, Biosensors and Bioelectronics 2012, 37, 82.

[74] Y. Ohno, K. Maehashi, K. Matsumoto, J Am Chem Soc 2010, 132, 18012.

[75] Q. He, H. G. Sudibya, Z. Yin, S. Wu, H. Li, F. Boey, W. Huang, P. Chen, H. Zhang, Acs Nano 2010, 4, 3201.

[76] D. J. Kim, I. Y. Sohn, J. H. Jung, O. J. Yoon, N. E. Lee, J. S. Park, Biosens Bioelectron 2013, 41, 621.

[77] S. J. Park, O. S. Kwon, S. H. Lee, H. S. Song, T. H. Park, J. Jang, Nano Lett 2012, 12, 5082.

[78] N. Li, X. M. Zhang, Q. Song, R. G. Su, Q. Zhang, T. Kong, L. W. Liu, G. Jin, M. L. Tang, G. S. Cheng, Biomaterials 2011, 32, 9374.

[79] P. Lin, F. Yan, J. Yu, H. L. W. Chan, M. Yang, Advanced Materials 2010, 22, 3655.

[80] B. Hofmann, V. Maybeck, S. Eick, S. Meffert, S. Ingebrandt, P. Wood, E. Bamberg, A. Offenhausser, Lab on a Chip 2010, 10, 2588.

[81] J. H. Chen, C. Jang, S. Adam, M. S. Fuhrer, E. D. Williams, M. Ishigami, Nature Physics 2008, 4, 377.

[82] Z. H. Sun, Z. K. Liu, J. H. Li, G. A. Tai, S. P. Lau, F. Yan, Advanced Materials 2012, 24, 5878.

[83] M. Vestergaard, K. Kerman, E. Tamiya, Sensors-Basel 2007, 7, 3442.

[84] G. F. Zheng, F. Patolsky, Y. Cui, W. U. Wang, C. M. Lieber, Nat. Biotechnol. 2005, 23, 1294.

[85] C. B. Jacobs, M. J. Peairs, B. J. Venton, Anal Chim Acta 2010, 662, 105.

[86] H. Tang, F. Yan, P. Lin, J. B. Xu, H. L. W. Chan, Advanced Functional Materials 2011, 21, 2264.

[87] L. C. Clark, C. Lyons, Annals of the New York Academy of sciences 1962, 102, 29.

[88] H. Tang, P. Lin, H. L. W. Chan, F. Yan, Biosensors and Bioelectronics 2011, 26, 4559.

[89] K. Hashizume, A. Yamatodani, T. Ogihara, Hypertension research: official journal of the Japanese Society of Hypertension 1995, 18, S205.

[90] T. H. Kim, S. H. Lee, J. Lee, H. S. Song, E. H. Oh, T. H. Park, S. Hong, Advanced Materials 2009, 21, 91.

[91] S. G. Amara, M. J. Kuhar, Annual review of neuroscience 1993, 16, 73.

[92] R. M. Wightman, J. A. Jankowski, R. T. Kennedy, K. T. Kawagoe, T. J. Schroeder, D. J. Leszczyszyn, J. A. Near, E. J. Diliberto, O. H. Viveros, P Natl Acad Sci USA 1991, 88, 10754.

[93] S. Ikemoto, Brain Res. Rev. 2007, 56, 27.

[94] J. R. Wickens, J. C. Horvitz, R. M. Costa, S. Killcross, Journal of Neuroscience 2007, 27, 8181.

[95] T. S. Tang, X. Chen, J. Liu, I. Bezprozvanny, Journal of Neuroscience 2007, 27, 7899.

[96] S. R. Laviolette, Schizophr. Bull. 2007, 33, 971.

[97] E. C. Y. Chan, P. Y. Wee, P. Y. Ho, P. C. Ho, J. Chromatogr. B 2000, 749, 179.

[98] M. E. P. Hows, L. Lacroix, C. Heidbreder, A. J. Organ, A. J. Shah, J. Neurosci. Methods 2004, 138, 123.

[99] H. M. Zhang, N. Q. Li, Z. W. Zhu, Microchem J. 2000, 64, 277.

[100] H. Zhao, Y. Z. Zhang, Z. B. Yuan, Anal Chim Acta 2001, 441, 117.

[101] S. M. Strawbridge, S. J. Green, J. H. R. Tucker, Chem Commun 2000, 2393.

[102] F. Yan, M. Zhang, J. Li, Advanced Healthcare Materials 2014, 3, 313.

[103] H. S. Wang, T. H. Li, W. L. Jia, H. Y. Xu, Biosens Bioelectron 2006, 22, 664.

[104] C. Z. Liao, M. Zhang, L. Y. Niu, Z. J. Zheng, F. Yan, Journal of Materials Chemistry B 2013, 1, 3820.

[105] C. Z. Liao, M. Zhang, L. Y. Niu, Z. J. Zheng, F. Yan, Journal of Materials Chemistry B 2014, 2, 191.

[106] D. A. Bernards, G. G. Malliaras, Advanced Functional Materials 2007, 17, 3538.

[107] D. A. Bernards, D. J. Macaya, M. Nikolou, J. A. DeFranco, S. Takamatsu, G. G. Malliaras, J Mater Chem 2008, 18, 116.

[108] Y. X. Sun, S. F. Wang, Microchim Acta 2006, 154, 115.

[109] S. M. Mok, F. Yan, H. L. W. Chan, Appl Phys Lett 2008, 93, 3.

[110] F. Yan, S. M. Mok, J. Yu, H. L. W. Chan, M. Yang, Biosensors and Bioelectronics 2009, 24, 1241.

[111] Z. H. Sun, J. H. Li, F. Yan, J Mater Chem 2012, 22, 21673.

[112] W. B. Nowall, W. G. Kuhr, Anal Chem 1995, 67, 3583.

[113] F. Malem, D. Mandler, Anal Chem 1993, 65, 37.

[114] R. M. Reynolds, P. L. Padfield, J. R. Seckl, Bmj 2006, 332, 702.

[115] Z. H. Sheng, X. Q. Zheng, J. Y. Xu, W. J. Bao, F. B. Wang, X. H. Xia, Biosens Bioelectron 2012, 34, 125.

[116] Z. D. Peterson, D. C. Collins, C. R. Bowerbank, M. L. Lee, S. W. Graves, J Chromatogr B 2002, 776, 221.

[117] N. J. Ronkainen, H. B. Halsall, W. R. Heineman, Chemical Society Reviews 2010, 39, 1747.

[118] T. Kuila, S. Bose, P. Khanra, A. K. Mishra, N. H. Kim, J. H. Lee, Biosens Bioelectron 2011, 26, 4637.

[119] A. Heller, B. Feldman, Chem Rev 2008, 108, 2482.

[120] Y. H. Lin, F. Lu, Y. Tu, Z. F. Ren, Nano Lett 2004, 4, 191.

[121] Y. J. Song, K. G. Qu, C. Zhao, J. S. Ren, X. G. Qu, Advanced Materials 2010, 22, 2206.

[122] Y. X. Liu, X. C. Dong, P. Chen, Chemical Society Reviews 2012, 41, 2283.

[123] Q. Y. He, S. X. Wu, Z. Y. Yin, H. Zhang, Chem Sci 2012, 3, 1764.

[124] M. Zhang, C. Liao, Y. Yao, Z. Liu, F. Gong, F. Yan, Advanced Functional Materials 2014, 24, 978.

[125] H. Tang, F. Yan, P. Lin, J. Xu, H. L. W. Chan, Advanced Functional Materials 2011, 21, 2264.

[126] M. H. Yang, Y. H. Yang, B. Liu, G. L. Shen, R. Q. Yu, Sensor Actuat B-Chem 2004, 101, 269.

[127] S. H. Lim, J. Wei, J. Y. Lin, Q. T. Li, J. KuaYou, Biosens Bioelectron 2005, 20, 2341.

[128] M. Yamaguchi, M. Mitsumori, Y. Kano, Ieee Eng Med Biol 1998, 17, 59.

[129] D. Khodagholy, J. Rivnay, M. Sessolo, M. Gurfinkel, P. Leleux, L. H. Jimison, E. Stavrinidou, T. Herve, S. Sanaur, R. M. Owens, G. G. Malliaras, Nature Communications 2013, 4.

[130] T. You, O. Niwa, M. Tomita, S. Hirono, Anal Chem 2003, 75, 2080.

[131] S. H. Lim, J. Wei, J. Lin, Q. Li, J. KuaYou, Biosensors and Bioelectronics 2005, 20, 2341.

[132] X. Kang, J. Wang, H. Wu, I. A. Aksay, J. Liu, Y. Lin, Biosensors and Bioelectronics 2009, 25, 901.

[133] R. Vaidya, P. Atanasov, E. Wilkins, Medical Engineering & Physics 1995, 17, 416.

[134] M. Lafkioti, B. Krauss, T. Lohmann, U. Zschieschang, H. Klauk, K. v. Klitzing, J. H. Smet, Nano Lett 2010, 10, 1149.

[135] S. Aydin, Journal of biochemistry and molecular biology 2007, 40, 29.

[136] J. El-Ali, P. K. Sorger, K. F. Jensen, Nature 2006, 442, 403.

[137] L. Z. Feng, Z. A. Liu, Nanomedicine 2011, 6, 317.

[138] H. Nj, B. Kj, O. C. K, C. R, M. Rl, J Long Term Eff Med Implants 1995, 5, 209.

[139] S. B. Prakash, P. Abshire, Sensors Journal 2007.

[140] A. Blau, Current Opinion in Colloid & Interface Science 2013, 18, 481.

[141] J. Wegener, C. R. Keese, I. Giaever, Experimental cell research 2000, 259, 158.

[142] A. C. Ferrari, J. C. Meyer, V. Scardaci, C. Casiraghi, M. Lazzeri, F. Mauri, S. Piscanec, D. Jiang, K. S. Novoselov, S. Roth, A. K. Geim, Phys Rev Lett 2006, 97, 187401.

[143] M. S. Dresselhaus, A. Jorio, M. Hofmann, G. Dresselhaus, R. Saito, Nano Lett 2010, 10, 751.

[144] P. Nguyen, V. Berry, The Journal of Physical Chemistry Letters 2012, 3, 1024.

[145] M. H. Bolin, K. Svennersten, D. Nilsson, A. Sawatdee, E. W. H. Jager, A. Richter-Dahlfors, M. Berggren, Advanced Materials 2009, 21, 4379.